The relation between geometry, hydrology and stability of complex hillslopes examined using low-dimensional hydrological models

Ali Talebi

The relation between geometry, hydrology and stability of complex hillslopes examined using low-dimensional hydrological models

Ali Talebi

Promotoren: Prof. dr. ir. P. A. Troch
Professor of Hydrology and Water Resources
University of Arizona, USA

Prof. dr. ir. R. Uijlenhoet
Hoogleraar Hydrologie en Kwantitatief Waterbeheer
Wageningen Universiteit

Samenstelling Promotiecommissie:

Prof. dr. ir. L. Stroosnijder (Wageningen Universiteit)
Prof. dr. M. S. Hassanizadeh (Universiteit Utrecht)
Dr. Th. W. J. Van Asch (Universiteit Utrecht)
Dr. T. A. Bogaard (Technische Universiteit Delft)

Dit onderzoek is uitgevoerd binnen de onderzoekschool WIMEK-SENSE.

The relation between geometry, hydrology and stability of complex hillslopes examined using low-dimensional hydrological models

Ali Talebi

Proefschrift
ter verkrijging van de graad van doctor
op gezag van de rector magnificus
van Wageningen Universiteit
Prof. dr. M.J. Kropff
in het openbaar te verdedigen
op donderdag 17 januari 2008
des morgens te 11.00 uur in de Aula

Talebi, Ali (2008),

"The relation between geometry, hydrology and stability of complex hillslopes examined using low-dimensional hydrological models"

Key words: Hillslope geometry, Hillslope hydrology, Hillslope stability, Complex hillslopes, Modeling shallow landslides, HSB model, HSB-SM model.

PhD-thesis, Hydrology and Quantitative Water Management Group, Wageningen University and Research center, Wageningen, The Netherlands.

ISBN: 978-90-8504-788-9

"... رب زد نی علما "

"... O my Lord!, advance me in knowledge."

(QS 20 Taahaa: 114)

This book is dedicated to:

my dearest wife, Shohreh

and my lovely son, Amin

Is this the real life
Is this just fantasy
Caught in a landslide
No escape from reality

© Queen – Bohemian Rhapsody (1975)

Abstract

Talebi, A. 2008. *The relation between geometry, hydrology and stability of complex hillslopes examined using low-dimensional hydrological models*, Doctoral thesis, Wageningen University, Wageningen, The Netherlands.

The hydrologic response of a hillslope to rainfall involves a complex, transient saturated-unsaturated interaction that usually leads to a water table rise. An increase of saturated groundwater flow can act as the triggering mechanism for slope failure. To account for the three-dimensional hillslope shape in which the groundwater flow and storage processes take place, simple (low-dimensional) but physically realistic models that represent hydrological processes at the hillslope scales are needed for reliable simulation of hillslope stability at the landscape scale. In this thesis the focus is on investigating the relation between hillslope geometry, hillslope hydrology and slope stability in complex hillslopes and hollows.

Several models have been presented in this thesis which examine the stability of nine characteristic hillslope types (landform elements) with three different profile curvatures (concave, straight and convex) and three different plan shapes (convergent, parallel and divergent). In addition to testing our models for nine characteristic hillslope types, a general relationship between plan shape and profile curvature of landform elements and the factor of safety is derived for a predefined hillslope length scale. Our results show that slope stability increases when profile curvature changes from concave to convex. In terms of plan shapes, changing from convergent to divergent, slope stability increases for all length profiles. Our analyses also show that the minimum safety factor occurs when the rate of subsurface flow is maximum. In fact, by increasing the subsurface flow, stability decreases for all hillslope shapes. Moreover, after a certain period of rainfall, the convergent hillslopes with concave and straight profiles become unstable faster than others whilst divergent convex hillslopes remain stable (even after intense rainfall). We also demonstrate that in hillslopes with non-constant soil depth (possible deep landslides), the ones with convex profiles and convergent plan shapes have slip surfaces with the minimum safety factor near the outlet region. Finally, we demonstrate that, in addition to bedrock slope, hillslope shape as represented by plan shape and profile curvature is an important control on hillslope stability.

With respect to the relation between rainfall occurrence and slope instability, a probabilistic model of rainfall-induced shallow landslides in complex hollows is also presented to investigate the relation between return period of rainfall, deposit thickness and landslide occurrence. A long term analysis of shallow landslides by the presented model illustrates that all hollows show a quite different behavior from the stability view point. Finally, we conclude that incorporating a more realistic description of hollow hydrology (the hillslope-storage Boussinesq model instead of the kinematic wave model) in landslide probability models is necessary, especially for hollows with a high convergence degree, which are more susceptible to landsliding. This model helps to theoretically investigate the relationship between return period of rainfall and landslide occurrence related to soil production (deposit thickness) in complex hollows.

In summary this thesis aims to understand theoretically how hydrological processes (subsurface flow and water table dynamics) affect slope stability in complex hillslopes and hollows. The presented models can widely be applied in many investigations of hillslope stability analysis because of their relative simplicity (low-dimensional).

Key words*: Hillslope geometry, Hillslope hydrology, Hillslope stability, Complex hillslopes, Modeling shallow landslides, HSB model, HSB-SM model.*

Acknowledgement

I would like to express my profound gratitude and praises to the Almighty Allah for all good graces and mercies he granted me in my life and career. I am also grateful of the Ministry of Science, Research, and Technology (MSRT) of Iran for granting me a fulltime scholarship to follow my PhD study abroad. The work presented in this thesis was made possible with the support and contribution of many individuals whom I like to sincerely acknowledge.

First, I respectfully render my regards and gratitude to my first promotor, Prof. Peter Troch. I appreciate his brilliant thoughts and inspiring guidance which kept me on the right way to the planned destination of PhD promotion. Two years after starting my PhD study, he moved to the University of Arizona in the United States. Dear Peter, if you had stayed in Wageningen I would have learned from you much more useful scientific qualities than what I have already acquired. Anyway, your comprehensive guidelines and support in all steps of my research enabled me to follow and finally get the job done. Thank you for everything.

My very special thanks go to my second promotor, Prof. Remko Uijlenhoet for his help, intellectual ideas, and valuable guidance. His enthusiastic ideas and prompt solutions to my technical questions convinced me to continue getting benefited by his creativity and supervision. Dear Remko, you gave all due attention to my work despite the limited time you had due to being the promotor or supervisor of many other PhD students. I deeply thank you and wish to keep in touch with you in the future.

I would also like to express my sincere gratitude to Prof. Rik Leemans (Director of graduate school, WIMEK) who supported and helped me when I had been involved in some problems during my PhD project.

I sincerely acknowledge Dr. Emiel van Loon, who was the first person in the Erosion, Soil and Water Conservation group with whom I communicated. He arranged all preliminary and logistic affairs before my arrival to the Netherlands.

I would also like to express my sincere gratitude to Theo van Asch and his colleagues (Thom Bogaard and Rens van Beek) in Utrecht University for their valuable comments.

I would like also to thank all office colleagues and section staff in the Hydrology group for providing a nice environment for work and discussion (especially Hidde, Arno and Anne). I experienced very pleasant times during our weekly meetings organized by the group. My special thanks go to Henny and Annemarie, always ready to translate so many letters and forms which I was receiving in Dutch language and to handle all the bureaucratic administration affairs which I was facing.

I would like to take the opportunity to express my gratitude to all the members of the Iranian student community here in Wageningen. Although we were far away from our parents, relatives, and our lovely country (Iran), our occasional gatherings and your emotional support prevented me and my family from getting homesick. Thanks to all. My special thanks go to Majid, Vahed and Kaka. We shared pleasant moments during our daily coffee and tea times talking and discussing about work, as well as personal matters. Dear Majid, you spent your free time to help me in programming with MATLAB and I appreciate you and never forget your help.

Finally, last and most of all, I am extremely grateful to my wife Shohreh and my son Amin. I am quite sure that it would not have been possible to accomplish my academic duties, particularly my PhD, without benefiting their patience, tolerance, good willing, and emotional support. My dears, I know that it is impossible to compensate by words what you suffered and whatever you lost in lieu of my academic achievements, but I would like to say THANK YOU for everything and I LOVE YOU.

Ali Talebi, Wageningen, 17th January 2008

Contents

List of symbols

Symbol	Description	Units (SI)
A	Upstream drainage area	m^2
a	Plan shape parameter	m^{-1}
c_e	Effective cohesion of saturated soil	kN m^{-2}
c_s	Degree of topographic convergence	-
c_t	Total soil cohesion	kN m^{-2}
c_w	Width of hillslope at the outlet	m
D	Soil depth (vertical)	m
D'	Soil depth (perpendicular to bedrock)	m
E	Minimum elevation of the surface above an arbitrary datum	m
f	Drainable porosity	m
H	Maximum elevation difference defined by surface	m
h	Water table depth (vertical)	m
h'	Water table depth (perpendicular to bedrock)	m
k	Hydraulic conductivity	m s^{-1}
k_s	Saturated hydraulic conductivity	m s^{-1}
L	Horizontal length of hillslope	m
L'	Length of hillslope on bedrock	m
m_v	Van Genuchten parameter	-
N	Recharge	m s^{-1}
n	Profile curvature parameter	-
n_v	Van Genuchten parameter	-
q	Subsurface flow rate	m^3s^{-1}
S	Subsurface storage (vertical)	m^3
S'	Subsurface storage (perpendicular to bedrock)	m^3
S_c	Subsurface storage capacity	m^3
S_n	Shear strength	kPa
T_n	Shear stress	kPa
u	Water pressure force	kPa

Symbol	Description	Units (SI)
u_a	Pore air pressure	kPa
u_v	Pore water pressure	kPa
W	Weight acting on the slice	kN
w	Width of hillslope	m
w_0	Hillslope width at upstream divide	m
x	Horizontal distance	m
x'	Distance on the bedrock	m
y	Horizontal distance from slope centre	m
Z_B	Elevation of each cell at bottom	m
Z_T	Elevation of each cell at top	m
z	Elevation	m
α	Gardner parameter	m^{-1}
α_v	Van Genuchten parameter	m^{-1}
β	Slope angle	deg
ϕ	Internal friction angle	deg
ϕ^b	Angle of shearing resistance with respect to matric suction	deg
γ_b	Buoyant bulk specific weight	kN m^{-3}
γ_m	Moist bulk specific weight	kN m^{-3}
γ_s	Saturated bulk specific weight	kN m^{-3}
γ_w	Water specific weight	kN m^{-3}
θ	Soil moisture	m^3 m^{-3}
θ_r	Residual soil moisture	m^3 m^{-3}
θ_s	Saturated soil moisture	m^3 m^{-3}
ρ_s	Saturated soil density	kg m^{-3}
ρ_w	Density of water	kg m^{-3}
σ	Relative saturated storage	m^3 m^{-3}
σ_n	Normal stress	kPa
ω	Plan shape parameter	m^{-1}
ψ	Soil water suction	m

Chapter 1

Introduction

1. Introduction

1.1. Problem definition

Landslides are common natural phenomena in many parts of the world. A landslide event is defined as "the movement of a mass of rock, debris, or earth (soil) down a slope (under the influence of gravity) (*Cruden*, 1991). This definition is the most widely used, and is also adopted by the International Geotechnical Societies UNESCO Working Party on the World Landslide Inventory (*Fell et al.*, 2000). Landslides constitute one of the major natural hazards that cause substantial damage to property and loss of life every year across the globe. The term *shallow landslide* is used to describe movements by which material is displaced more or less coherently over a discrete slip surface close to the land surface by disturbing gravitational forces (shear stress). It is well known that rainfall is the most important and frequent trigger of landslides in general and of shallow landslides in particular (*Giannecchini*, 2006). Commonly, it contributes to the triggering of the landslides by means of infiltration into the slope cover, which causes an increase in the pore pressure value and a decrease in the soil suction value.

In the study of hydrological processes in landslides, little attention has been paid to techniques to determine the origin of groundwater and groundwater flow within landslides (*Bogaard et al*., 2004). However, several studies have established that hydrological processes affect the landslide initiation on hillslopes (e.g. *Montgomery and Dietrich*, 1994; *Van Asch et al*., 1996; *Terlien*, 1997; *Ng and Shi*, 1998; *Iverson*, 2000; *Onda et al*., 2004; *Malet et al*., 2005; *Matsushi et al*., 2006). Shallow landslides are one of the most common types of landslides, which occur frequently in steep, soil-mantled landscapes in different climatic zones. In these shallow soils the soil water balance is controlled by infiltration of rain water, unsaturated percolation and a rapid response of the rise of (perched) groundwater during storm events (*Haneberg and Onder Gocke*, 1994). The infiltration of rainfall reduces shear strength at the slip surface by increasing pore water pressure and increasing soil weight, resulting in increased landslide movement. Although pore water pressure fluctuation is an important factor influencing landslide activity, it is difficult to observe its mechanism at various depths of the slip surface because of the complex hydrogeological structure (*Tsao et al*., 2005).

Studies of rainfall-induced landslides mainly focus on the statistical relation between landslide occurrence and rainfall (e.g. *Finlay et al*., 1997; *Terlien*, 1998; *Dai and Lee*, 2001; *Ibsen and Casagli*, 2004; *Floris and Bozzano*, 2007), or on the experimental description of landslides (e.g. *Reichenbach et al*., 1998; *Au*, 1998; *Magirl et al*., 2007; *Matsushi et al*. 2006). These approaches are important, but they provide no theoretical framework for understanding the slope transient pore pressure behaviors in response to rainfall, and its hydrological and physical influence on the occurrence of landslides.

Some researchers (e.g. *Montgomery and Dietrich*, 1994; *Wu and Sidle*, 1995; *Borga et al*., 1998; *Iida*, 1999; *Rosso et al*., 2006; *Claessens et al*. 2007) have investigated the effect of hydrological processes on slope stability by using the mathematical methods of slope stability analysis and modeling. They have defined a soil saturation index which helps predict the

groundwater table in function of the groundwater flow and rainfall intensity. These models are based on the assumption that groundwater flow is driven by gravity (kinematic wave approach), and thus parallel to the ground surface and equal to the total infiltration of rainfall in the upstream area. From a hydrological view point, these models are limited to moderate to steep slopes (*Hilberts et al*., 2004) with a straight or divergent plan shape. This is because convergent hillslopes tend to concentrate subsurface water into a small area of the hillslope, thereby generating rapid pore water pressure increases during storms (*Sidle and Ochiai*, 2006) and this process makes these hillslopes to be more susceptible to landslide occurrence. Therefore, Kinematic wave models loose their ability to accurately describe the water table and hydrographs for gentle and convergent hillslopes. Moreover, in assuming steady state rainfall, these models consequently neglect slope-normal redistribution of groundwater pressures associated with transient infiltration of rain (*Iverson*, 2000), indicating they are unable to predict the temporal response of landslides to varying rainfall patterns. Dynamic models are needed to take into account the transient conditions of hillslope hydrology.

To study the relation between water table dynamics, subsurface flow and slope stability, several researchers (e.g. *Iverson* 2000; *Tsaparas et al*., 2002; *Wilkinson et al*, 2002; *Frattini et al*., 2004; *Lan et al*., 2005; *D'Odorico et al*., 2005; *Tsai and Yang*, 2006; *Salciarini et al*., 2006) use numerical models based on the Richards equation (1D or 2D). Nevertheless, by considering the 1D-2D Richards equation, only the vertical redistribution of infiltrated rainfall can be examined along with the downslope movement of subsurface flow; topographic complexity (both surface and subsurface) is usually not represented (*Sidle and Ochiai*, 2006). None of these studies present models which account for the effect of the three-dimensional hillslope shape on storage and hillslope stability. Therefore, in order to improve our understanding of the role of (three-dimensional) hydrological processes on hillslope stability, an attempt to incorporate the topographic structure of hydrologic processes in hillslope stability models is required. These hydrological processes should preferably be modeled in a low-dimensional yet physically-based manner.

1.2. Objectives of the thesis

In attempting to accurately model the three-dimensional hillslope hydrological processes, 3D Richards equation models are often used. The 3D Richards equation is highly non-linear and requires the solution of extremely large systems of equations even for small problems (*Paniconi et al*., 2003). Moreover, the parameterization and calibration of these models is often cumbersome due to the small amount and low accuracy of the available data (*Hilberts*, 2006). Therefore, to account for the three-dimensional hillslope shape in which the groundwater flow and storage processes take place, simple (low-dimensional) but physically realistic models that represent hydrological processes at the hillslope scale are needed for reliable simulation of hillslope stability at the landscape scale. The general objective of this research is to investigate the relation between hillslope geometry, hillslope hydrology and slope stability in complex hillslopes and hollows. The main core consists of using the low-dimensional modeling of hillslope hydrological process to study the slope stability in

complex hillslopes, i.e. hillslopes with different plan shape (convergent, parallel and divergent) and different profile curvature (concave, straight and convex). The objectives of this study can, therefore be, divided into the following specific themes:

- To present an analytical hillslope stability model to study the role of topography (slope gradient, profile curvature and plan shape) on rain-induced shallow landslides.
- To investigate the relation between soil moisture storage and hillslope stability in complex hillslopes (investigating the effect of neglecting the unsaturated storage on the assessment of slope stability).
- To evaluate the critical slip surface in complex hillslopes with non-constant soil depth (deep landsliding) by incorporating the low-dimensional modeling of hillslope hydrology and a more complex approach of slope stability.
- To present a dynamic low-dimensional hillslope stability model, to investigate the relation between subsurface flow processes and slope stability in complex hillslopes.
- To generalize a probabilistic hydrogeomorphological model for the stability of complex hollows by incorporating the low-dimensional (yet physically-based) hydrological model to investigate the relation between rain return period and landslide return period in complex hollows.

Therefore, this thesis aims to investigate theoretically how hydrological processes (subsurface flow and water table dynamics) affect slope stability in complex hillslopes and hollows. The presented models can be widely be applied in many investigations of hillslope stability analysis because of their relative simplicity. In the following an introduction will be given to the models that are used and analyzed in this thesis.

1.3. Low-dimensional modeling of subsurface flow processes for slope stability in complex hillslopes

Rainfall-induced landslides are triggered hydrologically, i.e. by a rise in the groundwater depth at the slip plane. This raises the pore water pressure that carries part of the total weight that acts on the potential slip plane. Subsurface water and the associated pore-water pressure are the most important factors associated with the occurrence of most landslides. Because subsurface flow processes control the movement of infiltrated water through the hillslope, they influence both the temporal and spatial characteristics of the pore water pressure distribution.

Recently, some researchers (e.g. *Troch et al*., 2002, 2003; *Hilberts et al*., 2004, 2007; *Berne et al*., 2005) have shown that subsurface flow processes are influenced by plan shape and profile curvature and the hydraulic properties of the porous medium. The mathematical description of these flow processes results in the formulation of the 3D Richards equation which is expensive to solve numerically. To overcome difficulties associated with three-dimensional models, a series of low-dimensional hillslope models have been developed (*Troch et al*., 2002, 2003). These models are able to treat geometric complexity in a simple way based on a concept presented by *Fan and Bras* (1998), resulting in a significant reduction in model complexity. This reduction of the dimensionality is achieved by

introducing the subsurface storage capacity function, S_c. This function (*Fan and Bras*, 1998) defines the thickness of the pore space along the hillslope and accounts for plan shape, through the width function, and bedrock profile curvature, through the soil depth function. Assuming kinematic wave subsurface flow, *Troch et al*. (2002) derived the following equation:

$$f\frac{\partial S}{\partial t} = k\frac{\partial S}{\partial x}\frac{\partial z}{\partial x} + kS\frac{\partial^2 z}{\partial x^2} + fNw(x) \tag{1.1}$$

where f is the drainable porosity, S is the saturated storage, k is the hydraulic conductivity, N is the recharge rate, w is the width function, z is the elevation and x is the horizontal distance to the hillslope crest. At any position along the hillslope, the relative saturation of the soil (wetness index) can be defined as: $\sigma(x) = S(x)/S_c(x)$ which varies between 0 and 1.

The resulting hillslope-storage kinematic wave model shows quite different dynamic behavior during a free drainage and a recharge experiment (*Troch et al*., 2002; *Hilberts et al*., 2004). The authors conclude that the kinematic wave assumption is limited to moderate to steep slopes, and that for more gentle slopes a new model formulation based on the Boussinesq equation would be necessary. In *Troch et al*. (2003) the hillslope-storage Boussinesq (HSB) model together with several simplified versions (e.g. a linearized version) are derived and evaluated under free drainage and recharge scenarios. *Troch et al*. (2003) reformulated the continuity and Darcy equations in terms of storage along the hillslope, which leads to the hillslope-storage Boussinesq (HSB) equation for subsurface flow in hillslopes:

$$f\frac{\partial S'}{\partial t} = \frac{k\cos\beta}{f}\frac{\partial}{\partial x'}\left[\frac{S'}{w}\left(\frac{\partial S'}{\partial x'} - \frac{S'}{w}\frac{\partial w}{\partial x'}\right)\right] + k\sin\beta\frac{\partial S'}{\partial x'} + fNw \tag{1.2}$$

where k is the hydraulic conductivity, β is the slope angle, x' is distance to the outlet measured parallel to the impermeable layer and S' is the saturated storage at a given distance x' from the divide measured perpendicular to the bedrock. In this manner, the 3D soil mantle is collapsed into a 1D storage capacity profile, and thus the governing equation is expressed in terms of hillslope storage instead of water table height. The comparison between the hillslope-storage Boussinesq and Richards' equation models for various scenarios and hillslope configurations shows that the HSB model is able to capture the general features of the storage and outflow responses of complex hillslopes (*Paniconi et al*. 2003). In order to analyze the effect of non-constant profile curvature, *Hilberts et al*., (2004) developed the HSB model for complex hillslopes (hillslopes with different plan shape and profile curvature). Therefore, by calculating the saturated storage at each time step of the simulation, hillslope stability can be investigated for dynamic hydrological conditions. For long term analysis, the linearized steady-state solution of the HSB equation (*Berne et al*., 2005) can also be used to investigate the relation between rainfall characteristics (intensity and duration), water table depth and slope stability corresponding to the growth of colluvial deposits in complex hollows.

Generally, slope stability studies are based on the calculation of the factor of safety (*FS*) considering a failure surface. Among the slope stability analysis methods, the infinite

slope stability assumption has been widely applied in many investigations (e.g. *Montgomery and Dietrich*, 1994; *Wu and Sidle*, 1995; *Van Beek*, 2002; *Borga et al*., 2002; *D'Odorico and Fagherazzi*, 2003; *Hennrich and Crozier*, 2004; *Claessens*, 2005: *Rosso et al*., 2006) because of its relative simplicity, particularly where the thickness of the soil mantle is much smaller than the length of the slope and where the failure plane is approximately parallel to the slope surface. For hillslopes it is common to define the safety factor as the ratio of the available shear strength to the minimum shear strength needed for equilibrium. Shear strength (S_n) is a combination of forces, including the slope normal component of gravity or normal stress (σ_n), pore pressure (u) within the material, which counteracts the normal stress, total cohesion of the material (c_t), and the angle of internal friction (φ) (see Figure1.1). The driving force that may cause slope failure is shear stress (T_n), the slope parallel component of gravity (W) (Figure 1.1).

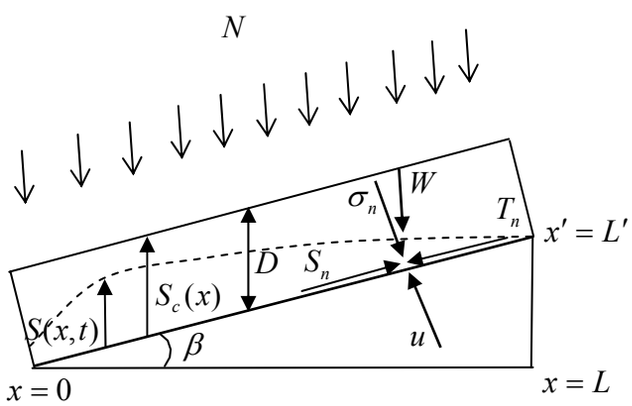

Figure 1.1: Definition sketch of cross section of a hillslope corresponding to the force diagram for translational landslides (modified from *Ritter*, 2004).

.

As we will show, all presented models in this thesis are composed of three parts: a topography model, a hydrological model and a slope stability model. By using a theoretical topography model based on the three-dimensional soil mantle (*Evans*, 1980) and *Fan and Bras's* work (1998) on collapsing the three-dimensional soil mantle into a one-dimensional profile, the stability of nine characteristic hillslope types (landform elements) with three different profile curvatures (concave, straight and convex) and three different plan shapes (convergent, parallel and divergent) has been studied. For the hydrological model, a steady-state hydrological model (based on kinematic wave hydrology) of hillslope saturated storage (*Troch et al*., 2002), applicable to a wide range of complex hillslopes, has been used. Moreover, to overcome the limitations of a kinematic wave hydrology in gentle slopes (*Hilberts et al*., 2004), the HSB model (*Troch et al*., 2003; *Hilberts et al*., 2004; *Berne et al*., 2005; *Hilberts et al*., 2007) has been used for determining shallow subsurface flow and water table depth for transient conditions.

Finally, by incorporating the relative saturated storage (σ, the ratio between actual storage and storage capacity) in the safety factor formulation, the average shallow landslide safety factor for complex hillslopes can be presented as follows:

$$\overline{FS} = \frac{\int_0^L \{c_t(x) + [(1-\sigma(x))\gamma_m(x) + \sigma(x)\gamma_b]D(x)\cos^2\beta(x)\tan\phi\}dx}{\int_0^L [(1-\sigma(x))\gamma_m(x) + \sigma(x)\gamma_s]D(x)\sin\beta(x)\cos\beta(x)dx} \quad (1.3)$$

where γ_m, γ_s and γ_b are respectively the moist, saturated and buoyant bulk density. Equation 1.3 illustrates how with varying the topographic characteristics and hydrological processes, slope stability changes in complex hillslopes.

To compare the stability of hillslopes with non-constant soil depth (deep landsliding) and different geometric characteristics and to find the critical slip surface in these hillslopes a more complex approach of slope stability analysis (*Janbu*, 1954; *Bishop*, 1955) has also been incorporated in the kinematic wave hydrology model based on relative saturated storage. Moreover, a linearized version of the HSB model (*Berne et al*., 2005) has been combined with the infinite slope method to analyze the stability of complex hollows corresponding to the long-term evolution of colluvial deposits through a probabilistic soil mass balance.

The advantages of the models presented in this thesis can be summarized as: (i) they operate at the hillslope scale and allow to more realistically simulate the space-time evolution of saturated storage; (ii) they are easy to connect to more complex slope stability methods (e. g. Bishop and Janbu methods) to find the critical slip surface in complex hillslopes; (iii) they mimic the three-dimensional behavior of saturated storage and subsurface flow well compared to the 3D Richards equation; (iv) they can form the basis of a simple yet effective landscape scale model of slope stability (especially for complex hillslopes); and finally (v) the presented models in this research help to understand theoretically how geometric characteristics and hydrological processes affect slope stability in complex hillslopes and hollows.

1.4. Thesis outline

Besides this introduction (**Chapter 1**), which sketches the outline of the work, this thesis contains five chapters with different aspects covering the main objective and research themes mentioned in the previous paragraph. These chapters (2-5) are based on and structured as scientific papers published in or submitted to peer reviewed journals (introduction, methodology, results, discussion, conclusions). **Chapter 2** presents a steady-state analytical slope stability model for complex hillslopes. We apply our analytical model to investigate the stability of nine different hillslope types with a constant length scale by a hydrology index (relative saturated storage). In **Chapter 3**, the analytical model (presented in Chapter 2) has been applied to investigate the effect of neglecting the unsaturated storage on slope stability. This model is applied also to hillslopes with non-constant soil depth to compare the stability of different hillslopes and to find the critical slip surface in hillslopes

with different geometric characteristics. In **Chapter 4**, a low-dimensional dynamic slope stability model, coupling the HSB model (*Troch et al*., 2003; *Hilberts et al*., 2004) and the infinite slope stability model for complex hillslopes (*Talebi et al*., 2007a), is presented. This model is applied to investigate the relation between rainfall, soil moisture storage, subsurface flow and slope stability in complex hillslopes. With respect to the relation between rainfall occurrence and slope instability, in **Chapter 5** a probabilistic model of rainfall-induced shallow landslides in complex hollows is presented to investigate the relation between return period of rainfall, deposit thickness and landslide occurrence. This model is based on an infinite-slope stability analysis for complex hollows, a more realistic description of hollow hydrology based on the linearized HSB model (*Berne et al*., 2005), a statistical model relating intensity, duration, and frequency of extreme precipitation, and a probabilistic soil mass balance (*D'Odorico and Fagherazzi*, 2003). Therefore, this model helps to theoretically investigate the relationship between return period of rainfall and landslide occurrence related to soil production (deposit thickness) in complex hollows. Finally, **Chapter 6** summarizes the findings of this thesis and provides some recommendations for future research.

Chapter 2

A steady-state analytical slope stability model for complex hillslopes

This chapter is based on the published paper **Talebi, A., P. A. Troch and R. Uijlenhoet (2007)**, A steady-state analytical slope stability model for complex hillslopes, *Hydrological Processes*, *21*, doi:10.1002/hyp.6881.

2. A steady-state analytical slope stability model for complex hillslopes

Abstract

This paper presents a steady-state analytical hillslope stability model to study the role of topography on rain-induced shallow landslides. We combine a bivariate continuous function of the topographic surface, a steady-state hydrological model of hillslope saturated storage, and the infinite slope stability assumption to investigate the interplay between terrain characteristics, saturated storage within hillslopes and soil mechanics. We demonstrate the model by examining the stability of nine characteristic hillslope types (landform elements) with three different profile curvatures (concave, straight and convex) and three different plan shapes (convergent, parallel and divergent). For each hillslope type, the steady-state saturated storage corresponding to given recharge rates is computed for three different average bedrock slope angles. Based on the infinite slope stability method, the factor of safety (*FS*) along the hillslopes is determined. Our results demonstrate that in the steep slopes, the least stable situation occurs in hillslopes with convergent plan shapes and concave length profiles, while the convex ones are more stable. In addition to testing our method for nine characteristic hillslope types, a general relationship between plan shape and profile curvature of landform elements and the factor of safety is derived for a predefined hillslope length scale. Our results show that slope stability increases when profile curvature changes from concave to convex. In terms of plan shapes, changing from convergent to divergent, slope stability increases for all length profiles. However, we find that the effect of plan shape is more pronounced for convex length profiles. Overall, we demonstrate that, in addition to bedrock slope, hillslope shape as represented by plan shape and profile curvature is an important control on hillslope stability.

Keywords: slope stability, hillslope hydrology, kinematic wave.

2.1. Introduction

In general, triggering of shallow landslides is controlled by the strength of the soil and the geometry of a slope, although other factors like soil depth (*Iida*, 1999) and storm properties (*D'Odorico et al*., 2005) also play an important role in the mechanism of landslide triggering. For shallow translational landsliding, topography, particularly slope angle and convergence, plays an important role in controlling stability (*Hennrich and Crozier*, 2004). Field studies and numerical simulation have shown that bedrock profile curvature and hillslope plan shape are the most significant controls on subsurface flow and saturation (*Troch et al.*, 2003). Since subsurface flow processes are strongly affecting slope stability, the occurrence of landslides is thus controlled twofold by topography (*Hennrich and Crozier*, 2004). *Montgomery and Dietrich* (1994) and *Borga et al*. (2002) have shown that shallow landslides are strongly controlled by surface topography through subsurface flow convergence, increased soil saturation, and shear strength reduction. *Iida* (1999) states that slope angle, slope shape (e.g. concavity or convexity) and the soil (regolith) depth are important controlling factors of shallow landsliding.

In quantitative slope stability studies, the effect of terrain on soil pore pressure during periods of extended rainfall has been modeled in two ways: by means of topographic (wetness) indexes (e.g. *Montgomery and Dietrich*, 1994) and through detailed modeling of the 3-D flow processes and unsteady rainfall infiltration in hillslopes (e.g. *Iverson*, 2000; *Wilkinson et al*., 2002 and *D'Odorico et al*., 2005). *Montgomery and Dietrich* (1994) combined a contour-based steady-state hydrologic model with the infinite slope stability model to define slope stability classes based upon slope and specific catchment area. *Wilkinson et al*. (2002) presented a more elaborate model that couples dynamic modeling of the hydrology with Janbu's non-circular slip surface stability analysis (*Janbu*, 1954) and Bishop's circular method (*Bishop*, 1955), accounting for soil cohesion, varying root strength and vegetation weight.

The approach taken in this paper is similar to that of *Montgomery and Dietrich* (1994) in that it combines steady-state hydrologic concepts with the infinite slope stability model, but has an important difference, viz. we present an analytical expression for the computation of the factor of safety (*FS*) for the different hillslope types that constitute a landscape.

This paper describes the development of a steady-state analytical hillslope stability model. We start by modeling profile curvature and plan shape of the land surface using a bivariate continuous function proposed by *Evans* (1980). This allows to analytically derive the hillslope width function and area function. Combining the hillslope width function with an assumed soil depth function and effective porosity results in the formulation of the soil moisture storage capacity function. The space-time evolution of saturated storage along such hillslopes is modeled by means of the mass conservation equation and a kinematic form of Darcy's equation. The resulting quasi-linear wave equation can be solved analytically for given boundary and initial conditions (*Troch et al.*, 2002). The steady-state storage profile corresponding to a given recharge rate forms the basis for the slope stability analysis. The

infinite slope stability model leads to an analytical expression for the factor of safety as function of position along the hillslope.

Finally, we apply our analytical model to investigate the stability of nine different hillslope types with a constant length scale. These nine characteristic hillslope types are formed by combining three profile curvatures (concave, straight, convex) with three plan shapes (convergent, parallel, divergent), and can be considered basic landform elements (*Pennock et al.*, 1987). We generalize our results by studying the relation between slope angle, profile and plan curvature, and landform stability.

2.2. Model formulation

2.2.1. Hillslope geometry

We consider only catchments with moderate to steep terrain and shallow (constant soil depth), permeable soil where subsurface storm flow is the dominant flow mechanism. To study the effect of topography on rain-induced shallow landsliding, we characterize the hillslopes of such catchments by the combined curvature in the gradient direction (profile curvature) and the direction perpendicular to the gradient (plan curvature). The profile curvature is important because it controls the change of velocity of mass flowing down the slope. The plan curvature defines topographic convergence which is an important control on subsurface flow concentration.

One can approximate a certain portion of the topographic surface of a catchment by a continuous function. Here we use a specific form of the bivariate function, suggested by *Evans* (1980), to describe the hillslope shape:

$$z(x,y) = E + H(1 - x/L)^n + \omega y^2 \tag{2.1}$$

where z is elevation, x is horizontal distance measured in the downstream length direction of the surface, y is horizontal distance from the slope centre in the direction perpendicular to the length direction (the width direction), E is the minimum elevation of the surface above an arbitrary datum, H is the maximum elevation difference defined by the surface, L is the total length of the surface, n is a profile curvature parameter, and ω is a plan shape parameter. Allowing profile curvature (defined by n) to assume values less than, equal to, or greater than 1 and plan curvature (defined by ω) to assume either a positive, zero, or negative value, one can define nine basic geometric relief forms. Figure 2.1 illustrates the three-dimensional view of a convergent hillslope on top of a convex bedrock profile explaining the symbols w, h, d and H used in this study.

The contour lines of the surface defined by Equation 2.1 can be obtained from the condition that z is constant, i.e.:

$$dz = \frac{\partial z}{\partial x}dx + \frac{\partial z}{\partial y}dy = 0 \Leftrightarrow \frac{dy}{dx} = -\frac{\partial z/\partial x}{\partial z/\partial y} = \frac{n\dfrac{H}{L}\left(1 - \dfrac{x}{L}\right)^{n-1}}{2\omega y} \tag{2.2}$$

Because the streamlines are perpendicular to the contour lines, the following differential equation defines the streamlines on this surface:

$$\frac{dy}{dx} = \frac{\partial z / \partial y}{\partial z / \partial x} = -\frac{2\omega y}{n\frac{H}{L}\left(1-\frac{x}{L}\right)^{n-1}} \tag{2.3}$$

which has as general solution:

$$\ln y = \frac{2\omega L^2}{n(2-n)H}\left(1-\frac{x}{L}\right)^{2-n} + C \tag{2.4}$$

where C is an integration constant. A specific value of C can be found by selecting a point on the surface which then defines the streamline passing through that point. Equation 2.4 describes all streamlines generated by Equation 2.1 and allows us to derive the shape of a hillslope (a stream tube) in the length direction. Figure 2.2 shows the location of the slope divides (streamlines) as well as some contour lines, generated by specific geometric relief forms, each belonging to a different basic type (for parameter values see Table 2.1).

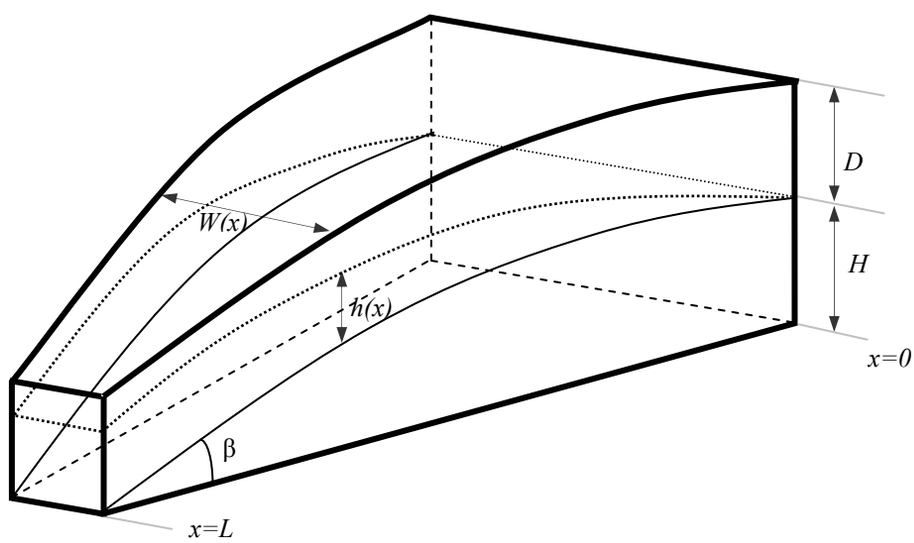

Figure 2.1: Three-dimensional view of a convergent hillslope on top of a convex bedrock profile.

Due to symmetry about the y=0 axis, the width of the hillslope measured in the y direction is given by:

$$w(x) = c_w \exp\left\{c_s\left(1-\frac{x}{L}\right)^{2-n}\right\} \tag{2.5}$$

and

$$c_s = \frac{2\omega L^2}{n(2-n)H} \tag{2.6}$$

where $c_w = 2\exp(C)$ defines the width of the hillslope at the outlet $(x = L)$ and c_s defines the degree of topographic convergence. The hillslope drainage area A at a distance x is:

$$A(x) = \int_0^x w(u)du \tag{2.7}$$

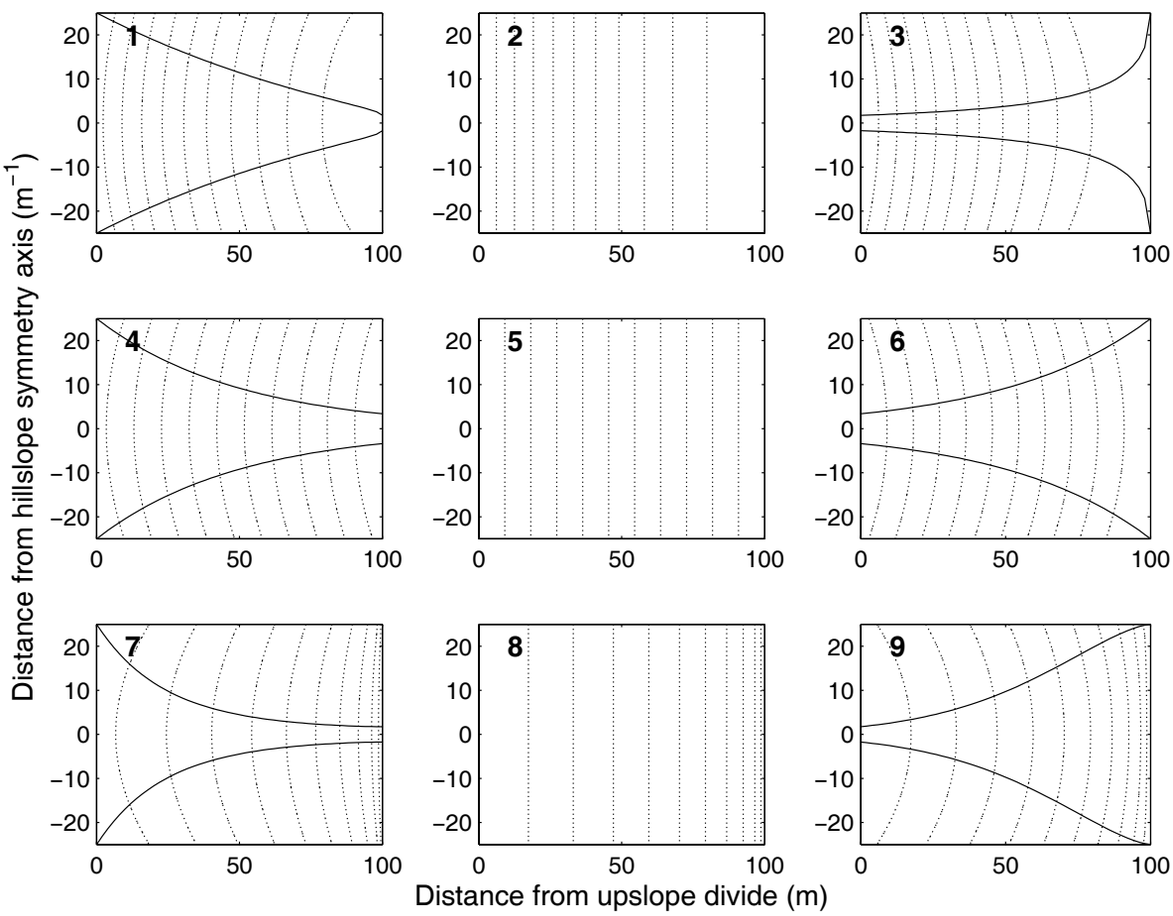

Figure 2.2: Plan view of the drainage divides (solid lines) and contour lines (dashed lines) for the nine basic hillslope types of Table 1. The upslope divide of each hillslope is at x=0, so the flow direction is from right to left. The hillslope length is 100 m and the average bedrock slope angle is $\beta = 20^{\circ}$. Hence, H (the maximum elevation difference) is equal to 36.40 m.

Table 2.1: Geometrical parameters for the nine characteristic hillslopes.

Hillslope Nr.	Profile Curvature	Plan Shape	n [-]	ω [10^{-3} m^{-1}]			Area* [m^2]
				$\beta/\phi = 0.5$	$\beta/\phi = 0.75$	$\beta/\phi = 0.9$	
1	concave	convergent	1.5	+3.6	+5.8	+7.3	2441
2	concave	parallel	1.5		0		5000
3	concave	divergent	1.5	-3.6	-5.8	-7.3	1049
4	straight	convergent	1	+3.6	+5.8	+7.3	2162
5	straight	parallel	1		0		5000
6	straight	divergent	1	-3.6	-5.8	-7.3	2162
7	convex	convergent	0.5	+3.6	+5.8	+7.3	1402
8	convex	parallel	0.5		0		5000
9	convex	divergent	0.5	-3.6	-5.8	-7.3	2268

* This is the area surrounded by two stream lines acting as drainage divides (assuming a maximum width of 50 m), x=0 and x=100 m.

2.2.2. Hillslope hydrology

Subsurface flow processes are influenced by plan and profile curvatures and the hydraulic properties of the porous medium. The mathematical description of these flow processes results in the formulation of the 3D Richards equation which is difficult to solve numerically. One way to overcome this problem is to reduce the dimensionality by introducing the subsurface storage capacity function, S_c (*Fan and Bras*, 1998):

$$S_c(x) = w(x)D(x)f \tag{2.8}$$

where $D(x)$ is the (width-averaged) soil depth at distance x and f is the specific yield or effective porosity (also sometimes referred to as drainable porosity). Equation 2.8 defines the thickness of the pore space along the hillslope and accounts for plan shape, through the width function, and bedrock profile curvature, through the soil depth function. If $d(x)$ is constant (as will be assumed in this paper), the bedrock follows the surface defined by Equation 2.1. $S(x,t)$ represents the saturated storage at a given distance x from the divide and at time t:

$$S(x,t) = w(x)h(x,t)f \tag{2.9}$$

where $h(x,t)$ is the (width-averaged) saturated depth, measured vertical from the bedrock up.

Subsurface flow rate Q is related to the storage S through Darcy's equation. In steep terrain, gravitational forces dominate pressure forces and a kinematic form of Darcy's equation becomes a reasonable simplification of the mathematical description of the flow process (e.g. *Fan and Bras*, 1998; *Hilberts et al.*, 2004; *Rezzoug et al.*, 2005):

$$Q = -K_s \frac{S}{f}\frac{\partial z}{\partial x} \tag{2.10}$$

where K_s is saturated hydraulic conductivity of the soil. Combining Equation 2.10 with the continuity equation

$$\frac{\partial S}{\partial t} + \frac{\partial Q}{\partial x} = N(t)w(x) \tag{2.11}$$

and assuming no spatial variability in K_s and f, one obtains a quasi-linear wave equation in terms of saturated storage that can be solved analytically with the method of characteristics (*Troch et al.*, 2002). N in Equation 2.11 is the recharge to the saturated storage and is defined as a vertical flux. For shallow permeable soils during heavy rainfall the recharge rate will be close to the rainfall intensity.

Given the hydrological conditions in steep terrain, it is reasonable to assume the following initial and boundary conditions:

$$\begin{cases} S(x,0) = g(x), & 0 \le x \le L \\ S(0,t) = 0, & \forall t \end{cases} \tag{2.12}$$

where $g(x)$ is the initial saturated storage along the hillslope. When N is considered to be a constant recharge rate the steady-state subsurface flow rate $Q(x) = NA(x)$ (from Equations 2.11 and 2.7 and the corresponding storage profile is given by (from Equations 2.10 and 2.1)):

$$S(x) = \frac{fL}{nK_sH}\left(1 - \frac{x}{L}\right)^{1-n} NA(x) \tag{2.13}$$

At any position along the hillslope the steady-state relative saturation of the soil is now given by:

$$\sigma(x) = \frac{S(x)}{S_c(x)} = a(x)\frac{N}{T}\frac{1}{|\partial z / \partial x|} \tag{2.14}$$

where $T = K_s D$ is soil transmissivity and $a(x) = A(x)/w(x)$ is drainage area per unit hillslope width. The variable σ describes the steady-state wetness of the soil and is similar to the wetness index W derived by *Montgomery and Dietrich* (1994).

2.2.3. Hillslope stability

Slope stability studies are based on the calculation of the factor of safety (*FS*) considering a failure surface. For hillslopes it is common to define the safety factor as the ratio of the available shear strength to the minimum shear strength needed for equilibrium. The infinite slope stability hypothesis has been widely applied in many investigations of natural slope stability (e.g. *Montgomery and Dietrich*, 1994; *Wu and Sidle*, 1995; *Van Beek*, 2002; *Borga et al.*, 2002; *D'Odorico and Fagherazzi*, 2003; *Zaitchik et al.*, 2003; *Hennrich and Crozier*, 2004; *Claessens*, 2005) because of its relative simplicity, particularly where the thickness of the soil mantle is much smaller than the length of the slope and where the failure plane is approximately parallel to the slope surface. The infinite slope model imposes the condition that the groundwater flow is parallel to the slope surface. Because of the geometry of an infinite slope, overall stability can be determined by analyzing the stability of a single, vertical element in the slope. Under these assumptions and with stability expressed by the factor of safety, *FS*, the infinite slope stability equation is given by (*Wu and Sidle*, 1995; *Van Beek,* 2002):

$$FS(x) = \frac{c_t + [(D - h(x))\gamma_m + h(x)\gamma_b]\cos^2\beta\tan\phi}{[(D - h(x))\gamma_m + h(x)\gamma_s]\sin\beta\cos\beta} \tag{2.15}$$

where c_t is the total soil cohesion, ϕ is the angle of internal friction, D is the depth to the shear plane, β is the local slope angle, h is the water level above this plane, and γ_m, γ_s and γ_b, are respectively the moist, saturated and buoyant bulk specific weights.

Applying Equation 2.15 together with the solution for $\sigma(x)$ (Equation 2.14), we can compute the shallow landslide safety factor for cohesionless soils as follows:

$$FS(x) = \frac{[(1 - \sigma(x))\rho_m + \sigma(x)\rho_b]\tan\phi}{[(1 - \sigma(x))\rho_m + \sigma(x)\rho_s]\tan\beta} \tag{2.16}$$

where $FS(x)$ is the factor of safety at location x along the hillslope, ρ_m is the moist soil density, ρ_s is the saturated soil density and ρ_b is the buoyant density defined as $\rho_b = \rho_s - \rho_w$, where ρ_w is density of water. If one assumes that the soil density above and below the water table is the same and equal to ρ_s, then Equation 2.16 can be written as:

$$FS = \left[1 - \sigma(x)\left(\frac{\rho_w}{\rho_s}\right)\right]\frac{\tan\phi}{\tan\beta} \tag{2.17}$$

Again, Equation 2.17 is the basic equation used by *Montgomery and Dietrich* (1994) to study shallow landslides. It should be noted that Equation 2.17 defines the factor of safety at a given location along the hillslope where soil depth and slope angle are constant. In order to derive the $\overline{FS}$ for the entire hillslope given a steady-state rainfall input, the following expression is proposed:

$$\overline{FS} = \frac{\int_0^L \left[1 - \sigma(x)\left(\frac{\rho_w}{\rho_s}\right)\right] \cos^2 \beta(x) dx \tan\phi}{\int_0^L \sin\beta(x)\cos\beta(x) dx} \tag{2.18}$$

2.2.4. Analytical solution for straight hillslopes

If β is constant along the hillslope, Equation 2.18 reduces to:

$$\overline{FS} = \left[1 - \overline{\sigma}\left(\frac{\rho_w}{\rho_s}\right)\right] \frac{\tan\phi}{\tan\beta} \tag{2.19}$$

where $\overline{\sigma}$ is the average relative saturation along the hillslope. Note that Equation 2.19 is simply the average of Equation 2.17. The assumption of a constant β is equivalent to taking $n = 1$ in Equation 2.1. In that case it is possible to obtain an analytical solution to Equation 2.19. If $n = 1$ (straight hillslopes) the width function (Equation 2.5) reduces to:

$$w(x) = w_0 \exp\left(-\frac{2\omega L}{H} x\right) \tag{2.20}$$

where w_0 is the hillslope width at the upstream divide $(x = 0)$. Note that Equation 2.20 is the exponential width function, which has been employed previously in hillslope hydrology (*Troch et al.*, 2003; *Berne et al.*, 2005). As a consequence the hillslope drainage area upstream of *x* becomes:

$$A(x) = \frac{w_0 H}{2\omega L}\left[1 - \exp\left(-\frac{2\omega L}{H} x\right)\right] \tag{2.21}$$

Recall that in the steady-state the subsurface flow rate at location *x* is simply $Q(x) = NA(x)$. Therefore, the saturated storage profile for straight hillslopes (where $\partial z / \partial x = -H / L$) can be calculated as:

$$S(x) = \frac{fNw_0}{2\omega K_s}\left[1 - \exp\left(-\frac{2\omega L}{H} x\right)\right] \tag{2.22}$$

Dividing by the subsurface storage capacity function $(S_c(x) = w(x)df)$ leads to the following steady-state relative soil saturation profile:

$$\sigma(x) = \frac{N}{2\omega K_s D}\left[\exp\left(\frac{2\omega L}{H} x\right) - 1\right] \tag{2.23}$$

Note that this reduces to a triangular profile ($\sigma(x) = NLx/(K_s DH)$) in the limit where ω approaches 0 (parallel hillslopes). Finally, taking the average of Equation 2.23 between $x = 0$ and $x = L$ yields:

$$\overline{\sigma} = \frac{N}{2\omega K_s D}\left\{\frac{H}{2\omega L^2}\left[\exp\left(\frac{2\omega L^2}{H}\right)-1\right]-1\right\} \tag{2.24}$$

which reduces to $\overline{\sigma} = NL^2/(2K_s DH)$ for parallel hillslopes ($\omega = 0$). Substitution of Equation 2.24 in Equation 2.19 gives the desired analytical solution for the hillslope factor of safety ($\overline{FS}$).

2.3. Stability of basic hillslope types

To study the effect of plan shape and profile curvature of the hillslope on its stability, we apply the model to a set of nine characteristic hillslopes. The nine characteristic hillslopes consist of three plan shapes (convergent, parallel, and divergent) and three profile curvatures (concave, straight, convex). Figure 2.2 illustrates the nine basic hillslope types used in this study. The parameters used to generate them are listed in Table 2.1. The horizontal length of the nine hillslopes is chosen to be constant (L = 100 m), whereas the average slope angle will be varied in subsequent applications.

These nine hillslopes represent a wide range of landforms traditionally considered in hydrology and geomorphology (*Pennock et al.*, 1987). For different hillslopes within a catchment each individual hillslope type can be fitted using the geometrical scaling parameters H, L, and n to the observed terrain profile curvature, and a proper choice of ω to represent plan curvature (obviously, $\omega = 0$ for parallel hillslopes). In order to reduce the number of free parameters that define the topographic surface of the hillslope we take ω equal to $+(H/L^2)$ for convergent hillslopes and equal to $-(H/L^2)$ for divergent hillslopes. This has the added advantage that streamlines do not converge immediately on the surface when the average gradient approaches zero (see Equation 2.6). A maximum hillslope width of 50 m is assumed, which defines the value of c_w in Equation 2.5.

Table 2.2: Hydrological and geotechnical parameters.

Parameter group	Parameter name	Symbol	Units	Value
Hydrological	Saturated hydraulic conductivity	K_s	m s^{-1}	0.0001
	Effective porosity	f	-	0.34
	Recharge	N	mm d^{-1}	10
Geotechnical	Total soil cohesion	c_t	kN m^{-2}	0
	Effective angle of internal friction	ϕ	°	40
	Slice length	dx	m	0.5
	Saturated soil density	ρ_s	kg m^{-3}	1600
	Density of water	ρ_w	kg m^{-3}	1000

Figure 2.3 shows the relative saturated storage along these hillslopes and Table 2.2 lists the values of the hydrological variables used to generate these storage profiles. The effect of plan shape and profile curvature on saturated storage is clear from inspection of Figure 2.3. Hillslopes with convergent plan shape (1, 4 and 7) and concave profile curvature (1, 2 and 3) have the largest saturated section. This should have important consequences on slope stability, as will be discussed hereafter.

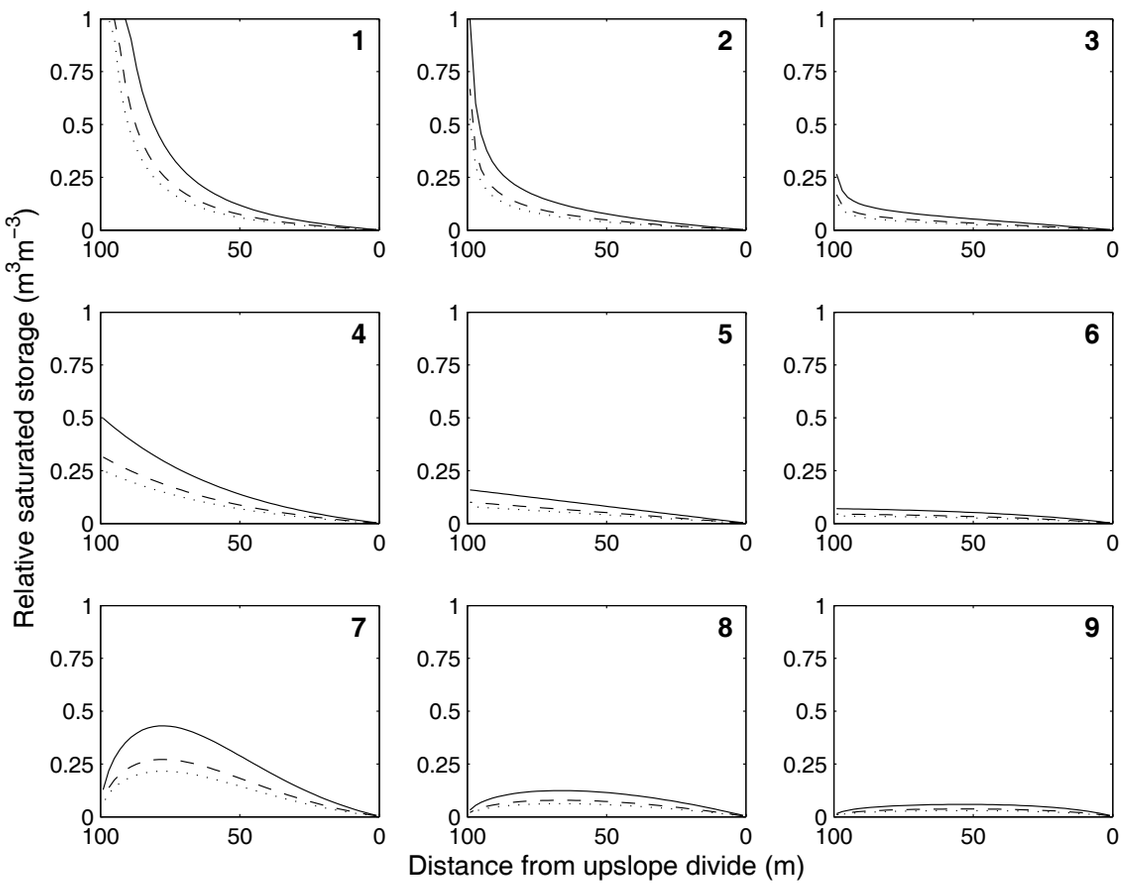

Figure 2.3: Relative saturated storage along the nine basic hillslopes of Table 2.1 for a constant recharge rate of 10 mm d^{-1} (solid line: β/ϕ=0.5; dashed line: β/ϕ=0.75; dotted line: β/ϕ=0.9). Relative storage in excess of one indicates surface saturation and overland flow regions.

Figure 2.4 reports the values of the average safety factor (Equation 2.18) for each hillslope and for three different average bedrock slope angles. For all profile curvatures, the overall slope stability increases when plan shape changes from convergent to divergent. For the parallel hillslopes (2, 5, and 8) the *FS* slightly drops when profile curvature changes from convex to concave. For the convergent hillslopes (1, 4, and 7) the same trend is observed: the *FS* increases slightly when profile curvature changes from concave to convex. In both cases, this is due to a decrease in saturated storage near the outlet when profile curvature changes from concave to convex (see Figure 2.3). For divergent hillslopes (3, 6, and 9) the *FS* stays almost the same, independent of profile curvature. This is due to the relatively small storages

in these hillslopes. In conclusion, it seems that the convergent concave hillslope (hillslope 1 in Figure 2.2) is the least stable among the nine basic hillslope types studied here and will be prone to failure as the constant rainfall rate would increase.

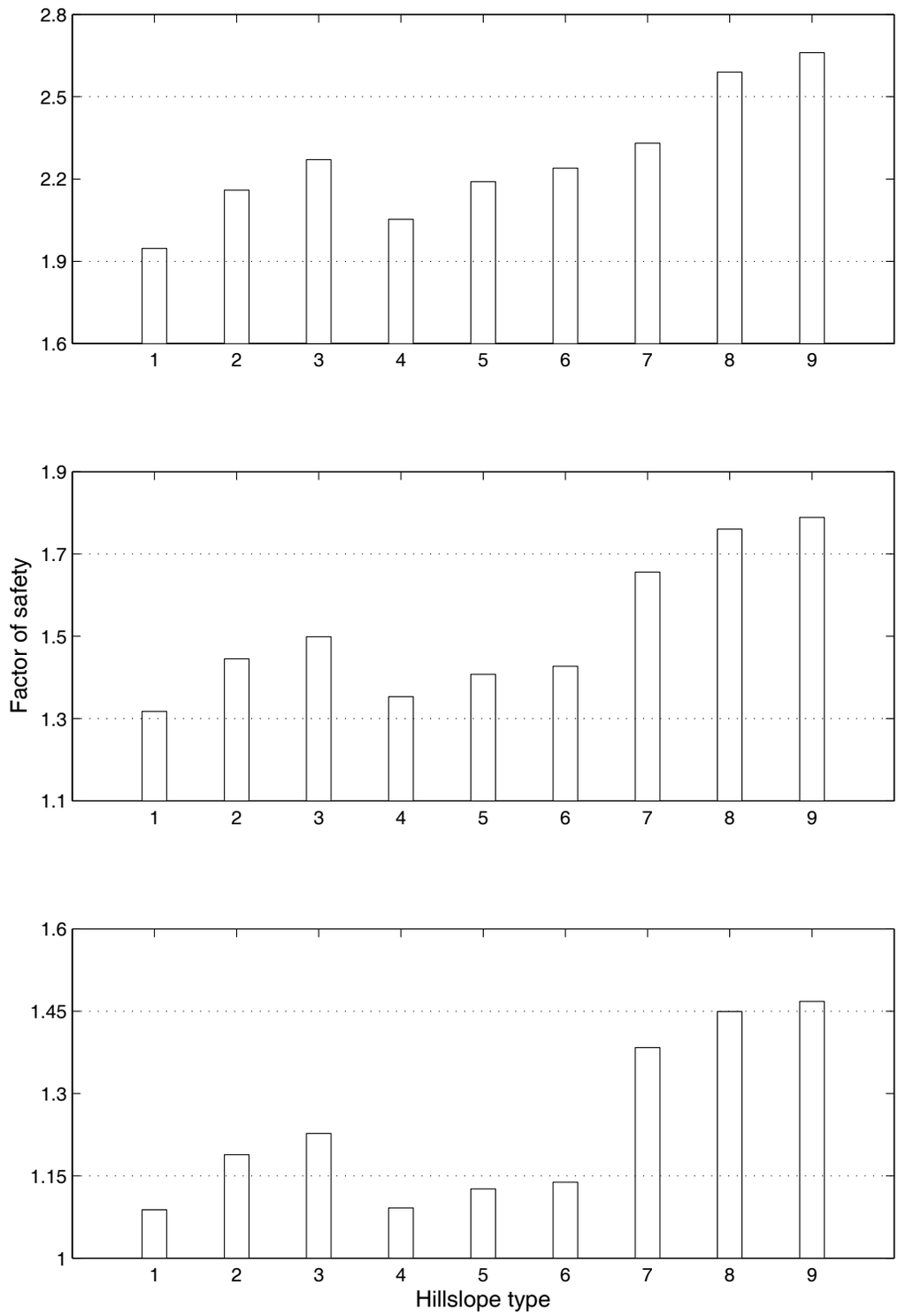

Figure 2.4: Factor of safety for the nine basic hillslopes of Table 2.1 as computed using Equation 2.18. Slope angle is equal to 20°, 30°, and 36° (β / ϕ = 0.5, 0.75, and 0.9) in the first, second and third panels, respectively.

In order to generalize these results we have computed the factor of safety for a wider range of plan shapes and profile curvatures. Figure 2.5 presents these results, where *FS* is plotted in (n,ω) space, again for three different ratio's of the average bedrock slope angle to the effective angle of internal friction (β/ϕ = 0.5, 0.75, and 0.9). For convenience the locations of the nine basic hillslopes treated above have been indicated as well. We see that the general shape of the *FS* surface does not change much with increasing bedrock slope angle, so that we can limit our discussion of the figure to the most critical case (β/ϕ = 0.9).

In general, the maximum stability is reached for small values of n, i.e. for convex hillslopes, and for negative values of ω, i.e. for divergent hillslopes. For concave bedrock profiles (n>1), stability decreases slightly when plan shape changes from divergent (ω<0) to convergent (ω>0). This is due to the increasing saturated storage near the outlet for convergent hillslopes. For strongly convex profiles (n<0.5) there is a large effect of plan shape: as plan shape changes from divergent to convergent, the *FS* drops quickly (the contour lines of the FS surface are closely aligned). As a final result, when profile curvature changes from concave to convex, stability increases. However, this effect is more pronounced when it changes from straight to convex (see Figure 2.5).

2.4. Discussion and conclusion

The approach described in this paper provides an analytical hillslope stability model for assessing the relation between slope geometry and slope stability. The model consists of a topography model, a steady-state hydrological model and the infinite slope stability assumption. The presented hydrological model takes account of the effects of topography on hillslope saturated storage through the plan shape and profile curvature. By varying these two parameters, nine basic hillslope shapes were used to compute their factor of safety (*FS*) for given hydraulic and hydrologic conditions. The proposed hillslope stability model generalizes the results from other studies (e.g. *Montgomery and Dietrich*, 1994; *Wu and Sidle*, 1995) in that slope geometry and its effect on steady-state saturated storage is explicitly taken into account in a closed (analytical) form.

We have demonstrated that these nine basic hillslopes show quite different behavior from the stability viewpoint. Based on this analysis, it is shown that in addition to average bedrock slope angle, topographic characteristics (especially profile curvature and plan shape) of the hillslope control the subsurface flow and this process affects slope stability by changing the soil strength. In particular, when the width function (plan shape) changes from convergent to divergent, hillslope stability generally increases. However, this effect is more pronounced for convex length profiles. As a result, for a given plan shape (convergent, parallel or divergent) convex hillslopes are generally more stable than either concave or straight hillslopes, particularly when the average bedrock slope angle approaches the effective angle of internal friction.

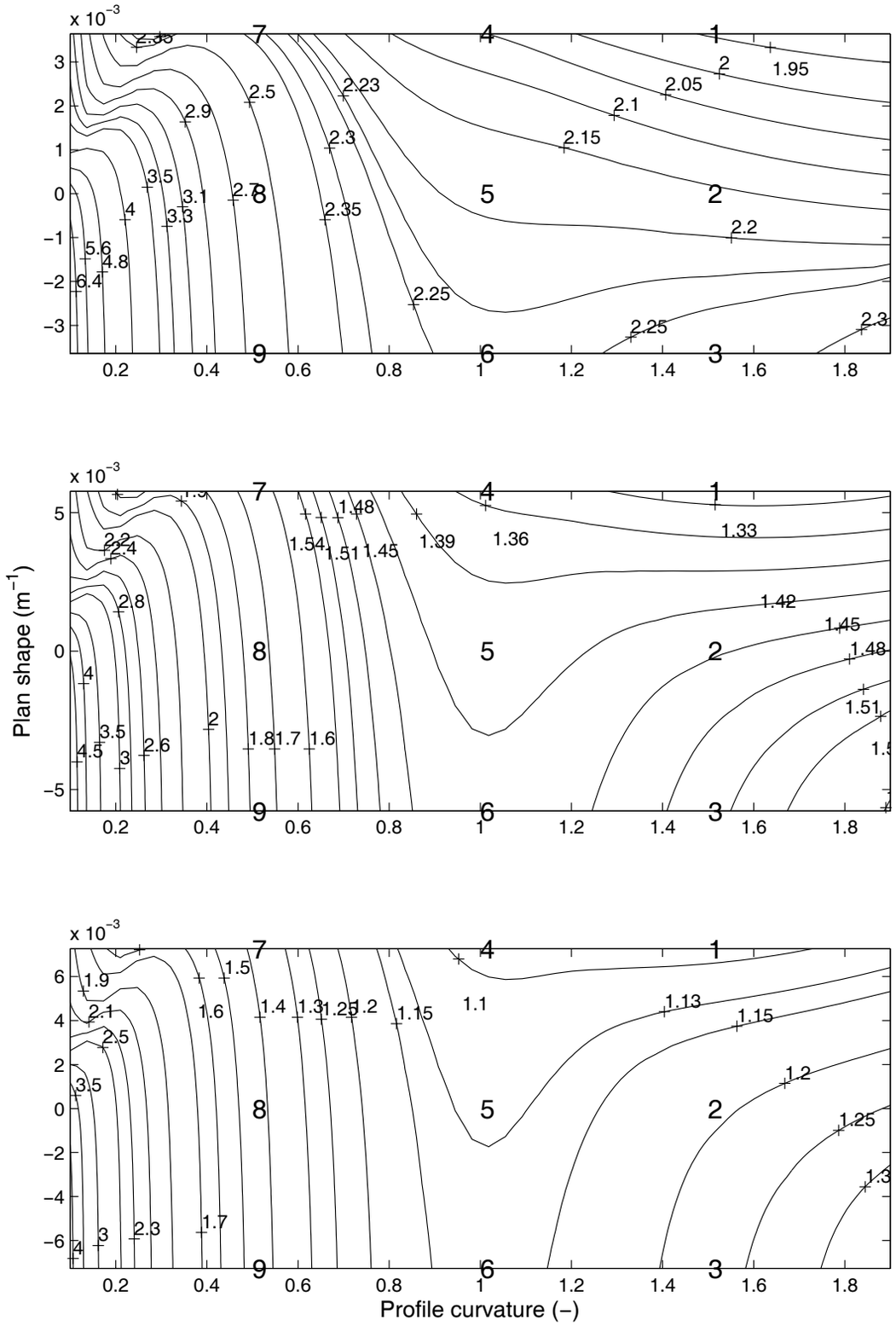

Figure 2.5: Relation between the factor of safety and profile curvature and plan shape changes for three different bedrock slope angles (β / ϕ = 0.5, 0.75, and 0.9 in the first, second and third panels, respectively). The bold numbers correspond to the nine basic hillslope types of Table 2.1 and Figure 2.4.

Several assumptions have been made to derive the relationships in this approach. Although the assumptions incorporated in the model limits its use, the model can determine relative stability in different hillslopes with different profile curvature and plan shape. The first assumption is the use of the kinematic wave approximation for subsurface flow. The advantages of the kinematic wave approximation are, first, that analytical solutions exist, and second, that the model accounts explicitly for the profile curvature and plan shape (*Troch et al.*, 2002). The main disadvantage of the kinematic wave approximation is that it does not account for diffuse drainage, hence the model is not applicable for gently to moderately sloping terrains. It should be noted that the key element for initiation of shallow landslides is the average bedrock slope angle, such that instability takes place only in steep sloping terrain. Therefore this assumption is not expected to have a large influence on the slope stability analysis.

Another assumption is that soil density above and below the water table is the same in the steady-state condition. Future research will attempt to relax this assumption by combining the saturated storage hydrological model with a steady-state unsaturated storage hydrological model. This will allow us to derive soil moisture profiles defined by the constant rainfall rate and the lower boundary condition (i.e. the groundwater level) from which the unsaturated soil density can be computed.

The steady-state hydrologic model requires the assumption that the predicted spatial pattern of critical steady-state rainfall represents that which occurs during an unsteady, landslide producing rainfall event (*Claessens*, 2005). In general, the notion of critical rainfall should only be considered as a relative measure of failure potential (*Borga et al.*, 2002). For the model presented in this paper, soil properties (hydraulic conductivity, soil depth and drainable porosity) are considered to be spatially uniform over the hillslope domain and constant in time.

It is important to recognize that all forces in the infinite slope analysis are assumed to vary only in the direction normal to the ground surface. The mathematical simplicity that results from this assumption makes the infinite slope analysis well-suited for drawing conclusions about the effects of ground water flow on slope stability (*Borga et al.*, 2002). The performance of the infinite slope hypothesis adopted here with respect to alternative approaches to estimate slope stability (such as the Bishop and Janbu methods) is the subject of ongoing investigations. The presented model proves to be an efficient tool for evaluating slope stability in hillslopes with different geometrical characteristics. One of its limitations lies in the steady-state hydrology. More research is needed to account for a dynamic slope stability model.

Chapter 3

Soil moisture storage and hillslope stability

This chapter is based on the published paper **Talebi, A., R. Uijlenhoet and P. A. Troch (2007),** Soil moisture storage and hillslope stability, *Natural Hazards and Earth System Sciences, 7*, 523-534.

3. Soil moisture storage and hillslope stability

Abstract

Recently, we presented a steady-state analytical hillslope stability model to study rain-induced shallow landslides. This model is based on kinematic wave dynamics of saturated subsurface storage and the infinite slope stability assumption. Here we apply the model to investigate the effect of neglecting the unsaturated storage on the assessment of slope stability in the steady-state hydrology. For that purpose we extend the hydrological model to compute the soil pore pressure distribution over the entire flow domain. We also apply this model for hillslopes with non-constant soil depth to compare the stability of different hillslopes and to find the critical slip surface in hillslopes with different geometric characteristics. In order to do this, we incorporate more complex approaches to compute slope stability (Janbu's non-circular method and Bishop's simplified method) in the steady-state analytical hillslope stability model. We compare the safety factor (*FS*) derived from the infinite slope stability method and the more complex approach for two cases: with and without the soil moisture profile in the unsaturated zone. We apply this extended hillslope stability model to nine characteristic hillslope types with three different profile curvatures (concave, straight, convex) and three different plan shapes (convergent, parallel, divergent). Overall, we find that unsaturated zone storage does not play a critical role in determining the factor of safety for shallow and deep landslides. As a result, the effect of the unsaturated zone storage on slope stability can be neglected in the steady-state hydrology and one can assume the same bulk specific weight below and above the water table. We find that steep slopes with concave profile and convergent plan shape have the least stability. We also demonstrate that in hillslopes with non-constant soil depth (possible deep landslides), the ones with convex profiles and convergent plan shapes have slip surfaces with the minimum safety factor near the outlet region. In general, when plan shape changes from divergent to convergent, stability decreases for all length profiles. Finally, we show that the applied slope stability methods and steady-state hydrology model based on the relative saturated storage can be used safely to investigate the relation between hillslope geometry and hillslope stability.

Keywords: soil moisture, hillslope stability, hillslope hydrology.

3.1. Introduction

Slope instability in steep mountainous terrain is a major problem to land managers worldwide. One of the types of hillslope instability occurs in the form of shallow landslides. Shallow landslides are one of the most common types of landslides in steep, soil-mantled landscapes in different climate zones. Recently, theoretical models have been developed to predict how landslide susceptibility depends on topographic and hydrologic variables (e.g. *Sidle*, 1992; *Montgomery and Dietrich*, 1994; *Wu and Sidle*, 1995; *Borga et al.*, 2002; *Van Beek*, 2002; *Claessens*, 2005). In all of these models, topography has been introduced as a factor affecting slope stability. The effect of terrain on soil pore pressure during periods of extended rainfall has been modeled in two ways: by means of topographic (wetness) indices (e.g. *Montgomery and Dietrich*, 1994; *Claessens*, 2005; *Rosso et al.*, 2006) and through detailed modeling of the 3-D flow processes along hillslopes (e.g. *Cai et al.*, 1998; *Wilkinson et al.*, 2000). *Montgomery and Dietrich* (1994) presented a simple model for the topographic influence on shallow landslide initiation by combining a contour-based steady-state hydrologic model with the infinite slope stability model to define slope stability classes based upon slope and specific drainage area. *Montgomery et al.* (1998) developed this model further (SHALSTAB) to evaluate slope instability associated with the potential occurrence of shallow landsliding. Although several applications show this approach to be capable of capturing the spatial variability of shallow landslide hazard, it only accounts for straight hillslopes with infinite length profile, neglecting other topographic characteristics (e.g. plan shape and profile curvature, as well as variable soil depth).

Anderson and Kemp (1991) presented a combined detailed hydrology and stability model (CHASM) that allows the simulation of changes in pore water pressures in response to individual rainfall events, and consider their role in maintaining slope stability. Further developments of this model presented by *Wilkinson et al.* (2002) couples dynamic modeling of the hydrology with Janbu's non-circular slip surface stability analysis (*Janbu*, 1954), accounting for soil cohesion, slope plan topography and vegetation.

To investigate the key role of geometric characteristics of hillslopes (plan shape and profile curvature) on shallow landslides, *Talebi et al.* (2007a) presented a steady-state analytical hillslope stability model based on kinematic wave subsurface storage dynamics. Their analytical approach is similar to the method of *Montgomery and Dietrich* (1994) in that it combines steady-state hydrologic concepts with the infinite slope stability model, but has an important difference. *Talebi et al.* (2007a) presented a complete analytical expression for the computation of the factor of safety (*FS*) for finite hillslopes. Possible shortcomings of their approach, however, are that the analytical model does not include the effect of unsaturated storage on slope stability, and that it applies infinite slope stability computations to finite hillslope types. The first purpose of this study is to investigate the appropriateness of those simplifying assumptions (neglecting the unsaturated zone storage and the infinite slope stability approach) for the accurate determination of the factor of safety for shallow landslides. Therefore, in this paper, the infinite slope stability method is replaced by a more complex approach (Janbu's non-circular method and Bishop's simplified method) to compute

the stability and the critical slip surface in hillslopes with different geometric characteristics and different soil depth (to allow for possible deep landslides). The latter approach is similar to *Wilkinson et al.* (2002) but it considers unsaturated zone storage by computing vertical soil moisture profiles from steady-state solutions to Richards' equation (*Rockhold et al.*, 1997).

Section 3.2 briefly summarizes the development of the steady-state analytical hillslope stability model (*Talebi et al.*, 2007a). This model computes the space-time evolution of saturated storage along hillslopes by means of the mass conservation equation and a kinematic form of Darcy's equation (*Troch et al.*, 2002). The steady-state storage profile corresponding to a given recharge rate forms the basis for the slope stability analysis. The infinite slope stability model leads to an analytical expression for the factor of safety as a function of position along the hillslope.

In section 3.3 we present an extension to the hydrological component of this model that accounts for unsaturated zone storage based on steady-state solutions to the 1D Richards' equation (*Rockhold et al.*, 1997). With respect to the influence of soil suction on soil cohesion (*Fredlund*, 1978), we also investigate the effect of the unsaturated zone storage on soil cohesion and thus slope stability. Therefore, the safety factor will be calculated with and without considering the soil moisture profiles in the unsaturated zone.

As soil depth usually is not constant and failures are often non-parallel to the bedrock (due to hydrological and geological discontinuities within the hillslope profile), the infinite slope stability assumption needs to be relaxed. In Section 3.4 we further extend the model to compute the factor of safety by using Bishop's circular method and Janbu's non-circular method. Bishop's method assumes zero interslice shear forces, satisfies moment equilibrium around the center of the circular failure surface and satisfies vertical force equilibrium. The Janbu method assumes that failure occurs through sliding of a block of soil on a non-circular slip surface. In this paper, we use Bishop's method to find the critical slip surface and Janbu's method to compare the stability of hillslopes with a common slip surface.

Section 3.5 explains the main results of the paper and describes the application of the analytical model and the more complex approach to investigate the stability of nine different hillslope types with a constant length scale. We generalize our results by studying the relation between slope angle, profile and plan curvature, and landform stability (with and without the effect of unsaturated zone storage). Hillslope stability is studied for two cases (constant and non-constant soil depth). The focus of this paper lies in a comparison of the two cases of slope stability analysis to determine the role of hillslope geometry (profile curvature and plan shape) on hillslope stability with and without considering the unsaturated zone storage. The first case is based on infinite slope assumption (constant soil depth) and the second one is based on Janbu's non-circular method (*Janbu*, 1954) and Bishop's simplified (*Bishop*, 1955) method (non-constant soil depth). Finally, Section 3.6 summarizes the main results of the paper.

3.2. Steady-state analytical hillslope stability model

Here we summarize the main features of the hillslope stability model recently developed by *Talebi et al.* (2007a). This model applies to catchments with moderate to steep

terrain and shallow, permeable soils where subsurface storm flow is the dominant flow mechanism. To study the effect of topography on rain-induced shallow landsliding, the hillslopes of such catchments are characterized by the combined curvature in the gradient direction (profile curvature) and the direction perpendicular to the gradient (contour or plan curvature). The profile curvature is important because it controls the change of velocity of mass flowing down the slope and the plan curvature defines topographic convergence which is an important control on subsurface flow concentration (*Troch et al.*, 2002). Other investigations (e.g. *Montgomery and Dietrich*, 1994; *Borga et al.*, 2002; *Hennrich and Crozier*, 2004) have also shown that shallow landslides are strongly controlled by subsurface flow convergence. The surface of an individual hillslope is represented by the following bivariate function (*Evans*, 1980):

$$z(x, y) = E + H(1 - x / L)^n + \omega y^2 \tag{3.1}$$

where z is the elevation, x is the horizontal distance measured in the downstream length direction of the surface, y is the horizontal distance from the slope centre in the direction perpendicular to the length direction (the width direction), E is the minimum elevation of the surface above an arbitrary datum, H is the maximum elevation difference defined by the surface, L is the total length of the surface, n is a profile curvature parameter, and ω is a plan curvature parameter. Allowing profile curvature (defined by n) to assume values less than, equal to, or greater than 1 and plan curvature (defined by ω) to assume either a positive, zero, or negative value, one can define different basic geometric relief forms. Subsurface flow processes are influenced by plan and profile curvatures and the hydraulic properties of the porous medium. The mathematical description of these flow processes results in the formulation of the 3D Richards equation which is difficult to solve analytically and numerically. One way to overcome this problem is to reduce the dimensionality by introducing the subsurface storage capacity function defined by the hillslope width at flow distance x, the average soil depth at that distance and the effective porosity. Assuming kinematic wave subsurface flow, *Troch et al.* (2002) derived the following analytical expression for steady-state saturated storage of the hillslope:

$$S(x) = \frac{fL}{nk_s H}\left(1 - \frac{x}{L}\right)^{1-n} NA(x) \tag{3.2}$$

where f is the drainable porosity, k_s is the saturated hydraulic conductivity, N is the (constant) recharge rate, $A(x)$ is the upstream drainage area at location x and $S(x)$ represents the saturated storage at a given distance x from the divide. Dividing by the storage capacity function, S_c one finds the relative saturated storage:

$$\sigma(x) = \frac{S(x)}{S_c(x)} \tag{3.3}$$

The variable σ describes the steady-state wetness of the soil. Note that $S_c(x) = fw(x)D(x)$ where $w(x)$ is the hillslope width function and $D(x)$ is the (width-averaged) soil depth at distance x.

Slope stability studies are based on the calculation of the factor of safety (*FS*) considering a failure surface. For hillslopes it is common to define the safety factor as the ratio of the available shear strength to the minimum shear strength needed for equilibrium. With stability expressed by the factor of safety, *FS*, the infinite slope stability equation is given by (*Wu and Sidle*, 1995; *Van Beek*, 2002):

$$FS(x) = \frac{c_t + [(D - h(x))\gamma_m + h(x)\gamma_b]\cos^2\beta\tan\phi}{[(D - h(x))\gamma_m + h(x)\gamma_s]\sin\beta\cos\beta} \tag{3.4}$$

where c_t is the total soil cohesion, ϕ is the angle of internal friction, D is the depth to the shear plane (vertical soil depth), β is the slope angle, h is the water level above this plane, and γ_m, γ_s and γ_b, are respectively the moist, saturated and buoyant bulk specific weights (the buoyant bulk specific weight is defined as $\gamma_b = \gamma_s - \gamma_w$). Applying Equation 3.4 together with the solution for $\sigma(x)$ (Equation 3.3), and by assuming the same soil density for whole soil profile (above and below the water table), *Talebi et al.* (2007a) presented the following simple equation to compute the shallow landslide safety factor for cohesionless soils:

$$\overline{FS} = \frac{\int_0^L \left[1 - \sigma(x)\left(\frac{\rho_w}{\rho_s}\right)\right]\cos^2\beta(x)dx\tan\phi}{\int_0^L \sin\beta(x)\cos\beta(x)dx} \tag{3.5}$$

where ρ_w and ρ_s are the density of water and saturated soil, respectively.

3.3. Incorporating the unsaturated zone storage

The computation of γ_m (moist bulk specific weight) and c_t (total soil cohesion) involves the assessment of the water storage in the unsaturated zone (the zone between the steady-state water table and the land surface). For steady vertical water flow in the unsaturated zone, Darcy's law gives (*Rockhold et al.*, 1997):

$$Z_T - Z_B = \int_{\psi_B}^{\psi_T} \frac{d\psi}{N / k(\psi) - 1} \tag{3.6}$$

where Z is the depth, ψ is the soil-water suction (negative pressure head), N is the steady-state recharge flux, $k(\psi)$ is the hydraulic conductivity, and subscripts T and B denote the top and bottom, respectively, of a layer with uniform, homogeneous hydraulic properties. Note that Equation 3.6 is written such that Z is positive downward and N is positive for infiltration. An exact analytical solution to Equation 3.6 was obtained by *Gardner* (1958) using the exponential $k(\psi)$ function:

$$k(\psi) = k_s \exp(-\alpha\psi) \tag{3.7}$$

where k_s is the saturated hydraulic conductivity and α is a parameter. The resulting analytical solution to Equation 3.6 is:

$$Z_T - Z_B = \psi_T - \psi_B + \frac{1}{\alpha}\ln\left[\frac{\lambda\, e^{\psi_B \alpha} - 1}{\lambda\, e^{\psi_T \alpha} - 1}\right] \tag{3.8}$$

where ψ_T and ψ_B are the soil-water suction head at the top and bottom of each layer respectively and $\lambda = N / k_s$. From Equation 3.8 and the soil water retention characteristic, the soil moisture (θ) profile can be determined. Here we use the van Genuchten equation (*van Genuchten*, 1980):

$$\theta(\psi) = \theta_r + (\theta_s - \theta_r)[1 + (\alpha_v \psi)^{n_v}]^{-m_v} \tag{3.9}$$

to model the soil water retention characteristic. The parameters α_v and n_v are empirical constants that affect the shape of the function and $m_v = 1\text{-}1/n_v$. The parameters θ_r and θ_s are the residual and saturated water content, respectively. Combining Equations 3.8 and 3.9 allows the computation of the soil moisture profile in the unsaturated zone. We are now able to derive the average soil moisture content in the unsaturated zone, which allows computing the moist bulk specific weight (γ_m) at each position along the hillslope.

With respect to the influence of soil suction on the slope stability, *Fredlund* (1978) proposed a linear shear strength equation for an unsaturated soil. According to this model, the total cohesion of the soil can be calculated as:

$$c_t = c_e + (u_a - u_v)\tan\phi^b \tag{3.10}$$

where c_e is the effective cohesion of saturated soil, $(u_a - u_v)$ is the matric suction of the soil on the plane of failure where u_a and u_v (kPa) are the pressures of pore air and pore water, respectively. In other words, $(u_a - u_v)$ equals the soil water suction expressed in kPa. For slope stability analysis, the pore air pressure is assumed to be atmospheric and constant. ϕ^b is the angle of shearing resistance with respect to matric suction (degrees). It has been demonstrated (e.g. *Gan et al.*, 1988; *Oeberg and Sallfors*, 1997) that ϕ^b is a nonlinear function of matric suction, however, it is difficult to determine the detailed pattern of decreasing ϕ^b with increasing suction (*Jiao et al.*, 2005). *Vanapalli et al.* (1996) proposed that the relation between ϕ^b and ϕ is determined by the degree of saturation as follows:

$$c_t = c_e + (u_a - u_v)\left(\frac{\theta - \theta_r}{\theta_s - \theta_r}\right)\tan\phi \tag{3.11}$$

Substituting the average soil moisture content and the average soil water suction into Equation 3.11 leads to a value of the soil cohesion in the unsaturated zone for each position along the hillslope. Finally, the total soil cohesion at each position is calculated as a weighted average of the soil cohesion in the unsaturated and saturated zone.

3.4. Different methods for hillslope stability analysis

3.4.1. Infinite slope method

First we generalize the infinite slope method by incorporating the effects of the unsaturated zone into Equation 3.4. If we assume the height of the water table, the moist bulk

specific weight and the total soil cohesion to be dependent on the *x*-coordinate, the local factor of safety can be calculated as:

$$FS(x) = \frac{c_t(x) + [(1-\sigma(x))\gamma_m(x) + \sigma(x)\gamma_b]D(x)\cos^2\beta(x)\tan\phi}{[(1-\sigma(x))\gamma_m(x) + \sigma(x)\gamma_s]D(x)\sin\beta(x)\cos\beta(x)} \tag{3.12}$$

where $FS(x)$ is the factor of safety at location x along the hillslope. Note that γ_m is calculated based on the weight of dry soil and the soil moisture content (Equation 3.9) at each position along the hillslope.

Obviously, Equation 3.12 defines the factor of safety at a given location along the hillslope where soil depth and slope angle are constant. In order to derive the $\overline{FS}$ for the entire hillslope given a steady-state rainfall input, the following expression is proposed:

$$\overline{FS} = \frac{\int_0^L \{c_t(x) + [(1-\sigma(x))\gamma_m(x) + \sigma(x)\gamma_b]D(x)\cos^2\beta(x)\tan\phi\}dx}{\int_0^L [(1-\sigma(x))\gamma_m(x) + \sigma(x)\gamma_s]D(x)\sin\beta(x)\cos\beta(x)dx} \tag{3.13}$$

3.4.2. More complex approaches toward hillslope stability

Limit equilibrium methods have been used for decades to safely design major geotechnical structures. Bishop's simplified method, utilizing a circular arc slip surface, is probably the most popular limit equilibrium method (*Han and Leshchinsky*, 2004). Although Bishop's method is not rigorous in the sense that it does not satisfy horizontal force limit equilibrium, it is simple to apply and, in many practical problems, it yields results close to rigorous limit equilibrium methods. In this paper Bishop's simplified method (*Bishop*, 1955) and Janbu's non-circular method (*Janbu*, 1954) are used for the hillslope stability analysis. Bishop's method assumes zero interslice shear forces, satisfies moment equilibrium around the center of the circular failure surface and vertical force equilibrium. The factor of safety according to this method is computed as:

$$FS = \frac{\int_0^L \left[c_t(x)/\cos\beta(x) + \left(P(x) - u(x)/\cos\beta(x)\right)\tan\phi\right]dx}{\int_0^L W(x)\sin\beta(x)dx} \tag{3.14}$$

where

$$P(x) = \left[W(x) - \frac{1}{FS}\left(c_t(x)\tan\beta(x) - u(x)\tan\beta(x)\tan\phi\right)\right] / M(x) \tag{3.15}$$

and

$$M(x) = (1 + \tan\beta(x)\frac{\tan\phi}{FS})\cos\beta(x) \tag{3.16}$$

In the Janbu method, the assumption is made that the interslice shear forces are zero and thus the expression obtained from the total normal force at the base of each slice is the same as that obtained by the Bishop method. To allow for the effect of the interslice shear

force, a correction factor f_0 is applied (taken to be 1 here); thus the factor of safety of the slope (*FS*) in the Janbu method is given as:

$$FS = f_0 \frac{\int_0^L \left[c_t(x)/\cos\beta(x) + \left(P(x) - u(x)/\cos\beta(x)\right)\tan\phi\right]/\cos\beta(x)dx}{\int_0^L W(x)\tan\beta(x)dx} \quad (3.17)$$

In these equations, c_t is the total soil cohesion, *dx* is the horizontal slice width, *u* is the pore water pressure, ϕ is the effective angle of internal friction and *W*(*x*)*dx* is the weight of a soil slice. The computation of *W* involves the assessment of the water storage in the unsaturated zone (Section 3.3). Since Equation 3.14 and 3.17 are implicit equations in *FS*, this set of equations must be solved iteratively.

3.4.3. Reference case: neglecting the effect of the unsaturated zone

For all three slope stability methods presented above, we also consider the simplifying situation where the unsaturated zone does not play a role in the steady-state hydrology. For the infinite slope method, the assumption of the same bulk specific weight above and below the water table leads to following simplification of Equation 3.13:

$$\overline{FS} = \frac{\int_0^L [c_t(x) + (\gamma_s - \sigma(x)\gamma_w)D(x)\cos^2\beta(x)\tan\phi]dx}{\int_0^L \gamma_s D(x)\sin\beta(x)\cos\beta(x)dx} \quad (3.18)$$

In case of the complex slope stability approach (Equations 3.14-3.17), the safety factor can be calculated by considering $u(x) = \gamma_w h(x)\cos\beta(x)$ and $W(x) = \gamma_s D(x)$, where $h = S/(wf)$ (see Troch et al., 2002). By incorporating *u* (based on *S*, the saturated soil storage) and *W* (based on γ_s, the specific weight of the saturated soil), the presented models can be used for hillslopes with different geometrical characteristics (plan shape and profile curvature) and constant or non-constant soil depth. They can help understanding the hydrologic control of shallow and deep landslides in the case of steady-state hydrology.

3.5. Results and discussion

3.5.1. Evaluation of different approaches to model hillslope stability

To investigate the critical slip surface and effect of the unsaturated zone storage on slope stability, we evaluate 6 possible slope stability computations: Case *A*: the same bulk specific weight for saturated and unsaturated storage and the infinite slope stability assumption (as in *Talebi et al.*, 2007a, our base case); Case *B*: considering the soil moisture profile (unsaturated storage) and the infinite slope stability assumption; Case *C*: the same bulk specific weight for saturated and unsaturated storage and Bishop's circular slip surface method; Case *D*: considering the soil moisture profile (unsaturated zone storage) and

Bishop's circular slip surface method; Case *E*: the same bulk specific weight for saturated and unsaturated storage and Janbu's non-circular slip surface method; and finally Case *F*: considering the soil moisture profile (unsaturated zone storage) and Janbu's non-circular slip surface method (see Table 3.1). We apply these 6 cases to nine different hillslope types. These nine characteristic hillslopes consist of three plan shapes (divergent, parallel, and convergent) and three profile curvatures (convex, straight, and concave). Figure 3.1 illustrates the nine basic hillslope types used in this study. The parameters to generate them are listed in Table 3.2. The horizontal length of the nine hillslopes is chosen to be constant (L=100 m), whereas the average slope is 26, 41 and 50 percent (β/ϕ= 0.5, 0.75 and 0.9) for the infinite slope method. As the soil depth is changed along the x direction in the complex slope stability approach, the bedrock slope and surface slope angle are assumed 30 and 50 percent (β/ϕ= 0.6 and 0.9), respectively. These nine hillslopes represent a wide range of landforms traditionally considered in hydrology and geomorphology (*Pennock et al.*, 1987). For different hillslopes within a catchment each individual hillslope type can be adjusted to the observed terrain profile curvature using the geometrical scaling parameters H, L, and n and a proper choice of ω to represent plan shape.

Table 3.1: Hydrological assumptions and stability methods used in this study.

		Stability	
Hydrology	Infinite slope	Bishop*	Janbu*
Constant bulk specific weight	*A*	*C*	*E*
Saturated/Unsaturated	*B*	*D*	*F*

* Note that for the Bishop and Janbu method, the soil depth is changed along the hillslope.

Table 3.2: Geometrical parameters for the nine characteristic hillslopes

Hillslope Nr.	Profile Curvature	Plan Shape	n [-]	ω [10^{-3} m^{-1}]*	Area [m^2]
1	concave	convergent	1.5	+2.7	2441
2	concave	parallel	1.5	0	5000
3	concave	divergent	1.5	-2.7	1049
4	straight	convergent	1	+2.7	2162
5	straight	parallel	1	0	5000
6	straight	divergent	1	-2.7	2162
7	convex	convergent	0.5	+2.7	1402
8	convex	parallel	0.5	0	5000
9	convex	divergent	0.5	-2.7	2268

* This parameter has been calculated based on $\beta = 15^\circ$ ($\beta/\phi = 0.5$).

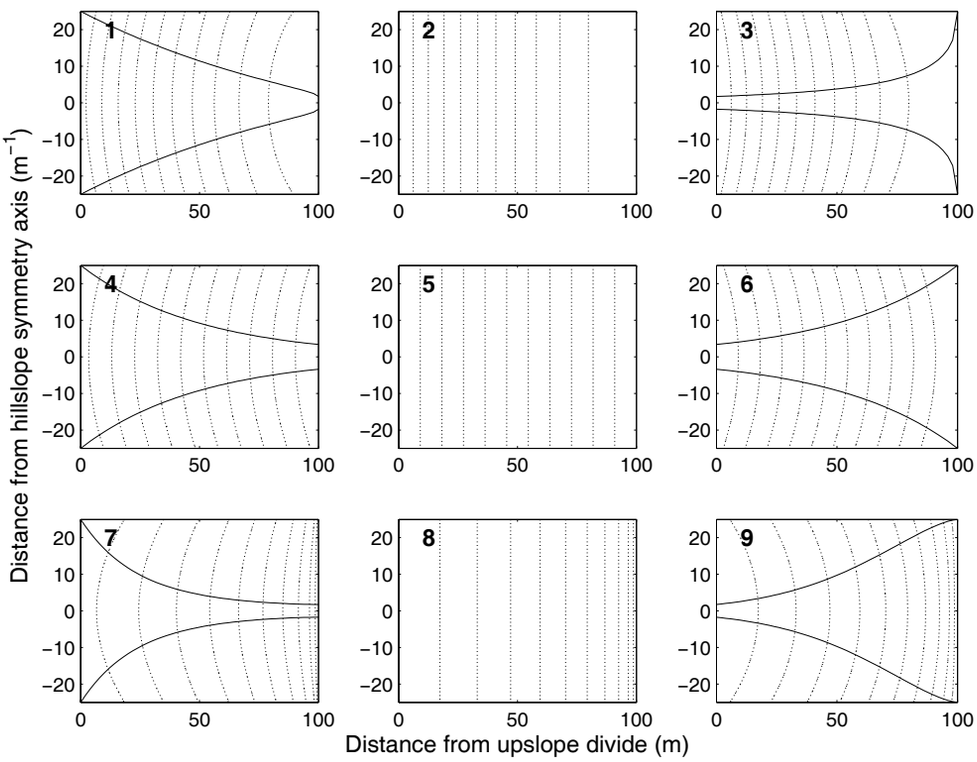

Figure 3.1: Plan view of drainage divides (solid lines) and contour lines (dashed lines) of nine hillslope types ($\beta / \phi = 0.9$). The upslope divide of each hillslope is at x=0.

3.5.2. Hydrology

Figure 3.2 shows the relative saturated storage along these hillslopes and Table 3.3 lists the values of the hydrological variables used to generate these storage profiles. The hydrological behavior of these hillslopes is quite different as can be seen from Figure 3.2, e.g. hillslopes with convergent plan shape (1, 4 and 7) have the largest saturated section. For the rainfall recharge rate (20 mm d^{-1}) and slope angle (27 degrees, $\beta = 0.9\phi$) chosen, hillslopes 1, 2, 4 and 7 saturate near the outlet. This hydrological behavior of hillslopes (storage changes) has important consequences for slope stability, as will be discussed hereafter.

In the procedure adopted to model the unsaturated zone pore water pressure and soil moisture, each hillslope is divided into a series of rectangular vertical columns or slices, each subdivided into regular cells. Using Equation 3.8 and considering $\psi_B = 0$ at the water table, ψ_T (the soil-water suction) for all cells in each column can be obtained. Figure 3.3 shows the steady state soil moisture profiles that develop in the unsaturated zone above the water table for each hillslope type (assuming a constant soil depth). In the hillslopes with a divergent plane shape, subsurface saturation is limited and as a result, the range of soil moisture profiles is small, in the sense that the depth to the saturated layer is more uniform in these cases (Figure 3.3). Although soil moisture dynamics is the result of complex interaction between many elements like climate, soil, and vegetation, this analysis shows that spatial soil moisture changes under steady-state conditions are strongly influenced by hillslope geometry

(especially plan shape). This has also been shown by other studies (e.g. *Qiu et al.*, 2001; *Pellenq et al.*, 2003; *Ridolfi et al.*, 2003; *Hilberts et al.*, 2007).

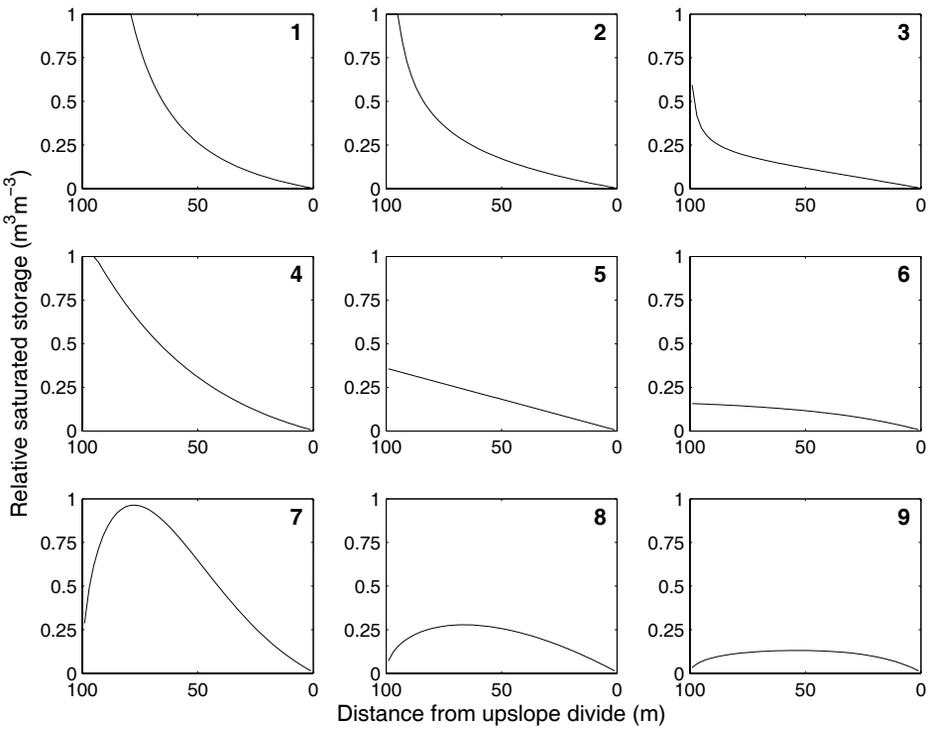

Figure 3.2: Relative saturated storage along the different hillslopes (D=2 m, N=20 mm d^{-1}, $\beta = 27^\circ$ and $\beta / \phi = 0.9$).

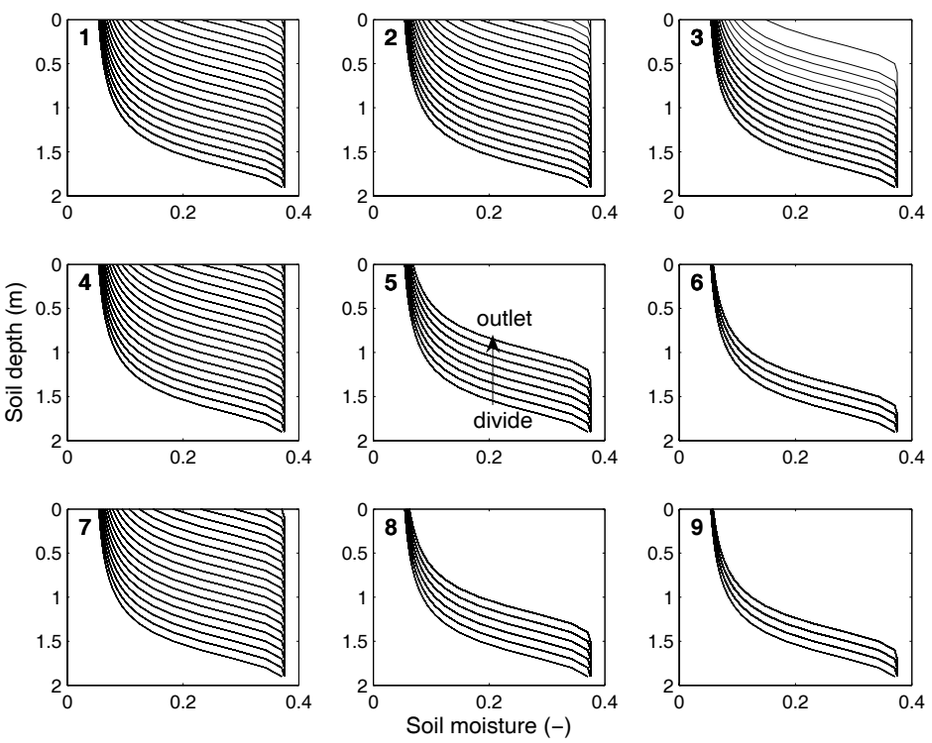

Figure 3.3: Range of soil moisture profiles corresponding to a steady-state recharge (20 mm d^{-1}) for the different hillslopes ($\beta = 27^\circ$, $\beta / \phi = 0.9$), between x=0 and x=L. The arrow (hillslope no. 5) indicates increasing values of the x-coordinate.

Table 3.3: Hydrological and geotechnical model parameters

Parameter group	Parameter name	Symbol	Units	Value
Hydrological	Saturated hydraulic conductivity	K_s	m s^{-1}	$6.383*10^{-5}$
	Effective porosity	f	-	0.34
	Recharge	N	mm d^{-1}	20 (infinite method) and 50 (complex approach)
	Van Genuchten parameter	α_v	m^{-1}	2.761
	Van Genuchten parameter	n_v	-	3.022
	Residual water content	θ_r	m^3 m^{-3}	0.044
	Saturated water content	θ_s	m^3 m^{-3}	0.375
Geotechnical	Effective soil cohesion	c_e	kN m^{-2}	7.85
	Effective angle of internal friction	ϕ	◦	30
	Slice width	dx	m	0.5
	Saturated bulk specific weight	γ_s	kN m^{-3}	20.35
	Water specific weight	γ_w	kN m^{-3}	9.81

3.5.3. Infinite slope stability analysis

Figure 3.4 reports the values of the safety factor for each hillslope and for a range of average bedrock slope angles using the infinite slope method (constant soil depth) for the two cases: with and without considering the unsaturated zone storage (Cases *A* and *B*). In this figure, the solid lines have been calculated by Equation 3.18 (case *A*) which assumes the bulk specific weight above and below the water table is equal. The dashed lines have been obtained by Equation 3.13 (case *B*), which is based on the calculation of the soil moisture profile in the unsaturated zone (Equation 3.8) and the relative saturated soil moisture storage (Equation 3.3). The effect of matric suction on soil cohesion also has been incorporated in the stability analysis (Equation 3.11). Because divergent hillslopes (3, 6 and 9) have the smallest saturated zone (see Figure 3.2), they exhibit the most stability in both cases. On the other hand, for a given profile curvature, convergent hillslopes (1, 4 and 7) have the least stability because they have the largest saturated zone (see Figure 3.2). As can be seen (Figure 3.4), both methods yield comparable results, illustrating the hillslope stability is determined by the water table dynamics (saturated soil moisture storage). This means that unsaturated zone storage does not play a critical role in determining the factor of safety for shallow landslides.

Hence, the bulk specific weight of the unsaturated zone can be considered equal to that of the saturated zone in the steady-state hydrology.

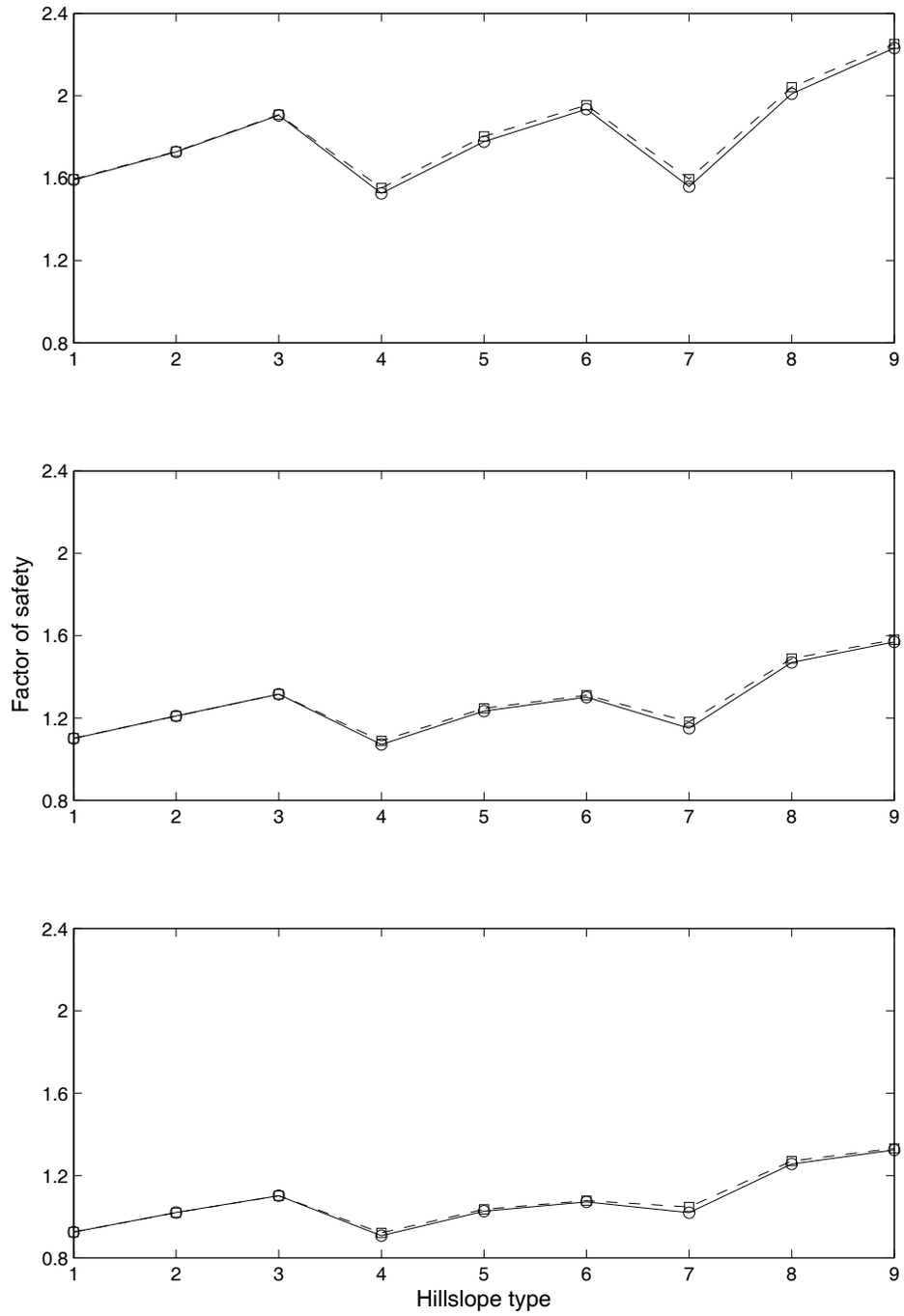

Figure 3.4: Factor of safety for nine hillslopes and different average slope angles. Solid lines (Case *A*): the bulk specific weight above and below the water table is the same and the infinite slope stability assumption is applied (as in *Talebi et al.,* 2007a); Dashed lines (Case *B*): the unsaturated storage is taken into account and the infinite slope stability assumption is applied; Average bedrock slope angle is different for each row; from top to bottom: 15, 22.5 and 27 degrees ($\beta/\phi = 0.5, 0.75, 0.9$).

To generalize the obtained results for the infinite slope method, the slope stability has also been investigated in the n-ω parameter space considering the unsaturated zone storage. On the basis of Equation 3.1, and for the parameter intervals $0.4 < n < 1.9$ and $-(H/L^2) < \omega < +(H/L^2)$ (for L=100), the factor of safety has been calculated. Figure 3.5 illustrates the relation of the safety factor with profile curvature (n) and plan shape (ω) for a critical slope angle ($\beta/\phi = 0.9$). For any given plan shape (ω=cst), when profile curvature (n) changes from convex to concave, stability decreases. In the case of plan shape, when it changes from $\omega < 0$ to $\omega > 0$ (from divergent to convergent), slope stability decreases in all profiles. This is due to the effect of plan shape on saturated soil storage (*Troch et al.*, 2002, *Hilberts et al.*, 2004). When plan shape changes from divergent to convergent, the soil moisture storage increases in all profiles (see Figure 3.2). In both cases, the convergent hillslopes with concave profile have the least stability. For the convex profiles (n<1), the effect of plan shape on hillslope stability is more pronounced than for the other profiles: as plan shape changes from divergent to convergent, *FS* drops quickly. For concave bedrock profiles (n>1), stability decreases slightly when plan shape changes from divergent (ω<0) to convergent (ω>0).

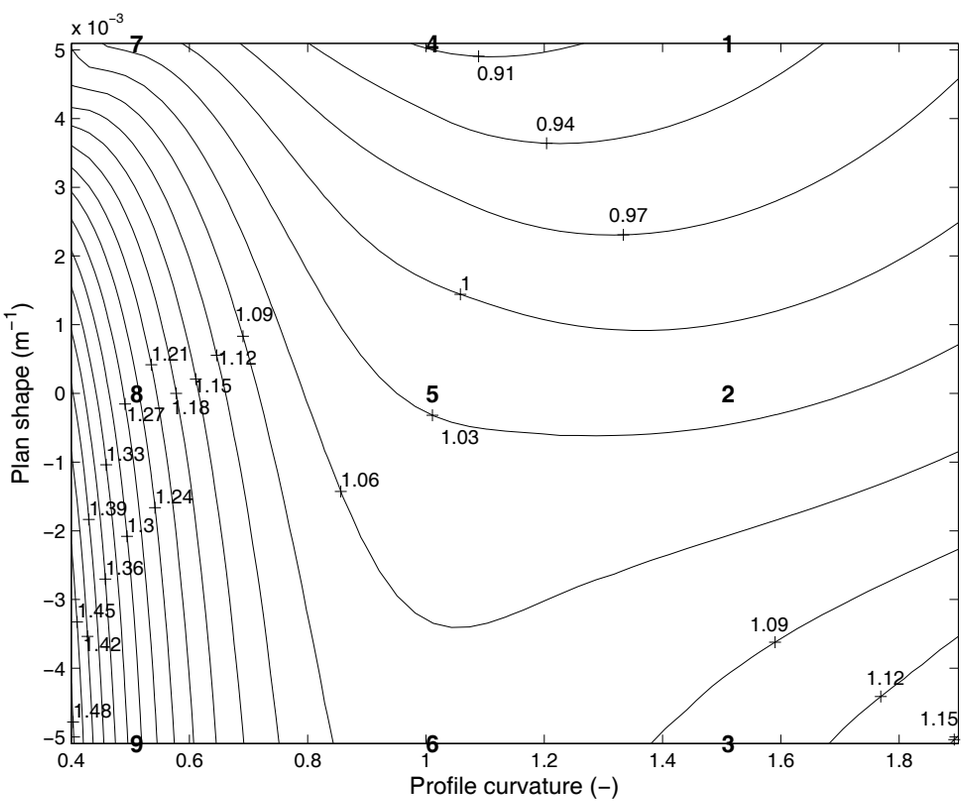

Figure 3.5: Factor of safety as a function of profile curvature (n) and plan shape (ω) for case *B*: considering the soil moisture profile in the unsaturated zone and the infinite slope stability assumption ($\beta/\phi = 0.9$). The bold numbers shows the location of the nine basic hillslopes.

3.5.4. Bishop and Janbu methods

Hillslope stability has also been investigated for hillslopes with non-constant soil depth (deep landslides) using more complex approaches: Bishop's and Janbu's methods taking the soil moisture in the unsaturated zone and its effect on soil cohesion into consideration. To do this, the Bishop circular method is incorporated into the analytical model to find the critical slip surface in hillslopes with different geometric characteristics. Here, we consider a series of slip circles of different radii but with the same center of rotation and find the minimum *FS* for this circle center. This procedure is repeated for several circles, each investigated from an array of centers. Each center will have a minimum *FS*, and the overall lowest *FS* from all the centers is considered to be the *FS* for the whole hillslope. Hence, a large number of possible slips (6000) has been considered for the calculation of the minimum safety factor. Finally, by assuming the same slip surface for all hillslopes (namely the bedrock), the safety factor is computed by Janbu's non-circular method.

Figure 3.6 shows the values of the minimum safety factor for each hillslope and for the two cases: with and without considering the unsaturated storage. The final results of both cases are similar and the previous conclusion that the unsaturated zone can be neglected is confirmed for hillslopes with non-constant soil depth. Figure 3.6 shows that when plan shape changes from convergent to divergent, for all profiles slope stability increases. In both cases the convex convergent hillslopes have the minimum safety factor as convex hillslopes have a large slope angle in the outlet region.

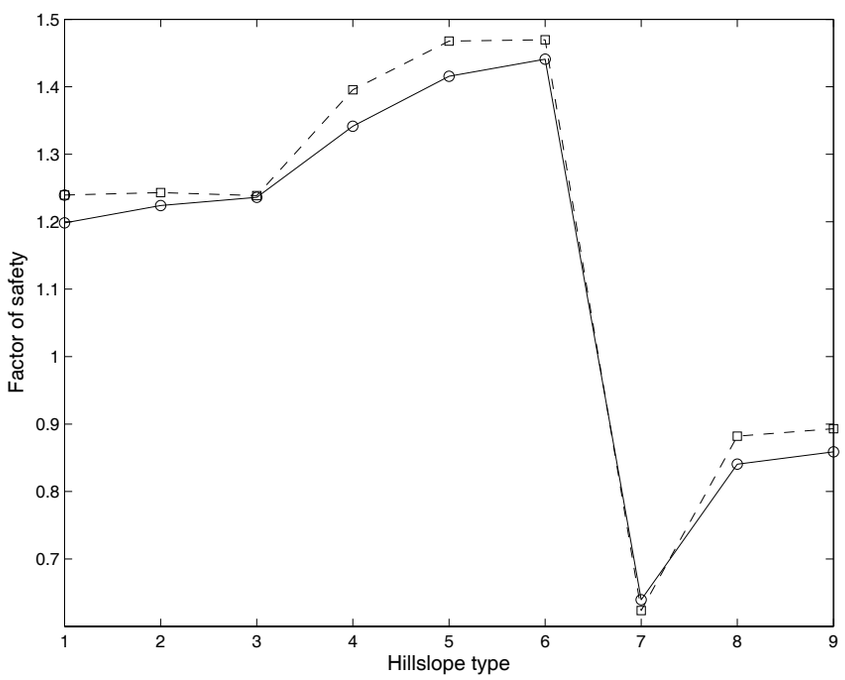

Figure 3.6: Factor of safety for nine hillslope shapes. Solid lines (Case *C*): considering the same bulk specific weight above and below the water table and Bishop's circular slip surface method. Dashed lines (Case *D*): taking into account the unsaturated storage and Bishop's circular slip surface method. Average bedrock slope is 30 and 50 percent for bedrock and surface, respectively.

The slip surface corresponding to the minimum *FS* has also been investigated. Figure 3.7 illustrates the location of the critical slip surface as computed by the Bishop simplified method (circular slip surface) for case *D*. The bedrock and surface slope angles are 30 and 50 percent, respectively (non-constant soil depth). As can be seen, not only the *FS* is different for all hillslopes, but also the location of the critical slip surface has changed. It is located in the upstream part of the slope for the concave and in the downstream part of the slope for the convex profiles. The location of the critical slip surface is dependent on the profile curvature but much less on plan shape (specifically for the convex profiles). This is because the stability strongly depends on the local slope angle, although plan shape also affects stability by increasing the saturated part near the outlet.

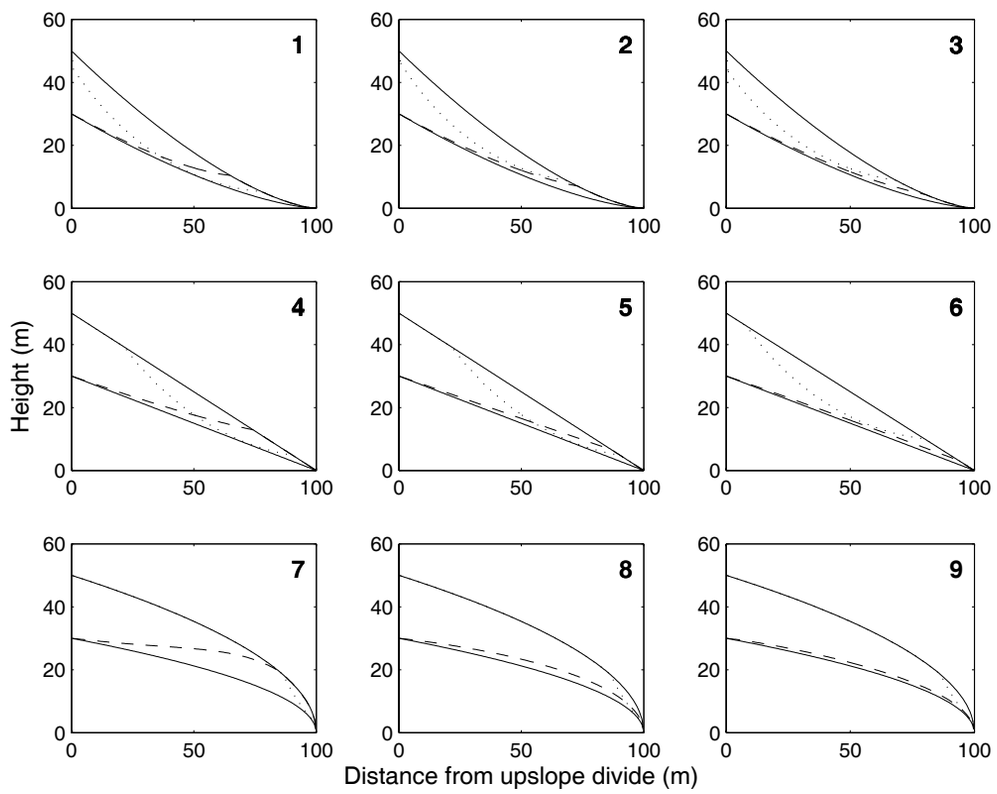

Figure 3.7: The critical slip surface (dotted lines) in hillslopes with different geometric characteristics as computed by Bishop's circular slip surface method and considering the unsaturated zone storage (case *D*). The dashed lines show the location of the water table. Average bedrock slope (bottom solid line) and surface slope angle (top solid line) are 30 and 50 percent, respectively.

In order to generalize the obtained results for hillslopes with non-constant soil depth, slope stability has again been investigated in the n-ω parameter space considering the unsaturated zone storage. Figure 3.8 indicates the obtained *FS* for the different values of n (profile curvature) and ω (plan shape). For any given plan shape (ω=cst), when profile curvature changes from straight to concave or convex, stability decreases because concave and convex hillslopes have a large slope angle in the upstream and downstream parts of the slope, respectively. Hillslopes with a small degree of convexity (n=0.9) have the maximum

safety factor (see Figure 3.8). For concave profiles (n>1), the contour lines are almost parallel, indicating a weaker effect of plan shape on stability. Finally, hillslopes with a convex length profile and convergent plan shape have the least stability. Furthermore, there is no significant difference between the results of both cases (*C* and *D*), which confirms again that the unsaturated zone storage can be neglected for the slope stability analysis in the case of steady-state hydrology.

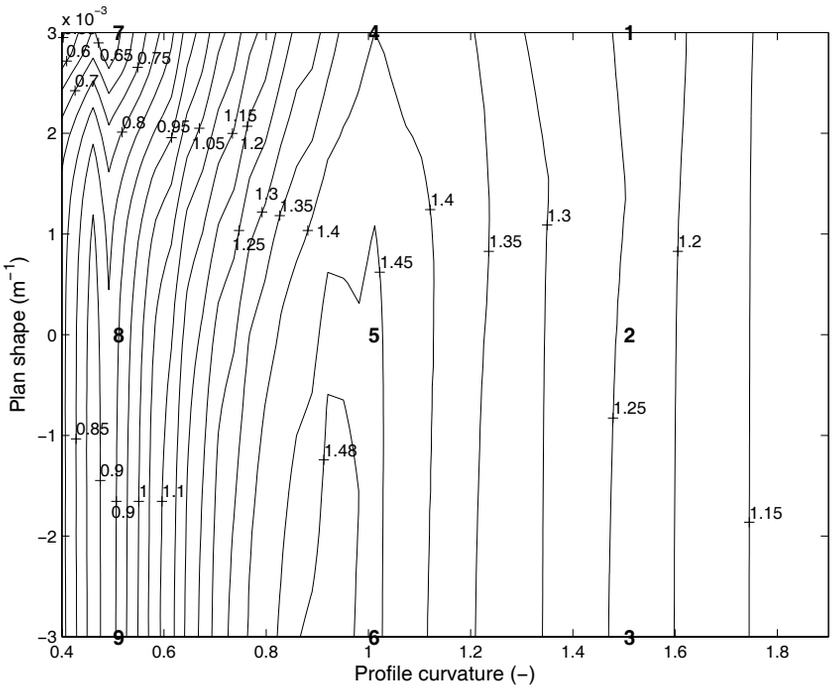

Figure 3.8: Factor of safety as function of profile curvature (n) and plan shape (ω) using the more complex approach (Bishop's circular slip surface method and non-constant soil depth), and considering the soil moisture in the unsaturated zone (case *D*). Average bedrock slope is 30 and 50 percent for bedrock and surface, respectively. The bold numbers shows the location of the nine basic hillslopes.

To compare the stability of hillslopes by assuming the same slip surface on the bedrock, the *FS* is also calculated by the Janbu non-circular method. Figure 3.9 shows the stability of nine hillslopes when the soil depth changes along the hillslopes. According to this method, when the slip surface lies on the bedrock, the convex hillslopes are the most stable and the concave ones are the least stable. For all profile curvatures, slope stability slightly increases when plan shape changes from convergent to divergent.

This is confirmed by Figure 3.10, where we have computed the *FS* for a wide range of plan shapes and profile curvatures. When profile curvature changes from concave to convex, stability decreases. The fact that the contour lines are nearly parallel indicates that plan shape only plays a minor role. With respect to the similarity of the Bishop and Janbu methods (see Equations 3.14 and 3.17), it should be kept in mind that in this paper, the slip surface with the minimum *FS* has only been determined with the Bishop circular method. However, the Janbu non-circular method has been used for comparison of slope stability for entire hillslopes

(when the slip surface lies on the bedrock). Overall, Figure 3.10 illustrates how slope stability is changed when hillslope geometry and thus hillslope hydrology is varied.

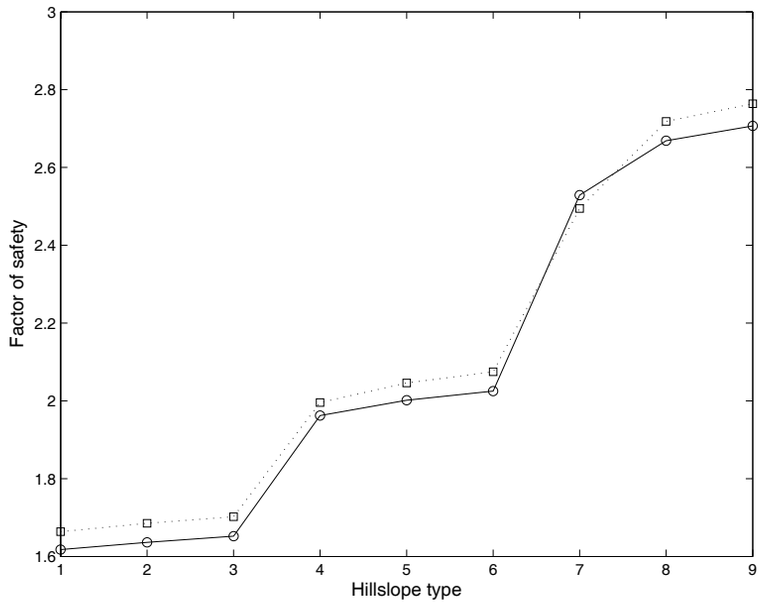

Figure 3.9: Factor of safety for nine hillslope shapes. Solid lines (Case *E*): considering the same bulk specific weight above and below the water table and Janbu non-circular slip surface method. Dashed lines (Case *F*): taking into account the unsaturated storage and Janbu non-circular slip surface method. Average bedrock slope is 30 and 50 percent for bedrock and surface, respectively.

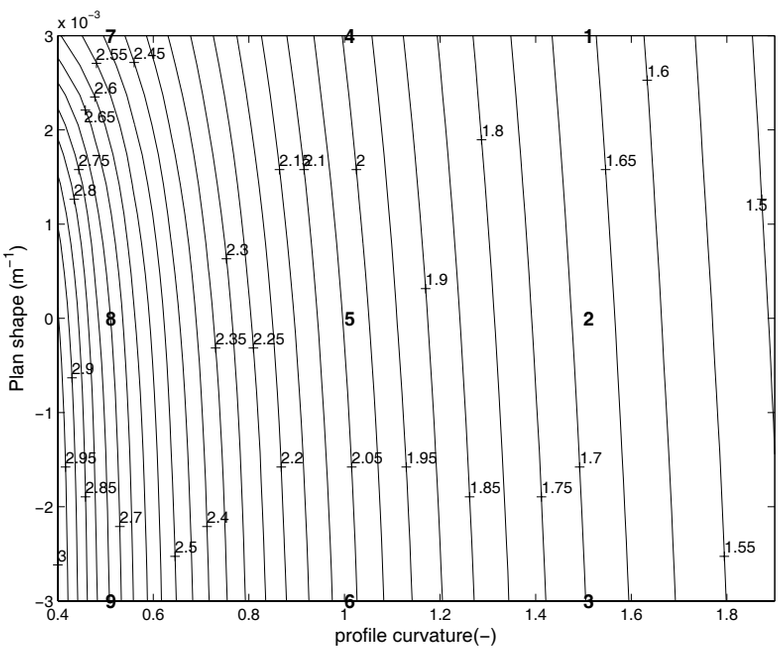

Figure 3.10: Factor of safety as function of profile curvature (n) and plan shape (ω) using the more complex approach (Janbu non-circular slip surface method and non-constant soil depth), and considering the soil moisture in the unsaturated zone (case *D*). Average bedrock slope is 30 and 50 percent for bedrock and surface, respectively. The bold numbers shows the location of the nine basic hillslopes.

3.6. Summary and conclusions

The aim of this paper was to analyze the role of the geometric characteristics of hillslopes as well as the effect of the unsaturated zone storage on the hillslope stability in the steady-state hydrology. This was studied on the basis of computing and analyzing the *FS* in two different manners. First, an analytical model (*Talebi et al.*, 2007a) that is based on kinematic wave dynamics of the saturated subsurface storage and the infinite slope stability assumption (for a constant soil depth and shallow landslides). Second, a more complex approach (for a non-constant soil depth associated with deep landslides) that accounts for the unsaturated zone storage and that relaxes the simplifying assumptions of the infinite slope stability model (Janbu's non-circular method and Bishop's simplified method). All methods were studied in two cases: with and without considering the soil moisture profile in the unsaturated zone. The effect of soil suction on soil cohesion has also been investigated.

We started our analysis from the observation that the geometry (that is plan shape and profile curvature) of a hillslope exerts a major control on the hydrologic storage, by defining the domain and boundary conditions of moisture storage (*Troch et al.*, 2002). The presented hydrological model (kinematic wave dynamics of saturated subsurface storage) takes into account the effects of topography on the hillslope-storage through the plan shape and profile curvature by computing the relative saturated soil moisture storage. We applied the considered hillslope stability models to nine characteristic hillslope types with three different profile curvatures (concave, straight, convex) and three different plan shapes (convergent, parallel, divergent). Furthermore, in order to generalize the results, we also applied the slope stability models to a wider range of plan shapes and profile curvatures. Our conclusions are the following:

i) When the width function (plan shape) changes from convergent to divergent, hillslope stability generally increases. In case of the infinite slope method for shallow landslides (with and without the unsaturated zone storage), the convergent hillslopes with concave profile curvature have the least stability in both cases. The divergent convex hillslopes have the most stability as they have less storage than other hillslopes.

ii) To find the critical slip surface in the hillslopes with non-constant soil depth, the simplified Bishop method was incorporated in the analytical model. In this case, not only the rate of *FS* is different in the hillslopes but also the location of the critical slip changes. In fact, the critical slip surface is located at the upstream end of the slope in the concave hillslopes and near the outlet in the convex hillslopes. This is because the local slope angle (profile curvature) plays a key role in the slope stability. Therefore, it can be concluded that the location of the critical slip surface is more dependent on profile curvature than on plan shape. Overall, for a given plan shape (convergent, parallel or divergent) convex convergent hillslopes have slip surfaces with the minimum safety factor in the outlet region.

iii) To compare the stability of entire hillslopes, the Janbu non-circular method was incorporated in the analytical model with its slip surface at the bedrock. This method also shows that the convergent hillslopes with concave profile curvature have the least stability.

iv) A comparison of the results of the different slope stability models with and without considering the unsaturated zone storage shows that there is no noticeable difference between the two cases. This means that the bulk specific weight of the unsaturated soil can be considered equal to that of the saturated soil in the steady-state hydrology. Hence, the hillslope stability (*FS*) is completely determined by the water table dynamics. Therefore the effect of the unsaturated zone storage can be neglected safely in the steady-state hydrology.

v) Finally, it can be stated that the incorporated more complex approaches (simplified Bishop method and Janbu's non-circular method) and steady-state hydrology model based on the relative saturated storage can help to predict the critical slip surface and slope stability for hillslopes with different geometrical characteristics. But due to its limitation (steady-state hydrology) more research is needed to account for dynamical slope stability effects.

Chapter 4

A low-dimensional physically-based model of hydrologic control on shallow landsliding in complex hillslopes

This chapter is based on the accepted paper **Talebi, A., R. Uijlenhoet and P. A. Troch (2007)**, A low-dimensional physically-based model of hydrologic control on shallow landsliding in complex hillslopes, *Earth Surface Processes and Landforms*, (in press).

4. A low-dimensional physically-based model of hydrologic control on shallow landsliding in complex hillslopes

Abstract

Hillslopes have complex three-dimensional shapes that are characterized by their plan shape, profile curvature of surface and bedrock, and soil depth. To investigate the stability of complex hillslopes (with different slope curvatures and plan shapes), we combine the hillslope-storage Boussinesq model (HSB) with the infinite slope stability method. The HSB model is based on the continuity and Darcy equations expressed in terms of storage along the hillslope. Solutions of the HSB equation account explicitly for plan shape by introducing the hillslope width function and for profile curvature through the bedrock slope angle and the hillslope soil depth function. The presented model is composed of three parts: a topography model conceptualizing three-dimensional soil mantled landscapes, a dynamic hydrology model for shallow subsurface flow and water table depth (HSB model), and an infinite slope stability method based on the Mohr-Coulomb failure law. The resulting Hillslope-Storage Boussinesq Stability Model (HSB-SM) is able to simulate rain-induced shallow landsliding in hillslopes with non-constant bedrock slope and non-parallel plan shape. We apply the model to nine characteristic hillslope types with three different profile curvatures (concave, straight, convex) and three different plan shapes (convergent, parallel, and divergent). In the presented model, the unsaturated storage has been calculated based on the unit head gradient assumption. To relax this assumption and to investigate the effect of neglecting the variations of unsaturated storage on the assessment of slope stability in the transient case, we also combine a coupled model of saturated and unsaturated storage and infinite slope stability method. The results show that the variations of the unsaturated zone storage do not play a critical role in hillslope stability. Therefore, it can be concluded that the presented dynamic slope stability model (HSB-SM) can be used safely for slope stability analysis in complex hillslopes. Our results show that after a certain period of rainfall, the convergent hillslopes with concave and straight profiles become unstable faster than others whilst divergent convex hillslopes remain stable (even after intense rainfall). In addition, the relation between subsurface flow and hillslope stability has been investigated. Our analyses show that the minimum safety factor (*FS*) occurs when the rate of subsurface flow is maximum. In fact, by increasing the subsurface flow, stability decreases for all hillslope shapes.

Key words: hillslope stability, subsurface flow, HSB-SM model

4.1. Introduction

Hillslopes can be considered as the basic landscape elements of many catchments. A proper understanding of the interaction and feedbacks between hillslope forms and the processes responsible for hillslope hydrology and stability are of great importance for catchment scale land management. Hillslope failures are complex natural phenomena that pose a serious natural hazard in many countries. Consequently, not only considerable financial costs are suffered, but also major ecological and environmental problems may arise in larger geographical areas (*Sidle and Ochiai*, 2006). To prevent or mitigate these damages, hillslope stability analysis requires an understanding and evaluation of the processes that are affected by the hydrologic behavior of the hillslopes.

The relationship between rainfall, water table fluctuations and landslide movement is often difficult to establish. *Keefer and Larsen* (2007) state that although major causes of landslides are well known, predicting just where and when a landslide will occur continues to be a complex proposition, because the properties of earth materials and slope conditions vary greatly over short distances, and the timing, location, and intensity of triggering events are difficult to forecast. Shallow slope failures, in general, are controlled by surface topography through shallow subsurface flow and increased soil saturation (*Montgomery and Dietrich*, 1994; *Iida*, 1999; *Borga et al.*, 2002). Many studies (e.g. *Sidle and Swanston*, 1982; *Harp et al.*, 1990; *Anderson and Sitar*, 1995; *Iverson*, 2000; *Dhakal and Sidle*, 2004; *Iida*, 2004; *Rosso et al.*, 2006), have indicated that hillslope instability can be caused by increased subsurface pore pressures during periods of intense rainfall which reduce the shear strength of hillslope materials. Although in these studies topography has been reported as an important factor in slope stability, in most of the models applied only slope angle has been investigated. From a slope stability view point, other topography parameters like profile curvature and plan shape are sometimes equally important. Former (*Beven and Kirkby*, 1979; *Sidle*, 1984; *Montgomery and Dietrich*, 1994) and more recent studies (e.g. *Tsuboyama et al.*, 2000; *Troch et al.*, 2002; *Troch et al.*, 2003; *Hilberts et al.*, 2004; *Berne, et al.*, 2005; *Rezzoug et al.*, 2005; *Sidle and Ochiai*, 2006) have shown that in addition to bedrock slope, hillslope form as represented by plan shape and profile curvature is an important control on subsurface flow response.

Because of the strong relation between hydrological processes, hillslope shape and slope stability, efficient tools are needed to investigate the effect of complex topography on slope stability at the landscape scale. Existing tools either neglect topographic curvature or model it in a very complex computationally inefficient manner. The main purpose of this study is therefore to present a dynamic low dimensional but physically-based model that includes both hydrological processes (saturated and unsaturated zone storage) and a stability model (based on the infinite slope assumption) for hillslopes with different topographic characteristics.

To study the effect of topography on rain-induced shallow landsliding, some researchers (e.g. *Montgomery and Dietrich*, 1994; *Sidle and Wu*, 1999; *Dhakal and Sidle*, 2003, 2004; *Talebi et al.*, 2007a) used the kinematic wave (KW) assumption for hillslope

hydrology and showed that, in addition to bedrock slope, plan shape and slope curvature play important roles in hillslope stability in case of a steady-state hydrology. However, by comparing the KW model with the fully three-dimensional Richards' equation, *Hilberts et al.* (2004) showed for convergent slope forms, the KW model looses its ability to accurately describe water table dynamics and the resulting hillslope drainage. Since the dynamic response of hillslopes is strongly dependent on plan shape, slope curvature and slope angle (*Troch et al.*, 2002; *Hilberts et al.*, 2004), a three dimensional model of dynamic hillslope hydrology would be necessary for stability analysis of complex hillslopes.

Recent studies (*Troch et al.*, 2003; *Paniconi et al.*, 2003; *Hilberts et al.*, 2004; *Hilberts et al.*, 2007) have generalized the Boussinesq equation to account for the three-dimensional soil mantle in which subsurface flow processes take place. This hillslope-storage Boussinesq (HSB) equation is formulated by expressing the continuity and Darcy equations in terms of soil water storage as the dependent variable. In this model, the method proposed by *Fan and Bras* (1998) is used to collapse the three-dimensional soil mantle of complex hillslopes into a one-dimensional drainable pore space. The resulting HSB model shows that the dynamic response of complex hillslopes during drainage and recharge events depends very much on the slope angle, plan shape and slope curvature. Because of the ability of the HSB model to analyze hydrological process in complex hillslopes in a very (computationally) efficient way, it is a good candidate to combine with the infinite slope stability method. The resulting model (HSB-SM) can be used for dynamic slope stability analyses in complex hillslopes.

To keep the model low-dimensional, the average soil moisture in the unsaturated zone has been calculated according to Campbell's method (*Campbell*, 1974), using Darcy's law with the unit-gradient assumption. As a result, in the HSB-SM model, the effect of the temporal variations of the unsaturated zone storage has been neglected. To investigate the effect of this simplification, a coupled model of the dynamic unsaturated and saturated zone is needed. Recently, *Hilberts et al.* (2007) developed a model that couples the one-dimensional Richard's equation for vertical unsaturated flow and the HSB equation for lateral saturated flow along complex hillslopes. By introducing the unsaturated zone matric pressure head as a system-state and reformulating the derived equations into state-space notation, they have solved the coupled system simultaneously as a set of ordinary differential equations. Considering the importance of the capillary fringe on groundwater flow, this component has also been included into the HSB flow domain (see *Hilberts, et al.*, 2007). Their model allows for an accurate investigation of the relationship between rainfall intensity, drainable porosity, unsaturated storage and recharge.

To investigate the importance of neglecting the variations of the unsaturated zone storage in the HSB-SM model, the coupled HSB model (*Hilberts et al.*, 2007) is combined with the infinite slope stability method. Moreover, the effect of unsaturated soil moisture on soil cohesion is incorporated in the slope stability model.

Hence, in this paper we present a methodology to investigate the effect of rainfall and water table variations on slope movement in complex hillslopes by coupling an integrated hydrologic model for the saturated and unsaturated zone with the infinite slope method for hillslope stability analysis. Specifically, the study aims (i) to present a dynamic hillslope

stability model (applicable in complex hillslopes), (ii) to investigate the relation between rainfall, soil moisture storage, subsurface flow and hillslope stability, and (iii) to investigate the changes of hillslope stability with respect to plan shape and slope curvature during rainfall.

4.2. Model formulation

In this study we combine a dynamic hillslope hydrology model with the infinite slope stability assumption for hillslopes with different topographic characteristics. Hence, this model incorporates three important aspects of a hillslope: its topography, hydrology and stability.

4.2.1. Hillslope topography

To study the effect of topography (plan shape and profile curvature) on rain-induced shallow landsliding, *Talebi et al.* (2007a) following *Evans* (1980), characterized hillslopes by the combined curvature in the gradient direction (profile curvature) and the direction perpendicular to the gradient (contour or plan curvature). The surface of an individual hillslope is represented by the following bivariate function (*Evans*, 1980):

$$z(x, y) = E + H(x / L)^n + \omega y^2, \quad (4.1)$$

where z is the elevation, x is the horizontal distance from the outlet, y is the horizontal distance from the slope centre in the direction perpendicular to the length direction (the width direction), E is the minimum elevation of the surface above an arbitrary datum, H is the maximum elevation difference defined by the surface, L is the total horizontal length of hillslope, n is a profile curvature parameter, and ω is a plan curvature parameter.

The presented model (HSB-SM) is applied to nine distinct hillslope types which can be viewed as a first-order approximation of the landscape elements (*Troch et al.*, 2002) that constitute a catchment. Figure 4.1 shows a hillslope with a three-dimensional soil mantle on top of an impermeable layer and a straight bedrock profile explaining the symbols w, L', D' and β in this study. By using Equation 4.1 and allowing profile curvature (defined by n) to assume values less than, equal to, or greater than 1 and plan curvature (defined by ω) to assume either positive, zero, or negative values, one can define different basic geometric relief forms. Figure 4.2 illustrates nine basic hillslope types that are formed by combining three plan and three profile curvatures. These nine hillslopes represent a wide range of hillslope types traditionally considered in hydrology and geomorphology (see also *Tsukamoto and Ohta*, 1988). The parameters for Equation 4.1 are different for each of these nine hillslopes, and are listed in Table 4.1. The values of the hydrological and geotechnical parameters have been listed in Table 4.2. The horizontal length of the nine hillslopes (measured along the bedrock) is chosen to be constant (L = 100 m). For different hillslopes within a catchment each individual hillslope type can be fitted using the geometrical scaling parameters H, L, and n to the observed terrain profile curvature, given a known soil depth function, and a proper choice of ω to represent the observed hillslope width function (*Troch et al.*, 2002).

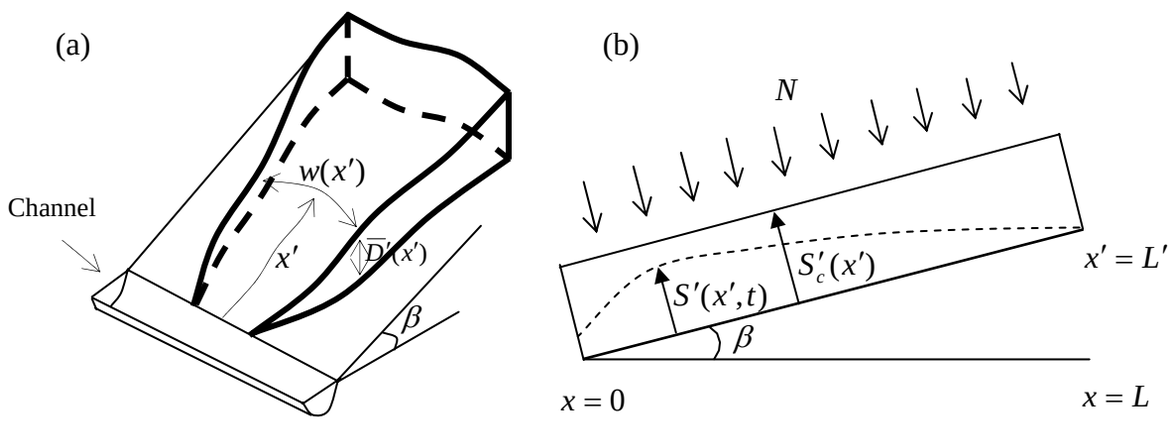

Figure 4.1: ***a)*** A three dimensional view of a convergent hillslope overlying a straight bedrock profile, ***b)*** a definition sketch of the cross section of a one-dimensional hillslope aquifer overlying a bedrock with a constant bedrock slope angle (modified from *Troch et al.*, 2003).

Table 4.1: Geometrical parameters for the nine characteristic hillslopes

Hillslope Nr.	Profile Curvature	Plan Shape	n [-]	ω [10^{-3} m^{-1}]*	Area [m^2]
1	concave	convergent	1.5	+2.7	2441
2	concave	parallel	1.5	0	5000
3	concave	divergent	1.5	-2.7	1049
4	straight	convergent	1	+2.7	2162
5	straight	parallel	1	0	5000
6	straight	divergent	1	-2.7	2162
7	convex	convergent	0.5	+2.7	1402
8	convex	parallel	0.5	0	5000
9	convex	divergent	0.5	-2.7	2268

* This parameter has been calculated based on $\beta = 15^\circ$ ($\beta / \phi = 0.5$).

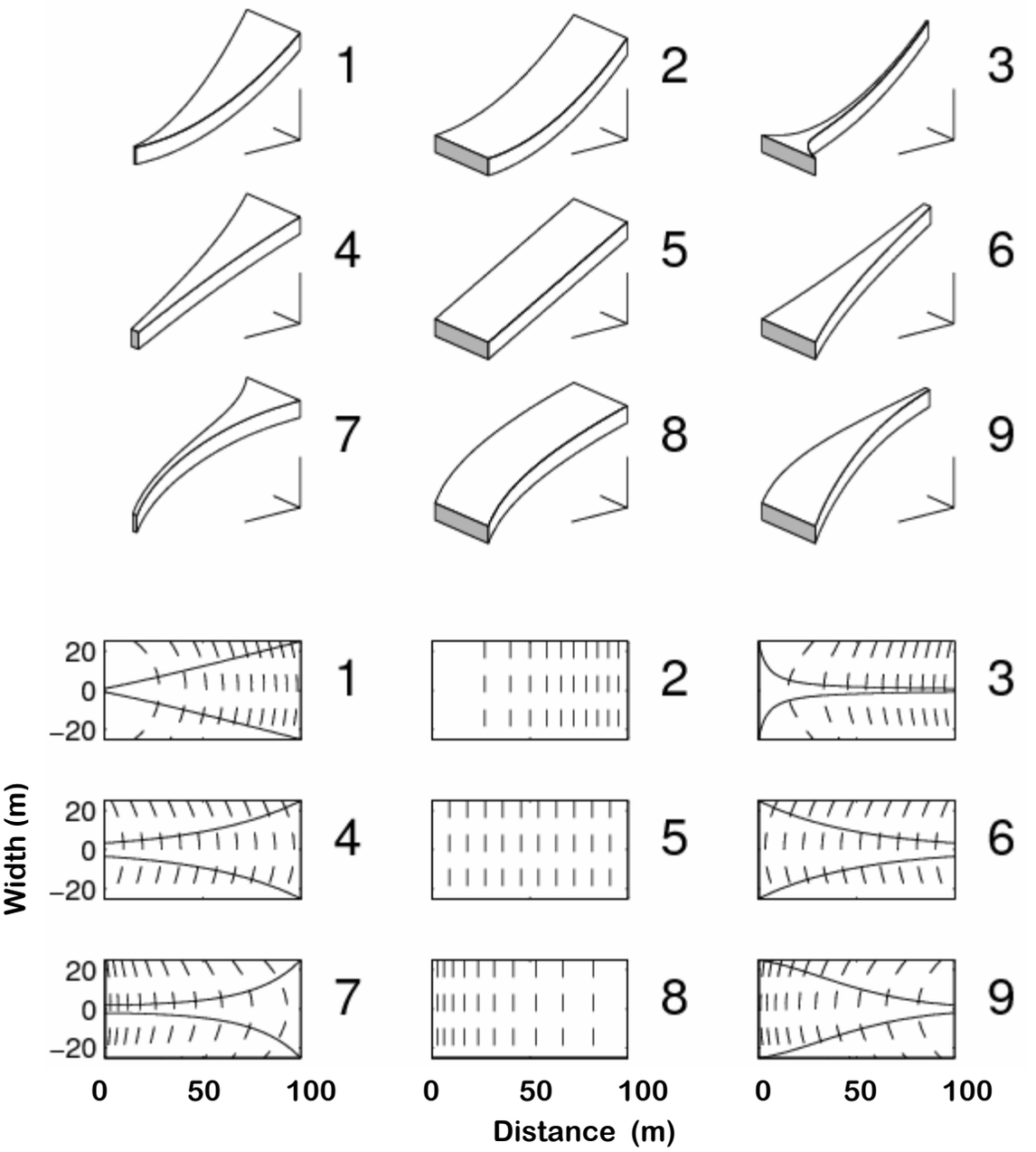

Figure 4.2: Three-dimensional view (top) and a two-dimensional plot of the contour lines and slope divides (bottom) of the nine hillslopes considered in this study (after Hilbert et al., 2004).

Table 4.2: Hydrological and geotechnical model parameters

Parameter group	Parameter name	Symbol	Units	Value in this paper
Hydrological	Saturated hydraulic conductivity	k_s	md^{-1}	5.0
	Effective porosity	f	-	0.35
	Recharge	N	$mm\ d^{-1}$	50
	Van Genuchten parameter	α_v	m^{-1}	-2.54
	Van Genuchten parameter	n_v	-	1.953
	Residual water content	θ_r	m^3m^{-3}	0.054
	Saturated water content	θ_s	m^3m^{-3}	0.408
Geotechnical	Effective soil cohesion	c_e	kNm^{-2}	5.0
	Soil depth	D'	m	2.0
	Effective angle of internal friction	ϕ	∘	30
	Slice length	dx	m	0.5
	Saturated bulk specific weight	γ_s	kNm^{-3}	17.66
	Water specific weight	γ_w	kNm^{-3}	9.81

4.2.2. Hillslope hydrology

The hillslope hydrological model used here is the hillslope-storage Boussinesq (HSB) model for subsurface flow (*Troch et al.*, 2003) in complex hillslopes. The Darcy equation along a unit-width hillslope with sloping bedrock reads:

$$q = -kh'\left(\frac{\partial h'}{\partial x'}\cos\beta + \sin\beta\right) \tag{4.2}$$

Substituting in the continuity equation:

$$f\frac{\partial h'}{\partial t} = -\frac{\partial q}{\partial x'} + N \tag{4.3}$$

yields the Boussinesq equation (*Boussinesq*, 1877):

$$\frac{\partial h'}{\partial t} = \frac{k}{f}\left[\frac{\partial}{\partial x'}\left(h'\frac{\partial h'}{\partial x'}\right)\cos\beta + \frac{\partial h'}{\partial x'}\sin\beta\right] + \frac{N}{f} \tag{4.4}$$

where $h'(x',t)$ is the elevation of the groundwater table measured perpendicular to the underlying impermeable layer which has a slope angle β, k is the hydraulic conductivity, f is the drainable porosity, x' is the distance from the outlet measured parallel to the

impermeable layer, *t* is time and *N* represents the rainfall recharge to the groundwater table. Note that the flow lines for these equations are assumed to be parallel to the bedrock.

As the application of Equation 4.4 is limited to one-dimensional soil mantle, *Troch et al.* (2003) reformulated the continuity and Darcy equations in terms of storage along the hillslope which leads to the hillslope storage Boussinesq (HSB) equation for subsurface flow in complex hillslopes:

$$f\frac{\partial S'}{\partial t} = \frac{k\cos\beta}{f}\frac{\partial}{\partial x'}\left[\frac{S'}{w}\left(\frac{\partial S'}{\partial x'} - \frac{S'}{w}\frac{\partial w}{\partial x'}\right)\right] + k\sin\beta\frac{\partial S'}{\partial x'} + fNw \tag{4.5}$$

where $S' = S'(x',t) = wf\overline{h'}$ is the subsurface water storage, $\overline{h'} = \overline{h'}(x',t)$ is the water table height averaged over the width of the hillslope, and $w(x')$ is the hillslope width function. The total storage capacity along the hillslope can be expressed as $S'_c(x') = fw(x')\overline{D'}(x')$, where $\overline{D'}$ is the soil depth averaged over the width of the hillslope. *Paniconi et al.* (2003) have shown that the HSB model is able to capture the general features of the storage and outflow response of complex hillslopes, as compared to a 3D Richards equation based simulations.

Equation 4.5 allows us to investigate the hydrological behavior of the original Boussinesq equation on hillslopes of variable plan geometry. In order to analyze the effect of non-constant profile curvature, *Hilberts et al.* (2004) presented the HSB model as:

$$f\frac{\partial S'}{\partial t} = \frac{k}{f}\cos\beta(x')\left[B\frac{\partial S'}{\partial x'} + S'\frac{\partial B}{\partial x'} + fS'\frac{\partial\beta(x')}{\partial x'}\right] + \frac{k}{f}\sin\beta(x')\left[f\frac{\partial S'}{\partial x'} - S'B\frac{\partial\beta(x')}{\partial x'}\right] + fNw \tag{4.6}$$

where $B = \partial/\partial x'(S'/w)$. The model is solved numerically, can handle spatially and temporally variable parameters, and allows for the computation of subsurface flow and saturation excess overland flow. By determining the saturated storage (S') at each time step (daily) of the simulation, the relative saturated storage ($\sigma = S'/S'_c$) is calculated and is directly coupled to the infinite slope stability method for determining the factor of safety.

During wet conditions, as will occur in the case of shallow landsliding, precipitation as an input parameter can be assumed equal to the recharge rate. The average soil moisture content in the unsaturated zone (θ) can then be calculated according to *Campbell* (1974) by using Darcy's law with the unit-gradient assumption as:

$$\theta = \mu\left(\frac{N}{k_s}\right)^{\frac{1}{2b+3}} \tag{4.7}$$

where θ is the volumetric soil moisture content averaged over a depth ($D' - h'$), μ is the porosity, *N* is the recharge rate, k_s is the saturated hydraulic conductivity and *b* is a pore size distribution parameter. Since μ and *b* are generally correlated with k_s, we related these to k_s by linear regression with $\ln(k_s)$, fitted to the data provided by *Clapp and Hornberger* (1978). This yields $\mu = -0.0147\ln(k_s) + 0.545$ and $b = -1.24\ln(k_s) + 15.3$ where k_s is expressed in mm d^{-1} (*Teuling and Troch*, 2005). Hence, at each time step (daily), the average soil moisture content in the unsaturated zone can be changed based on the recharge rate (rainfall).

4.2.3. Hillslope stability

Next, from the water table depth along the hillslope and the average soil moisture in the unsaturated zone, the factor of safety (*FS*) can be calculated at each time step. The safety factor is the ratio of the available shear strength to the minimum shear strength that is needed for equilibrium. Many variables are involved in slope stability evaluation and the calculation of the *FS* requires geometrical data, physical data on the geologic materials and their shear-strength parameters (cohesion and angle of internal friction), information on pore-water pressures, etc. In general, the infinite slope stability analysis has been widely applied in many investigations of natural slope stability (e.g. *Montgomery and Dietrich*, 1994; *Wu and Sidle*, 1995; *Van Beek*, 2002; *Borga et al.*, 2002; *D'Odorico and Fagherazzi*, 2003; *Hennrich and Crozier*, 2004; *Claessens*, 2005: *Rosso et al.*, 2006) because of its relative simplicity, particularly where the thickness of the soil mantle is much smaller than the length of the slope and where the failure plane is approximately parallel to the slope surface. The infinite slope model imposes the condition that the groundwater flow is parallel to the slope surface, which is consistent with the HSB model. In order to derive the $\overline{FS}$ for the entire hillslope, *Talebi et al.* (2007a, 2007b) presented the shallow landslide safety factor for complex hillslopes by incorporating the relative saturated storage (the ratio between actual storage and storage capacity) in the safety factor formulation as follows:

$$\overline{FS} = \frac{\int_0^{L'} \{c_t(x') + [(1-\sigma(x'))\gamma_m(x') + \sigma(x')\gamma_b]D'\cos\beta(x')\tan\phi\}dx'}{\int_0^{L'} [(1-\sigma(x'))\gamma_m(x') + \sigma(x')\gamma_s]D'\sin\beta(x')dx'} \tag{4.8}$$

where L' is the total length of hillslope (measured parallel to bedrock), c_t is the total soil cohesion, ϕ is the angle of internal friction, β is the slope angle, and $\sigma(x')$ is the relative saturated storage. γ_m, γ_s and γ_b are respectively the moist, saturated and buoyant bulk density (note that in this equation, x' is measured along the bedrock and $x' = 0$ in the outlet).

With respect to the influence of soil suction on the slope stability, *Fredlund* (1978) proposed a linear shear strength equation for unsaturated soils. According to this model, the total cohesion of the soil (c_t) can be calculated as:

$$c_t = c_e + (u_a - u_v)\tan\phi^b \tag{4.9}$$

where c_e is the effective cohesion of saturated soil (kPa), $(u_a - u_v)$ is the matric suction of the soil on the plane of failure (kPa), where u_a and u_v are the pressures of pore air and pore water, respectively. For slope stability analysis, the pore air pressure is assumed to be atmospheric and constant. ϕ^b is the angle of shearing resistance with respect to matric suction. *Vanapalli et al.*, (1996) proposed that the relation between ϕ^b and ϕ can be replaced by the degree of saturation as follows:

$$c_t = c_e + (u_a - u_v)\left(\frac{\theta - \theta_r}{\theta_s - \theta_r}\right)\tan\phi \tag{4.10}$$

Equation 4.10 shows how the total cohesion of the soil (c_t) is changed as a function of the soil moisture in the unsaturated zone (θ) in each slice and each time step. As can be seen, by substituting the average soil moisture content and the average soil water suction into Equation 4.11, the soil cohesion in the unsaturated zone for each *x*-position along the hillslope is computed. Finally, the total soil cohesion at each *x*-position along the slip surface is calculated as a weighted average of the soil cohesion in the unsaturated and saturated zone.

4.2.4. Numerical analysis

After determining the plan shape and slope curvature (Equation 4.1) for each hillslope (see *Talebi et al.*, 2007a), the dynamic model of hillslope stability is solved starting from the initial condition $h' = 0$ at time *0* and the following steps are performed with a time step, Δt, of one day: (i) the saturated soil moisture storage and the relative saturated storage are calculated from Equation 4.6; (ii) the averaged soil moisture content in the unsaturated zone is estimated from Equation 4.7; (iii) Equation 4.10 is used to calculate the influence of soil suction on soil cohesion; (iv) the factor of safety is determined by Equation 4.8 and (v) back to step *i* for the subsequent time step. For the saturated zone, it is assumed that the downhill boundary condition is $h'(0,t) = 0$ and the uphill boundary condition is a zero-flux boundary as are all sides and the bedrock. In this manner, *FS* is obtained for the hillslope, with any temporal variations arising from dynamic hydrological responses. This will be used for the investigation of its relation with water table fluctuations and subsurface flow.

4.3. Results and Discussion

4.3.1. Effect of the unsaturated zone storage

In the HSB-SM model, the rate of daily precipitation is substituted by the recharge rate directly. This means that the variations of the unsaturated zone storage have been ignored (note that soil moisture in the unsaturated zone has been calculated by Darcy's law with a unit gradient assumption (see Equation 4.7)). To relax this assumption, the slope stability analysis has also been investigated based on coupling the saturated and unsaturated storages. *Hilberts et al.* (2007) presented a coupling between the one-dimensional Richards' equation for vertical unsaturated flow and the one-dimensional hillslope-storage Boussinesq equation (HSB model) for lateral saturated flow along hillslopes with different plan shapes. They also incorporated the capillary fringe in the Boussinesq flow domain. In this paper, to investigate the effect of the unsaturated zone storage on hillslope stability under time-varying conditions, this model has been combined with the infinite slope stability method. Figure 4.3 reports the values of the safety factor for hillslopes with different plan shape using the original HSB model (solid line) and coupled HSB model (dashed line) (*Hilberts et al.*, 2007). As can be seen (Figure 4.3), both methods yield comparable results, illustrating the hillslope stability is mainly determined by the water table dynamics (saturated soil moisture storage). Based on our analysis (see Figure 4.3) and for both methods, after the onset of rainfall, stability starts

to decrease in all hillslopes. Obviously, after a certain period of rainfall (depending on hillslope type), stability becomes constant as the hydrological conditions approach the steady-state. As can be seen, the *FS* obtained from the original HSB model is a little less than that from the coupled HSB model; this is because the original HSB model produces a higher water table than the coupled HSB model (*Hilberts et al.*, 2007).

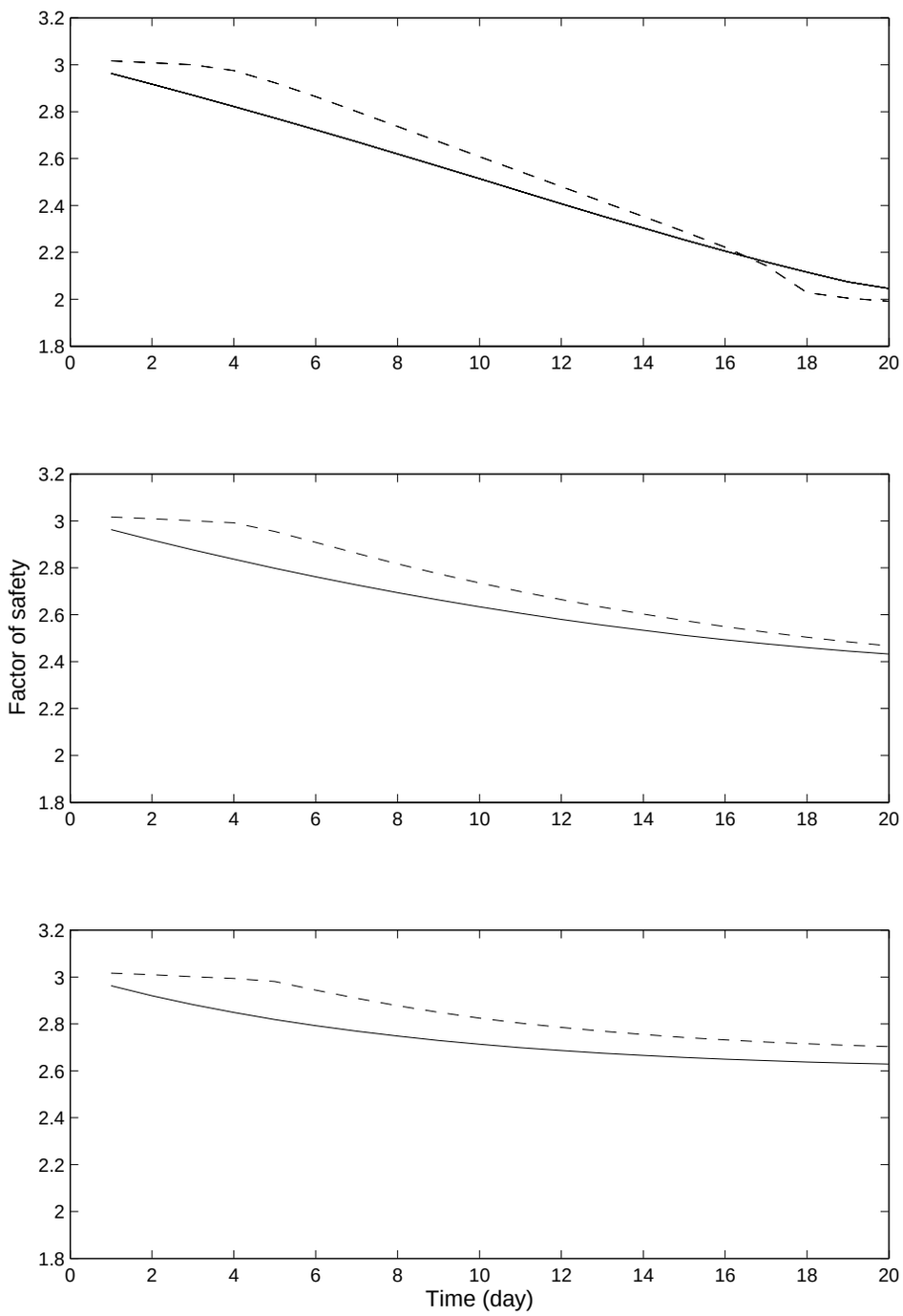

Figure 4.3: Variations of the safety factor in hillslopes with different plan shapes computed using the original HSB model (solid line) and the coupled HSB model (dashed line), assuming $\beta = 0.5\phi$ and N=20 mmd^{-1}. Top panel: convergent, middle panel: parallel and bottom panel: divergent hillslope (profile curvature is constant).

These results are confirmed by other studies (e. g. *Iverson*, 2000; *Iida*, 2004; *Rosso et al.*, 2006) that have shown slope stability is controlled mainly by the water table dynamics. Therefore, with respect to the obtained results (Figure 4.3) and limitation of the coupled model (*Hilberts et al.*, 2007) for hillslopes with non-constant bedrock, we can safely use the original HSB model (*Troch et al.*, 2003; *Hilberts et al.*, 2004) for stability analysis in hillslopes with different plan shapes and profile curvatures. To compare the stability of these nine hillslopes by the Janbu method (Janbu, 1954), we also computed the FS by two methods (Equation 4.8 and Janbu method) (see Table 4.3). As can be seen, the results of both methods are closely following each other.

Table 4.3: The results of computed *FS* by the HSB_SM model and Janbu method for the nine hillslopes in Figure 4.2 ($\beta = \phi$ and N=50 mmd^{-1}).

Hillslope shapes	**1**	**2**	**3**	**4**	**5**	**6**	**7**	**8**	**9**
HSB_SM model	0.95	1.11	1.25	0.93	1.05	1.20	1.04	1.14	1.36
Janbu equation	1.03	1.21	1.32	1.01	1.13	1.27	1.02	1.07	1.29

4.3.2. The relation between recharge rate and slope stability

The results of the stability analysis for three recharge rates equal to 10, 20 and 50 mmd^{-1} (Figure 4.4) indicate clear differences in the stability of different hillslope types for the same soil condition. In all cases (different recharge rates), convergent hillslopes with concave and straight profiles (Figure 4.4, no. 1 and no. 4) become unstable faster than others ($FS < 1$). This is because the convergent hillslopes drain much more slowly than the divergent hillslopes (*Troch et al.*, 2003) and this process increases the saturated zone storage which consequently decreases the factor of safety quickly. In contrast, in the divergent hillslopes (Figure 4.4, no. 3, 6 and 9) which drain fast, even with 50 mm recharge per day, the slopes remain stable ($FS > 1$).

As can be seen, by increasing the recharge rate from 10 to 50 mm per day the stability duration decreases, however, the time to reach instability is different in all hillslopes. For instance, when the recharge is 10 and 20 mmd^{-1}, all hillslopes are stable, whilst by increasing the recharge to 50 mmd^{-1} all convergent hillslopes become unstable after 8-10 days. As a result, it can be stated that from the plan shape view point, the convergent hillslopes and from the profile curvature view point, the straight and concave hillslopes become unstable faster than the others.

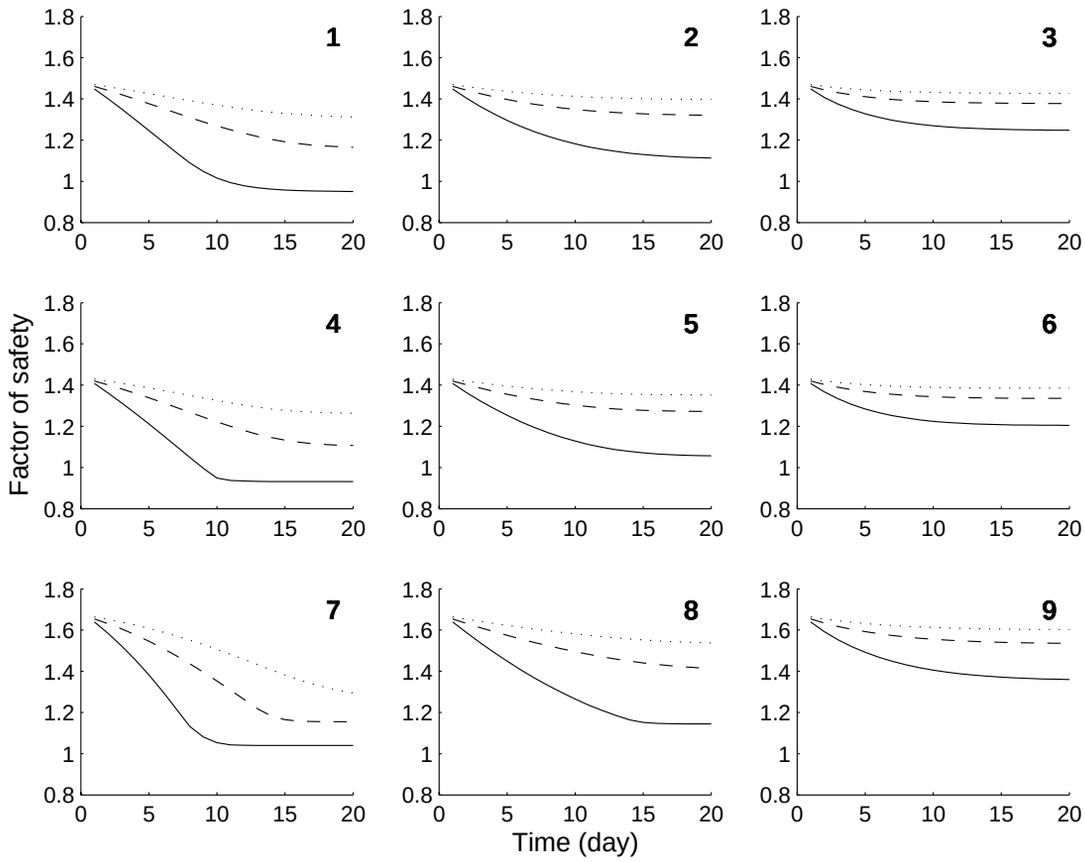

Figure 4.4: Variations of the safety factor in different hillslopes (Figure 4.2) by changing the recharge rate from 10 (dotted line), via 20 (dashed line) to 50 (solid line) mmd^{-1} ($\beta = \phi$).

4.3.3. Effect of slope angle change

The hillslope stability has also been investigated for different slope angles. Figure 4.5 illustrates how by varying the slope angle, *FS* is changed. The variations are completely regular in all hillslopes and for all slope angles. Comparison of Figures 4.4 and 4.5 shows that in a specific hillslope, by changing the slope angle, *FS* also changes regularly whilst by changing the plan shape and slope curvature, the variations of *FS* are different for each hillslope type. This means that in addition to the slope angle, the plan shape and slope curvature should be incorporated as additional key factors in slope stability models. As can be seen in Figure 4.5, when $\beta = \phi$, all convergent hillslopes (1, 4, and 7) become unstable ($FS < 1$) a few days after the onset of rainfall, whilst other hillslopes remain stable. This means that for steep slopes and for shallow landslides, the effect of plan shape on hillslope stability is much more important than that of profile curvature.

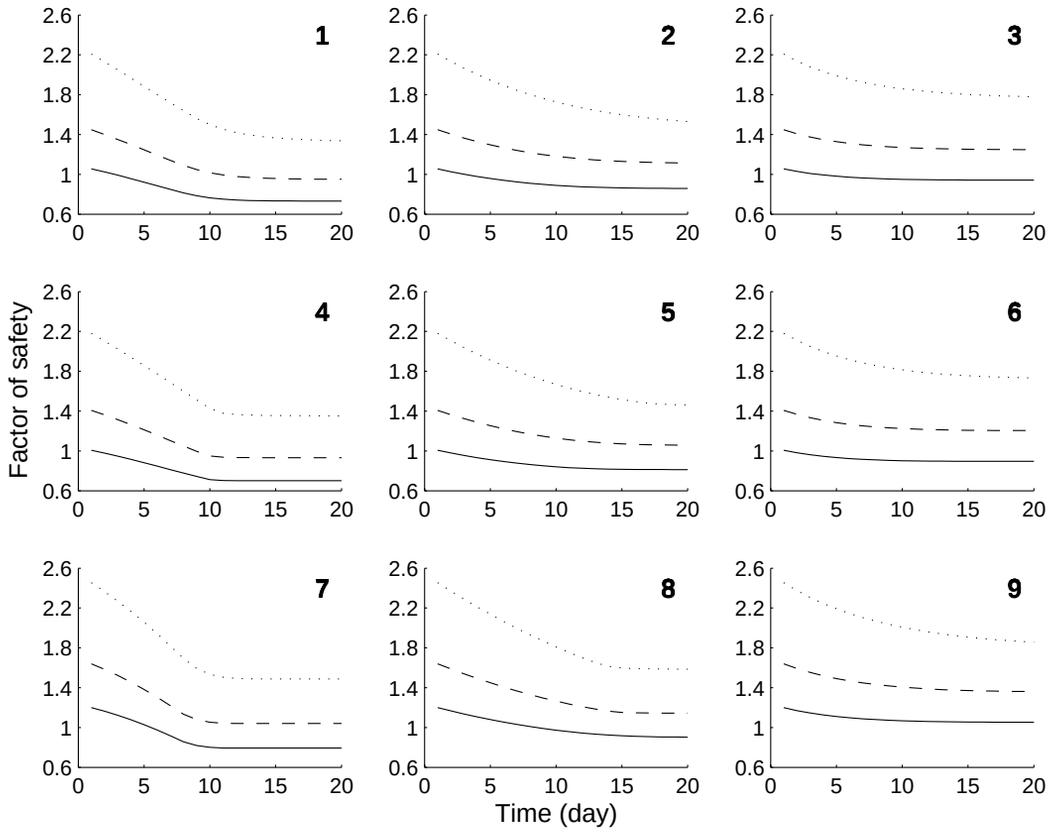

Figure 4.5: Variations of the safety factor in different hillslopes (Figure 4.2) by changing the slope angle from 20 (dotted line), via 30 (dashed line) to 40 (solid line) degrees (N=50 mmd^{-1}).

4.3.4. The relation between subsurface flow and hillslope stability

With respect to the important role of subsurface flow on slope stability (e.g. *Borga et al.*, 2002; *Matsushi et al.*, 2006), the relation between variations of subsurface flow and *FS* has also been studied. Figure 4.6 illustrates how the variations of *FS* and subsurface flow at the outlet are almost each other's mirror image: when subsurface flow increases, slope stability decreases in all hillslopes and vice versa. When the water table reaches a constant (steady-state), subsurface flow and *FS* obviously also become constant. Also at the moment when subsurface flow rate becomes maximum, the *FS* approaches its minimum. Moreover, the time to reach the steady-state condition and constant *FS* are different in all hillslopes. In the concave convergent hillslopes (Figure 4.6, no.1), it takes less time and in the convex divergent hillslopes (Figure 4.6, no. 9) it takes longer than in the others. This is because the convergent hillslopes, due to the reduced flow domain near the outlet, drain much slower than the divergent hillslopes (*Troch et al.*, 2003), and as a result build up saturated storage much quicker. Note that when the subsurface flow reaches a constant (steady-state) with respect to recharge rate (N=50 mmd^{-1}), the subsurface flow at the outlet for some hillslopes is less than 20 mmd^{-1}. This is because in these hillslopes flow concentrates near the outlet region, resulting in overland flow. Finally, based on the Figure 6 it can be concluded that when the hillslope shape changes from divergent to convergent (with the same rainfall), hillslopes

become unstable earlier. On the other hand, when profile curvature changes from convex to concave, hillslopes also become unstable faster.

Sidle and Ochiai (2006) note that spatial and temporal variability in subsurface flow may be strongly linked to three-dimensional preferential flow networks at the hillslope scale and may can exert a huge effect on landslide initiation. However, our model cannot address this issue and to better understand the effect of preferential flow on hillslope stability, it is necessary to evaluate or spatially simulate a likely array of pathways rather than simply preferential fluxes (*Sidle and Ochiai*, 2006).

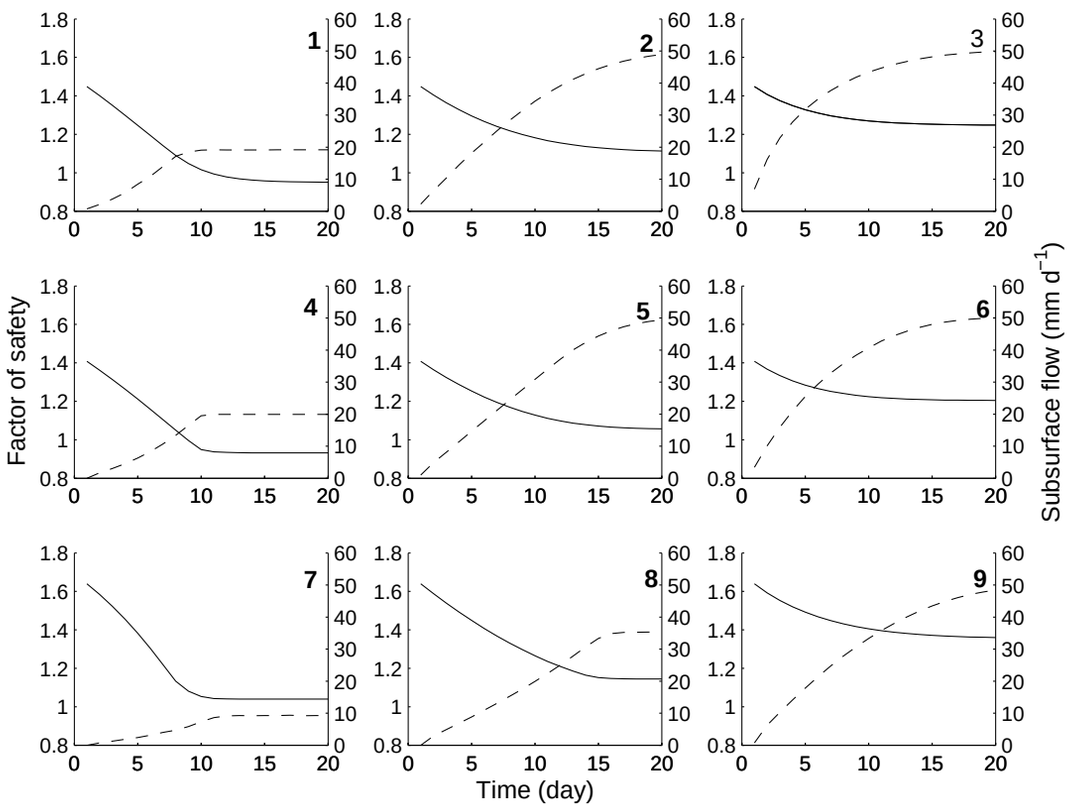

Figure 4.6: The relation between subsurface flow (dotted line) and hillslope stability (solid line) in different hillslopes ($\beta = \phi$ and N=50 mmd^{-1}).

4.4. Conclusion

In this paper we have presented a physically-based hillslope stability model to investigate the hydrologic control of shallow landsliding for complex hillslopes (HSB-SM). The model is based on a combination of the hillslope-storage Boussinesq model (HSB) (*Troch et al.*, 2003; *Hilberts et al.*, 2004) and the infinite slope stability method based on the Mohr-Coulomb failure law. The HSB model is based on the continuity and Darcy equations in terms of storage along the hillslope. The resulting HSB-SM model shows that the dynamic response of complex hillslopes during drainage and recharge events depends very much on the slope angle, plan shape and slope curvature. We have focused on the study of flow

processes in the situation where the topographic relief and the shallow subsurface moisture control the storage and stability of the hillslope.

We have also combined the coupled system for soil moisture storage in the saturated and unsaturated zone (*Hilberts et al.*, 2007) with the infinite slope method to investigate the effects of unsaturated storage variations on hillslope stability in complex hillslopes. Our analysis shows that there is not a large difference between both methods, illustrating that the variations of the unsaturated zone storage can be ignored safely in the dynamic slope stability analysis for shallow landslides. Therefore, it can be concluded that the presented model (HSB-SM) can be used safely for hillslope stability analysis in complex hillslopes under dynamic hydrological conditions. Furthermore, this model allows to investigate the relation between subsurface flow and slope stability in hillslopes with different plan shapes and different slope curvatures.

Based on our analysis, the minimum safety factor (*FS*) coincides with the maximum rate of subsurface flow. In fact, an increase of subsurface flow, leads to a decrease of stability in all hillslopes and vice versa. Consequently, after a certain period of rainfall, the convergent hillslopes with concave and straight profiles become unstable faster than others. However, the divergent convex hillslopes remain stable even after intense rainfalls. Finally, it can be concluded that, in addition to the average bedrock slope angle, topographic characteristics (especially profile curvature and plan shape) of the hillslope control the subsurface flow as well and this process affects hillslope stability by changing the soil strength. As the current model is limited to event-based analyses, further research is needed to present a probabilistic model of rainfall-triggered shallow landslides for complex hillslopes with changing rainfall input and soil depth.

Chapter 5

Application of a probabilistic model of rainfall-induced shallow landslides to complex hollows

This chapter is based on the submitted paper **Talebi, A., R. Uijlenhoet and P. A. Troch (2007),** Application of a probabilistic model of rainfall-induced shallow landslides to complex hollows, *Natural Hazards and Earth System Sciences*

5. Application of a probabilistic model of rainfall-induced shallow landslides to complex hollows

Abstract

Recently, *D'Odorico and Fagherazzi* (2003) proposed "A probabilistic model of rainfall-triggered shallow landslides in hollows" (Water Resour. Res., 39(9), 2003). Their model describes the long-term evolution of colluvial deposits through a probabilistic soil mass balance at a point. Further building blocks of the model are: an infinite-slope stability analysis; a steady-state kinematic wave model (KW) of hollow groundwater hydrology; and a statistical model relating intensity, duration, and frequency of extreme precipitation. Here we extend the work of *D'Odorico and Fagherazzi* (2003) by incorporating a more realistic description of hollow hydrology (hillslope storage Boussinesq model, HSB) such that this model can also be applied to more gentle slopes and hollows with different plan shapes. We show that results obtained using the KW and HSB models are significantly different as in the KW model the diffusion term is ignored. We generalize our results by examining the stability of several hollow types with different plan shapes (different convergence degree). For each hollow type, the minimum value of the landslide-triggering saturated depth corresponding to the triggering precipitation (critical recharge rate) is computed for steep and gentle hollows. Long term analysis of shallow landslides by the presented model illustrates that all hollows show a quite different behavior from the stability view point. In hollows with more convergence, landslide occurrence is limited by the supply of deposits (supply limited regime) or rainfall events (event limited regime) while hollows with low convergence degree are unconditionally stable regardless of the soil thickness or rainfall intensity. Overall, our results show that in addition to the effect of slope angle, plan shape (convergence degree) also controls the subsurface flow and this process affects the probability distribution of landslide occurrence in different hollows. Finally, we conclude that incorporating a more realistic description of hollow hydrology (instead of the KW model) in landslide probability models is necessary, especially for hollows with high convergence degree which are more susceptible to landsliding.

Key words: probabilistic model, shallow landslides, complex hollows, HSB model

5.1. Introduction

The relationship between the return period of rainfall and shallow landslides has attracted the interest of numerous researchers (e.g. *Dietrich and Dunne*, 1978; *Montgomery et al.*, 1998; *Iverson*, 2000; *D'Odorico et al.*, 2005; *Rosso et al.*, 2006) because rainfall is the most frequent landslide-triggering factor in many regions in the world. In steep soil-mantled landscapes, landslides tend to occur in topographic hollows due to convergence of water and accumulation of colluvial soils that leads to a cycle of periodic filling and excavation by landsliding (*Dietrich and Dunne*, 1978).

Shallow landsliding is a stochastic process, and understanding what controls the return period is crucial for risk assessment (*Sidle et al.*, 1985; *Iida*, 1999; *D'Odorico and Fagherazzi*, 2003). Observations of repeated landslides in certain areas indicate that for some slopes and soil properties there exist a threshold of soil thickness, beyond which failure must occur, provided the slope gradient is greater than the angle of internal friction of the failure surface (*Sidle and Ochiai*, 2006). Therefore, to estimate the long-term susceptibility to shallow landsliding, a combined model of soil depth development and rainstorm occurrence is needed, since both of these factors control the recurrence interval of shallow landsliding (*Iida*, 2004).

Recently *D'Odorico and Fagherazzi* (2003) have presented a probabilistic model of rainfall-triggered shallow landslides in hollows and showed that landslide frequency is linked to the rainfall intensity-duration-frequency characteristics of the region. They developed a stochastic model that computes the temporal evolution of regolith thickness in a hollow and hollow hydrologic response to rainfall based on a steady-state kinematic wave model for subsurface flow. In this research, we will use some elements of this model (stochastic soil mass balance) to simulate the soil production (colluvial deposit) and soil erosion (landslide) in time for hollows with complex shapes. Although our model is similar to that presented by *D'Odorico and Fagherazzi* (2003) in that it is a probabilistic model of rainfall-induced shallow landslides, there is an important difference. Convergent plan shapes or concave profile curvatures cause the kinematic wave model to perform relatively poorly even in steep slopes (*Hilberts et al.*, 2004). *Troch et al.* (2003) observed that hillslope plan shape rather than mean bedrock slope angle determines the validity of the kinematic wave approximation to describe the subsurface flow process along complex hillslopes. Therefore, incorporating a more realistic description of hollow hydrology in the stochastic landslide model is needed, as hollows are generally convergent (e.g. *Hack*, 1965; *Reneau and Dietrich*, 1987) and hollows with more convergence have more potential for landslide occurrence.

To investigate the role of rain infiltration on landslide triggering, some investigators (e.g. *Iverson*, 2000) have employed the Richards equation to assess the effects of transient rainfall on the timing, rate and location of landslides. However, the Richards equation is highly complex and requires the solution of large systems of equations even for small problems (*Paniconi et al.*, 2003). *Troch et al.* (2003) introduced the hillslope-storage Boussinesq (HSB) model to describe subsurface flow and saturation along geometrically complex hillslopes. This model is formulated by expressing the continuity and Darcy

equations in terms of soil storage as the dependent variable. The resulting HSB model shows that the dynamic response of complex hillslopes during drainage and recharge events depends very much on the slope angle, plan shape and profile curvature (*Troch et al.*, 2003; *Hilberts et al.*, 2004; *Berne et al.*, 2005; *Hilberts et al.*, 2007). The HSB model can be linearized and further reduced to an advection-diffusion equation for subsurface flow in hillslopes with constant bedrock slopes and exponential width functions (*Berne et al.*, 2005).

To relax the KW assumptions, in this paper we substitute the linearized steady-state HSB model in the work of *D'Odorico and Fagherazzi* (2003) for complex hollows (hollows with different length, slope angle and convergence degree). In fact, using an exponential width function, hollows with different convergence degree is presented and then for each hollow the critical soil depth, the minimum value of landslide-triggering saturated depth and the minimum rainfall intensity needed to trigger a landslide along hollow length are computed. Moreover, the temporal evolution of colluvium thickness is studied through a stochastic soil mass balance. Therefore, by considering the soil production function and hydrology condition in the different hollows, stability of each hollow is analyzed by the infinite slope stability method. Finally, the generalized model helps to investigate the relation between rainfall characteristics (intensity and duration), water table depth and slope stability of colluvial deposits in complex hollows.

5.2. Model formulation

5.2.1 Hollow geometry

Topography influences shallow landslide initiation through both concentration of subsurface flow and the effect of slope gradient on slope stability (*Montgomery and Dietrich*, 1994). Slope failure often occurs in areas of convergent topography where subsurface soil water flow paths give rise to excess pore-water pressures downslope (*Wilkinson et al.*, 2002; *Talebi et al.*, 2007a, 2007c). In most models of slope stability only the slope angle is considered. Although slope gradient is an important factor in landslide initiation, other geometric characteristics (such as profile curvature and plan shape) also control the hydrological process (*Hilberts et al.*, 2004) and as such affect hillslope stability (*Talebi et al.*, 2007b). The plan shape defines topographic convergence which is an important control on subsurface flow concentration. Several investigations (e.g. *Fernandes et al.*, 1994; *Montgomery et al.*, 1997; *Tsuboyama et al.*, 2000; *Troch et al.*, 2002; *Hilberts et al.*, 2004) have shown that hillslopes with convergent plan shape tend to concentrate subsurface water into small areas of the slope, thereby generating rapid pore water pressure increases during rain storms.

We consider only hollows with moderate to steep slopes and shallow, permeable soils overlying a straight bedrock where subsurface storm flow is the dominant flow mechanism. Shallow soils are most prone to rain-induced landslides. It is assumed that the plan shape of the hollow can be described using an exponential width function:

$$w(x') = w_o e^{ax'} \Rightarrow A(x') = \frac{w_0}{a}\left(e^{aL'} - e^{ax'}\right), \tag{5.1}$$

where w is the hollow width (deposits) along the x' direction (see Figure 4.1), x' is the distance from the outlet of hollow parallel to bedrock), w_o is the hollow width at the outlet, A is the hollow area, L' is the hollow length and a is a plan shape parameter. Allowing this plan shape parameter to assume either a positive, zero, or negative value, one can define several basic geometric relief forms: $a>0$ for convergent, $a<0$ for divergent and $a=0$ for parallel shapes. As hollows are generally convergent (e.g. *Hack*, 1965; *Reneau and Dietrich*, 1987), we will assume a wide range of positive numbers for convergent hollows.

As the purpose of this study is to investigate the effect of hollow geometry and hydrology on landslide probability, we employ the subsurface flow similarity parameter for complex hollows proposed by *Berne et al.* (2005). This dimensionless parameter, the hillslope Péclet number, is defined for subsurface flow as the ratio between the characteristic diffusive time and the characteristic advective time, taken from the middle of the hillslope:

$$Pe = \left(\frac{L'}{2pD'}\right)\tan\beta - \left(\frac{aL'}{2}\right), \tag{5.2}$$

where p is a linearization parameter, D' is the soil depth and β is the bedrock slope angle. As can be seen, Pe is a function of three independent dimensionless groups: $L'/(2pD')$, $\tan\beta$ and $aL'/2$; $L'/(2pD')$ represents the ratio of the half length and the average depth of the aquifer (related to the hollow hydrology), and $\tan\beta$ and $aL'/2$ define the hollow geometry (see *Berne et al.*, 2005).

5.2.2 Hollow stability

Planar infinite slope analysis has been widely applied to the determination of natural slope stability, particularly where the thickness of the soil mantle is small compared with the slope length and where landslides are due to the failure of a soil mantle that overlies a sloping drainage barrier (*Borga et al.*, 2002). *Iida* (1999) used the same approach in his stochastic hydro-geomorphological model for shallow landsliding due to rainstorms. He states that the two-layer model of soil (regolith) and bedrock, which assumes a potential landsliding (soil) layer, is suitable for the slope stability analysis in case of shallow landsliding. In this study the slope stability model is based on a Mohr-Coulomb failure law applied to an infinite planar slope. The failure condition can be expressed as (e.g. *Montgometry and Dietrich*, 1994; *D'Odorico and Fagherazzi*, 2003):

$$\gamma_{sat} D' \sin\beta = c_t + \left(\gamma_{sat} D' \cos\beta - \gamma_w h' \cos\beta\right)\tan\phi \tag{5.3}$$

where γ_{sat} and γ_w are the specific weights of saturated soil and water respectively, β is the bedrock slope angle, ϕ is the soil repose angle, c_t is the soil cohesion and h' is the saturated water depth, with both h' and D' (deposit thickness) being measured perpendicularly to the bedrock.

By solving Equation (5.3) for h', the minimum value of landslide-triggering saturated depth (h_{cr}) can be obtained as (*D'Odorico and Fagherazzi*, 2003):

$$h_{cr} = \frac{\gamma_{sat}}{\gamma_w} D' \left(1 - \frac{\tan\beta}{\tan\phi} \right) + \frac{c_t}{\gamma_w \tan\phi \cos\beta} \tag{5.4}$$

When the soil depth (D') is equal to h_{cr}, the critical soil depth or immunity depth (D_{cr}) is given as follows (e. g. *Iida*, 1999; *D'Odorico and Fagherazzi*, 2003):

$$D_{cr} = \frac{c_t}{\gamma_w \tan\phi \cos\beta + \gamma_{sat} \cos\beta (\tan\beta - \tan\phi)} \tag{5.5}$$

As long as $D' < D_{cr}$, no shallow landslide will occur as the depth h' of the saturated layer cannot reach the critical value h_{cr}, even following an intense rainstorm. For this reason the period during which $D' < D_{cr}$ may be named "immunity period" (*Iida*, 1999; *D'Odorico and Fagherazzi*, 2003). In gentle slopes (in contrast to steep slopes), an increase in colluvium thickness increases stability. Hence, for gentle slopes the likelihood of landslide occurrence is maximum when $D' = D_{cr}$ and decreases for larger values of D' (e.g. *Iida*, 1999; *D'Odorico and Fagherazzi*, 2003). For steep slopes the occurrence of a rainstorm can lead to landsliding as soon as the soil depth starts to exceed the critical depth.

The hydrogeomorphological significance of these equations is as follows:

-When $D' < D_{cr}$, no shallow landsliding occurs and the slope is stable (independent of rainfall).

-When $D' > D_{cr}$, the water table depth (h') can exceed h_{cr} during a rainstorm, potentially leading to shallow landsliding.

In the case of relatively steep slopes ($\beta > \phi$), h_{cr} decreases linearly (i.e. stability decreases) with an increase of soil depth D' (see Equation (5.4)). The soil depth $D_{\max}$ for which shallow landsliding can occur without saturated throughflow (corresponding to $h_{cr} = 0$) is (*Iida*, 1999):

$$D_{\max} = \frac{c_t}{\gamma_{sat} \cos\beta (\tan\beta - \tan\phi)} \tag{5.6}$$

In practice, $D_{\max}$ is never reached because the soil depth increases slowly with time (see section 5.2.5) and periodic rainstorms will produce at least some saturated subsurface flow and consequently destabilization at thicknesses less than $D_{\max}$. Therefore, according to this model, shallow landsliding occurs when the soil depth D' ranges between D_{cr} and $D_{\max}$. Note that in the case of relatively gentle slopes ($\beta < \phi$), h_{cr} increases linearly (i.e. stability increases) with an increase of D', hence no upper limit to the soil depth ($D_{\max}$) exists. This means that for gentle slopes, the likelihood of landslide occurrence is maximum when $D' = D_{cr}$.

5.2.3 Hollow Hydrology

Hillslope hydrological response has traditionally been studied by means of hydraulic groundwater theory (*Troch et al.*, 2003). In many regions, groundwater flow is the main source of streamflow between rainfall events. The basic macroscopic equation describing the movement of water in the soil is known as the three-dimensional Richards' equation. It is highly complex and requires the solution of relatively large systems of equations even for small problems (*Paniconi et al.*, 2003).

To incorporate the hydrological process in hillslope stability analysis, many researchers (e.g. *Montgomery and Dietrich*, 1994; *Wu and Sidle*, 1995; *D'Odorico and Fagherazzi*, 2003) have used kinematic wave hydrology (KW). When water table gradients are high and bedrock slopes are relatively small, diffusive effects become important. In such hillslopes (e.g. convergent and gentle hillslopes) the KW model shows a relatively poor match to the Richards' model (*Hilberts et al.*, 2004). Therefore, we propose to relax the KW assumption in hillslope stability analysis.

Troch et al. (2003) reformulated the continuity and Darcy equations in terms of storage along the hillslope, which leads to the hillslope storage Boussinesq (HSB) equation for subsurface flow in hillslopes. Extending *Brutsaert's* (1994) analysis, they linearized this equation as:

$$\frac{\partial S'}{\partial t} = K\frac{\partial^2 S'}{\partial x'^2} + U\frac{\partial S'}{\partial x'} + Nw \tag{5.7}$$

with $K = \dfrac{k_s pD' \cos\beta}{f}$ and $U = \dfrac{k_s \sin\beta}{f} - aK$

where S' is the subsurface saturated storage, N is the recharge to the ground water table, k_s is the saturated hydraulic conductivity and f is the drainable porosity (note that the value of p is determined iteratively as pD' should be equal to the average water table height $\int_0^{L'} S'(x')dx'/(Af)$ where A is the hollow drainage area). The assumptions are that the recharge rate of subsurface flow is equal to the rainfall intensity and that water flows parallel to bedrock. Comparison between the hillslope-storage Boussinesq and Richards' equation models for various scenarios and hillslope configurations shows that the HSB model is able to capture the general features of the storage and outflow responses of complex hillslopes (*Paniconi et al.*, 2003; *Hilberts et al.*, 2004). *Berne et al.* (2005) derived the steady-state solution of Equation (5.7), with a zero-storage downstream boundary condition and a zero-flux upstream boundary condition, for a given recharge N as:

$$S'(x') = \frac{Nw_0}{a}\left[\frac{e^{aL'}}{U}\left(1 - e^{-\frac{U}{K}x'}\right) + \frac{1}{(Ka+U)}\left(e^{-\frac{U}{K}x'} - e^{ax'}\right)\right] \tag{5.8}$$

For parallel hillslopes ($a = 0$), this reduces to:

$$S'(x') = \frac{Nw_0}{U}\left[\left(\frac{K}{U} + L'\right)\left(1 - e^{-\frac{U}{K}x'}\right) - x'\right] \tag{5.9}$$

According to the definition of the storage S', the mean groundwater table height (over the hillslope width) is:

$$\overline{h'}(x') = \frac{S'(x')}{fw(x')} = \frac{Ne^{-ax'}}{af}\left[\frac{e^{aL'}}{U}\left(1-e^{-\frac{U}{K}x'}\right)+\frac{1}{(Ka+U)}\left(e^{-\frac{U}{K}x'}-e^{ax'}\right)\right] \tag{5.10}$$

Again, for parallel hillslopes this reduces to:

$$\overline{h'}(x') = \frac{N}{fU}\left[\left(\frac{K}{U}+L'\right)\left(1-e^{-\frac{U}{K}x'}\right)-x'\right] \tag{5.11}$$

The x-coordinate x'_m where the mean groundwater table height is maximum (the critical point for slope stability), can be obtained by solving $\overline{h'}(x'_m)=0$ (see *Berne et al.*, 2005):

$$x'_m = \frac{K}{U}\ln\left[1+\frac{U}{Ka}\left(1-e^{-aL'}\right)\right] \tag{5.12}$$

which for parallel hillslopes reduces to $x'_m = \frac{K}{U}\ln\left(1+\frac{UL'}{K}\right)$.

Now, by substituting the Equation (5.12) into Equations (5.10) or (5.11), we can obtain the maximum groundwater table depth in each hillslope (which is critical for landslide occurrence):

$$\overline{h'}(x'_m) = \frac{N}{fa(aK+U)}\left\{e^{aL'}\left[1+\frac{U}{aK}\left(1-e^{-aL'}\right)\right]^{-\frac{aK}{U}}-1\right\} \tag{5.13}$$

which for parallel hillslopes reduces to:

$$\overline{h'}(x'_m) = \frac{N}{fU}\left[L'-\frac{K}{U}\ln\left(1+\frac{UL'}{K}\right)\right] \tag{5.14}$$

Equating $\overline{h'}(x'_m)$ and h_{cr}, the critical rainfall intensity for triggering landslides (R_{cr}) can now be calculated as:

$$R_{cr} = \frac{h_{cr}fa(aK+U)}{\left\{e^{aL'}\left[1+\frac{U}{aK}\left(1-e^{-aL'}\right)\right]^{-\frac{aK}{U}}-1\right\}} \tag{5.15}$$

which for parallel hillslopes ($a=0$) reduces to:

$$R_{cr} = \frac{fUh_{cr}}{L'-\frac{K}{U}\ln\left(1+\frac{UL'}{K}\right)} \tag{5.16}$$

Note that Equations (5.15) and (5.16) illustrate how R_{cr} (the minimum rainfall intensity needed to trigger a landslide) is a function of the deposit thickness (D_{cr}).

To compare with the linearized HSB model, we also derive the steady-state solution of Equation (5.7) for a given recharge *N* under the KW assumption $(K=0)$as:

$$S'(x') = \frac{Nw_0}{Ua}\left(e^{aL'} - e^{ax'}\right) \Rightarrow \overline{h'}(x') = \frac{S'(x')}{fw(x')} = \frac{N}{Uaf}\left(e^{a(L'-x')} - 1\right) \tag{5.17}$$

As $x'_m = 0$ (in the KW case), then:

$$\overline{h'}(x'_m) = \frac{N}{Uaf}\left(e^{aL'} - 1\right) \tag{5.18}$$

Now, the critical rainfall intensity for triggering landslides (R_{cr}) can be calculated as:

$$R_{cr} = \frac{Uafh_{cr}}{e^{aL'} - 1} \tag{5.19}$$

Note that for parallel hillslopes ($a = 0$), these equations reduce to:

$$S'(x') = \frac{Nw_0}{U}\left(L' - x'\right) \Rightarrow \overline{h'}(x') = \frac{N}{Uf}\left(L' - x'\right) , \tag{5.20}$$

$$\overline{h'}(x'_m) = \frac{NL'}{Uf} \tag{5.21}$$

and

$$R_{cr} = \frac{Ufh_{cr}}{L'} = \frac{h_{cr}k_s \sin\beta}{L'} \tag{5.22}$$

D'Odorico and Fagherazzi (2003) have presented critical rainfall intensity equal to $R = h'k_s w_0 \sin\beta / A$ for all hollow shapes and based on the KW assumptions. As can be seen, this equation is similar to Equation (5.22) which has been presented based on the KW assumptions and for parallel hollows. As we will show, the results of the KW and HSB models for hollow hydrology differ significantly (especially for hollows with high convergence degree) and this affects landslide probability.

The analysis of landslide frequency also requires the estimation of the duration of the triggering rainfall. For this purpose, *D'Odorico and Fagherazzi* (2003) applied the rational method (e.g. *Chow et al.*, 1988) to the subsurface flow in hollows to determine the most critical storm duration for a given return period. The rational method assumes that the time of concentration (T_c) is the most critical storm duration. Thus the maximum saturated depth generated by storms of a given frequency is due to events of duration T_c . Here, we update the way in which the time of concentration is calculated to make it fully consistent with the linearized steady-state HSB model. Hence, the concentration time can be expressed as:

$$T_c = \int_{x_m}^{L'} \frac{S'(x')}{Q(x')} dx' \tag{5.23}$$

with $Q(x) = \begin{cases} \dfrac{Nw_0}{a}\left(e^{aL'} - e^{ax'}\right) & (a \neq 0) \\ Nw_0\left(L' - x'\right) & (a = 0) \end{cases}$

In the KW limit this reduces to $T_c = L'/U$, which for parallel hillslopes can be written as $T_c = L'f/\left(k_s \sin\beta\right)$. *D'Odorico and Fagherazzi* (2003) expressed the concentration time as $T_c = C\sqrt{A}/\left(k_s \sin\beta\right)$, where C is a dimensionless coefficient accounting for other factors

affecting the concentration time and A is the hollow contributing area. This suggests that an equivalent hollow length can be estimated as $L' = C\sqrt{A}/f$. According to the exponential width function, Equation (5.1), the contributing area is $A = w_0\left(e^{aL'} - 1\right)/a$. This provides an implicit equation to estimate the degree of convergence of an equivalent exponential hollow from given values of A, w_o, and L'.

5.2.4 Return period of the triggering rainfall

Rainfall is considered to be the most important factor in triggering slope failure. To accomplish a hazard analysis of the landslide phenomenon, a probability analysis of intense rainfall occurrence for different return periods is needed. The objective of rainfall frequency analysis is to estimate the amount of rainfall falling at a given point for a specified duration and return period. The frequency of extreme rainfall is usually defined by reference to the annual maximum series, which comprises the largest values observed in each year. The Gumbel distribution has been the most common probabilistic model used in modelling hydrological extremes (*Brutsaert*, 2005). Since landslides are triggered by extreme rainfalls, following *D'Odorico and Fagherazzi* (2003), we use a Gumbel distribution to express the dependence between annual maximum rainfall intensity for events of duration T_c and return period T_r as follows:

$$\frac{1}{T_r} = \lambda = 1 - \exp\left[-\exp\left(-\frac{R(T_c) - u}{v}\right)\right] \tag{5.24}$$

where T_r is the return period, $R(T_c)$ is the annual maximum rainfall intensity of duration T_c, u and v are the parameters of the Gumbel distribution and λ is the probability that the maximum intensity exceeds $R(T_c)$ in a given year. As our model is applied to a parameter set (for four realistic hollows) derived from published data from the Oregon Coastal range (e.g. *Montgomery et al.*, 1997; *Torres et al.*, 1998; *Stock and Dietrich*, 2003; *D'Odorico and Fagherazzi*, 2003), based on rainfall data available for the Oregon Coastal range (*Montgomery et al.*, 1997) the relation between u, v and T_c is found to be $u/v = 2.6$ and $v = 4.75\,T_c^{-0.6}$. From the value of T_c in a hollow, the parameters u and v are computed and the return period of the critical rainfall intensity will be determined. Note that $\lambda = 1/T_r$ is a function of the soil depth due to the dependence between the intensity of the triggering precipitation, R_{cr}, and D_{cr} (see Equations (5.15), (5.16), (5.19), and (5.22)).

5.2.5 Temporal evolution of deposit thickness

The temporal evolution of colluvial deposits in hollows can be characterized by a continuous process of deposit accretion, and a discontinuous random process of denudation caused by rainfall-triggered landslides, which scour to the bedrock large portions of the hollow (*D'Odorico and Fagherazzi*, 2003). The temporal evolution of colluvium thickness can thus be studied through a stochastic soil mass balance, accounting for the supply of debris

from the adjacent slopes and for random denudation due to landsliding. The description of the probabilistic soil mass balance model we apply in this study largely follows that of *D'Odorico and Fagherazzi* (2003).

Many studies analyzed the soil production and landscape evolution to investigate the spatial and temporal patterns of soil thickness (e.g. *Kirkby*, 1985; *Dietrich et al.*, 1986; *Heimsath et al.*, 1997; *Heimsath et al.*, 2001). Based on the conservation of mass equation for a tipped triangular trough and slope-dependent transport, *Dietrich et al.* (1986) presented an expression for the rate of colluvium accumulation in hollows. They showed that the rate of accumulation is a function of the side-slope gradient and the difference between the side-slope and hollow gradient. For a hollow composed of a tipped triangular trough and two planar side slopes, the accretion of colluvial deposits can be obtained as (*Dietrich et al.*, 1986):

$$D' = \left[2D_c \cos\beta\left(\tan^2\alpha - \tan^2\beta\right)t\right]^{0.5}, \tag{5.25}$$

where D_c is the soil creep diffusivity, α is the angle between the side slopes and a horizontal plane and t is time. *Dietrich et al.* (1986) also showed that basin form, consisting of noses, side slopes, and a hollow appears to be well represented by the geometry of a tipped triangular trough and typically the ratio of hollow slope to side slope is about 0.8. If we assume that α and β do not vary substantially with time, then Equation (5.25) can be expressed as (*D'Odorico and Fagherazzi*, 2003):

$$D' = \sqrt{Mt}\ ;\ M = 2D_c \cos\beta\left(\tan^2\alpha - \tan^2\beta\right) \tag{5.26}$$

with M being independent of time. The differentiation of Equation (5.26) with respect to time leads to:

$$\frac{dD'}{dt} = l(D') = \frac{M}{2D'} \tag{5.27}$$

showing that the rate of colluvium accretion decreases with the depth, D', of the deposit (*D'Odorico and Fagherazzi*, 2003). Now, the overall temporal evolution of the deposit thickness (D') can be stated as:

$$\frac{dD'}{dt} = l(D') - J(D',t) \tag{5.28}$$

where $l(D')$ is a depth-dependent function of net colluvium accretion expressed by Equation (5.27) and $J(D',t)$ is the rate of soil removed by debris flow and shallow landslides. The latter is modelled as a stochastic Poisson process (*D'Odorico and Fagherazzi*, 2003):

$$J(D',t) = \zeta(D')\sum_i \delta\left(t - t_i\right) \tag{5.29}$$

where

$$\zeta(D') = \begin{cases} 0;\ 0 \le D' \le D_{cr} \\ D';\ D' > D_{cr} \end{cases} \tag{5.30}$$

In this equation δ represents a Dirac-δ function and the sequence t is such that the interarrival time of the triggering precipitation, $\tau = t_{i+1} - t_i$, is an exponentially distributed

random variable. As a result, the temporal variability of colluvium thickness is controlled by the rates of colluvium accretion and erosion (i.e., landslides), and both of them depend on the actual state (i.e., deposit thickness) of the system. Note that the time needed to accumulate a colluvium thickness $D' = D_{cr}$ (T_{im}) is computed as:

$$T_{im} = D_{cr}^2 / \left[2D_c \cos\beta\left(\tan^2\alpha - \tan^2\beta\right)\right] \quad (5.31)$$

.

5.2.6 Numerical simulation of landslide occurence

To simulate the dynamics of complex hollows, the following steps are performed:

- The deposit thickness of a simulated hollow is D'=0 at t=0.
- The linearization parameter (p) is determined iteratively as $p\,D'$ should be equal to average water table depth in each hollow ($\overline{h'}$) and $\overline{h'}$ is calculated using S' (saturated storage, Equation (5.8) and (5.9)). Note that N is also computed iteratively by substituting D_{cr} (in stead of h_{cr}) in Equations (5.15) and (5.16).
- The time of concentration (T_c) of each hollow is determined by Equation (5.23).
- Gumbel rainfall parameters (u and v) are estimated for extreme precipitation of duration T_c.
- The minimum saturated depth (h_{cr}) able to trigger a landslide is calculated from Equation (5.4).
- The critical rainfall intensity (R_{cr}) corresponding to h_{cr} is computed from Equations (5.15) and (5.16).
- The probability that R is exceeded in given year is estimated by from Equation (5.24).
- A random number to determine if a landslide occurs is drawn; if a triggering storm occurs, the landslide scours the hollow entirely.
- The deposit thickness D' increases by transport from uphill based on Equation (5.27). Note that in this model, a landslide occurs when $D_{\max} > D' \geq D_{cr}$.

The presented model, which is an extension of that of *D'Odorico and Fagherazzi* (2003), simulates the long term evolution of soil depth. The extension lies in the fact that the probability distribution of scar depth, landslide return period and colluvium thickness is calculated for complex hollows based on a more realistic description of hollow hydrology (the linearized HSB model). As the aim of this paper is to investigate the effect of geometry and hydrology of hollows on landslide probability, we compare the different approaches of hollow hydrology (KW and HSB models) in hollows with different geometries.

The model is applied to a parameter set (for four hollows) derived from published data from the Oregon Coastal range (e.g. *Montgomery et al.*, 1997; *Torres et al.*, 1998; *Stock and Dietrich*, 2003; *D'Odorico and Fagherazzi*, 2003). To apply the exponential width function to these four hollows (which are convergent, see Figure 2, Montgomery et al., 1997), Equation (5.1) is fitted using the total contributing areas (A), the outlet width (w_o) and the dimensionless coefficient affecting concentration time (C coefficient in Equation 6, *D'Odorico and Fagherazzi*, 2003), as was explained previously after equation (5.23). The

hollow length assuming exponential geometry is estimated by $L' = C\sqrt{A}/f$. Now, from the equivalent hollow length (L'), the plan shape parameter (a) is calculated using the Equation (5.1). Finally, by computing pD' (see Equation (5.2)) in each hollow (iteratively), the subsurface saturated storage is obtained by the HSB model (Equations 5.8 and 5.9).

Table 5.1 lists the values of the hydrological and geotechnical variables used to perform stability analyses in the different hollows and Table 5.2 shows the geometric characteristics of these four hollows. To generalize the obtained results, we also apply the model for a wide range of hollows with different geometric characteristics and different hydrology conditions (different Péclet numbers).

Table 5.1: Hydrological and geotechnical model parameters (Published data from Montgomery et al., 1997).

Parameter name	Symbol	Units	Value in this paper
Saturated hydraulic conductivity	k_s	m d^{-1}	65
Effective porosity	f	-	0.30
Soil cohesion	c_t	kN m^{-2}	11.0
Soil repose angle	ϕ	°	33
Saturated unit weight of soil	γ_{sat}	kN m^{-3}	20.0
Unit weight of water	γ_w	kN m^{-3}	9.81
Diffusivity coefficient	D_c	m^2 yr^{-1}	0.0032
Side slope angle	α	°	$\arctan(\tan\beta / 0.8)$

Table 5.2: Geometric characteristics of four hollows used in this study (Published data from *Montgomery et al.*, 1997; *D'Odorico and Fagherazzi*, 2003). L' and a are determined from Equation (5.1), D_{cr} from Equation (5.5) and T_{im} from Equation (5.31).

Parameter	Symbol	Units	1	2	3	4
Drainage area	A	m^2	3700	860	7500	4500
Bedrock slope angle	β	°	43	43	30	30
Outlet width	w_0	m	12	6	12	12
Length	L'	m	77	37	110	85
Convergence degree	a	m^{-1}	0.030	0.061	0.026	0.029
Immunity depth	D_{cr}	m	1.25	1.25	2.58	2.58
Immunity period	T_{im}	yr	682	682	6389	6389

5.3. Results and discussion

Based on Equation (5.5), the critical soil depth (D_{cr}) for the two steep hollows ($\beta > \phi$) is found to be 1.25 m and for the two gentle hollows ($\beta < \phi$) 2.58 m (see Table 5.2). Table 5.3 and Table 5.4 show the results of the landslide probability analysis for the KW and the HSB model, respectively. They illustrate how the hydrological properties and stability of hollows change as a function of hollow geometry. As can be seen, the values of the concentration time (T_c) are slightly longer for the HSB model than for the KW model. This is because in the KW model the diffusion term is ignored (K=0 in Equation (5.7)). As a result, other parameters (R_{cr} and T_r) for all hollows are also larger for the HSB model. This affects the stability regime, especially in gentle and convergent hollows (see Table 5.4).

Based on the obtained results (Tables 5.3 and 5.4), the immunity period (T_{im}, i.e. the time needed to accumulate a colluvium thickness $D' = D_{cr}$) of hollows 1 and 3 are significantly longer than the return period of the triggering rainfall (T_r). This means that landslide occurrence is limited by the supply of debris from the adjacent slopes, rather than by the occurrence of triggering rainfall. As soon as the soil depth reaches D_{cr}, a landslide will occur shortly. *D'Odorico and Fagherazzi* (2003) denote this regime as "supply limited", indicating that the landslide return period depends first and foremost on soil production. On the other hand, in hollow 2 (where T_{im} is the same as for hollow 1), a higher rainfall intensity is needed to trigger landslides ($T_{im} < T_r$). In that case landslides occur when an extreme

rainfall intensity is able to produce the critical saturated depth (h_{cr}) required for landslide occurrence. This is called the event-limited regime. Hence, it can be concluded that hollow geometry is an important control on subsurface flow response (*Troch et al.*, 2003; *Hilberts et al.*, 2004) and this process affects slope stability (*Talebi et al.*, 2007b).

Table 5.3: Characteristics of hollows based on the kinematic wave assumption.

Parameter	Symbol	Units	1	2	3	4
Time of concentration	T_c	hr	12.5	6.0	24.3	18.8
Critical rainfall intensity	R_{cr}	mm hr^{-1}	7.5	16.1	5.6	9.3
Return period of triggering rainfall	T_r	yr	98	1581	216	6623
Condition	-	-	Supply-limited	Event-limited	Supply-limited	Event-limited to unconditionally stable

Table 5.4: Characteristics of hollows based on the HSB model.

Parameter	Symbol	Units	1	2	3	4
Péclet number	Pe	-	170	74.16	91.7	55.8
Linearization parameter	p	-	0.168	0.184	0.132	0.167
Time of concentration	T_c	hr	13.5	6.4	24.7	19.2
x-coordinate where $h' = h_{\max}$	x'_m	m	1.10	1.02	2.46	2.85
Critical rainfall intensity	R_{cr}	mm hr^{-1}	7.8	17.6	6.1	10.5
Return period of triggering rainfall	T_r	yr	191	5948	481	32342
Condition	-	-	Supply-limited	Event-limited	Supply-limited	Unconditionally stable

Figure 5.1 shows long term simulations of deposit thickness evolution in the four hollows (from top to bottom) and illustrates how shallow landsliding occurs when the soil thickness (D') ranges between D_{cr} and $D_{\max}$. In this figure, left and right columns show the time series of deposit thickness for the KW and HSB models, respectively. As can be seen, the landslide probability analysis for the HSB model (using a more realistic description of hollow hydrology) shows significant differences with respect to the results of the KW model (especially in gentle and convergent hollows, Figure 5.1, last row). Comparison of the results reported in Tables 5.3 and 5.4 with Figure 5.1 also illustrate that the KW model looses its ability in gentle hollows, such as in hollow no. 4, where the stability regime has also been changed. Figure 5.1 also indicates how, as a function of the hollow geometry from steep slopes (top) to gentle slopes (bottom), the landslide probability is changed as well. For instance in hollow 4 (where $T_r >> T_{im}$), landslides never occur and the system can be termed "unconditionally-stable".

Figure 5.2 illustrates the probability distribution of colluvium thickness when a landslide occurs as simulated by the KW model (left column) and the HSB model (right column) (D_{slide}). Note that hollow 4 lies in the unconditionally-stable regime, hence the distribution of D_{slide} can only be presented for the three remaining hollows. These histograms show that not only the different hollows have different distributions of scar depth, but also the results of the KW and HSB models are significantly different. The average (*m*) and standard deviation (*sd*) of histograms in each row shows these differences clearly. As can be seen, the probability of distribution of D_{slide} is concentrated close to the immunity depth (D_{cr}) for the supply-limited case, whereas it is concentrated at significantly larger depths for the event-limited cases.

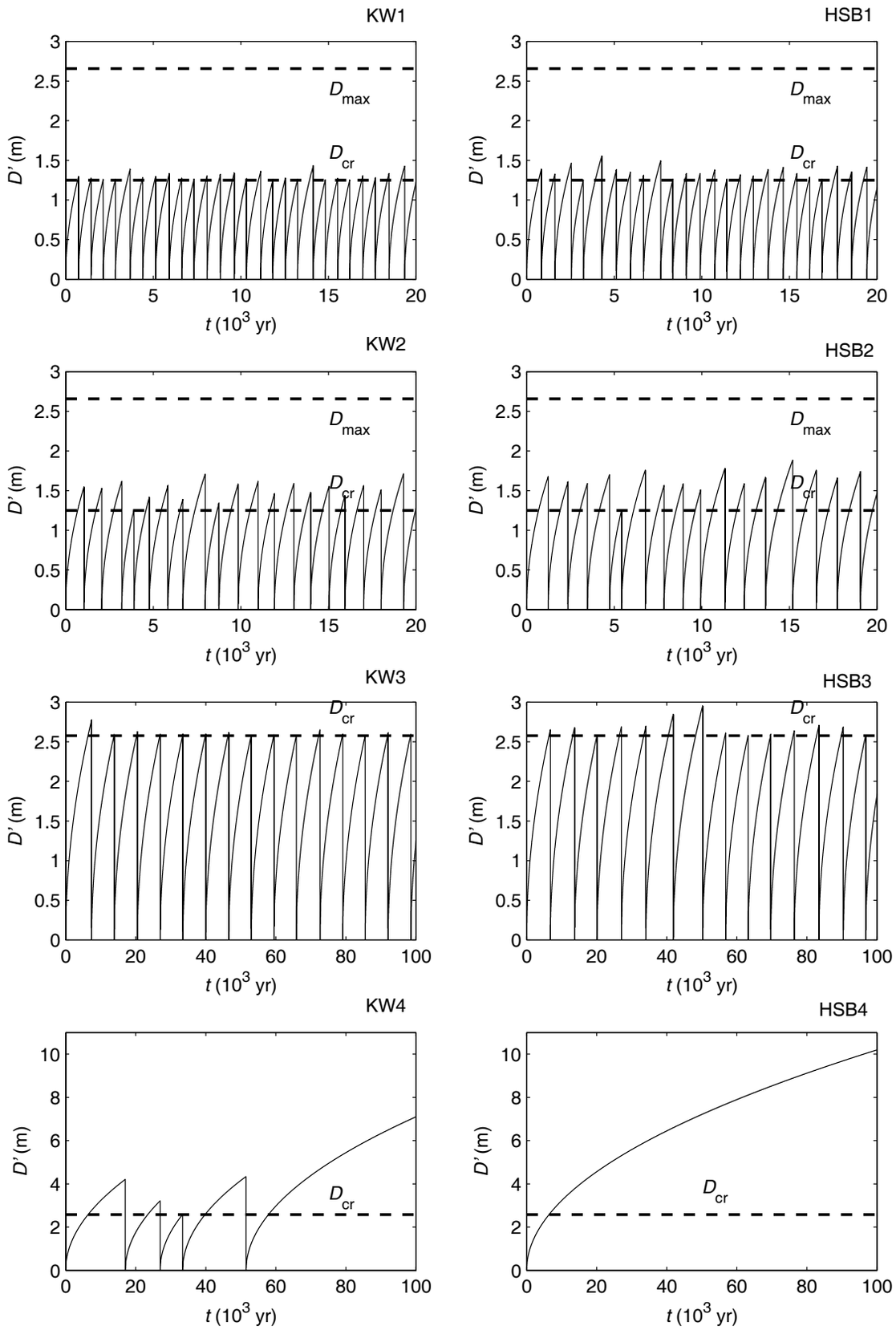

Figure 5.1: Long term simulation of deposit thickness for the four hollows in Table 5.1 (from first to fourth row, respectively). Left column: KW; right column: HSB model.

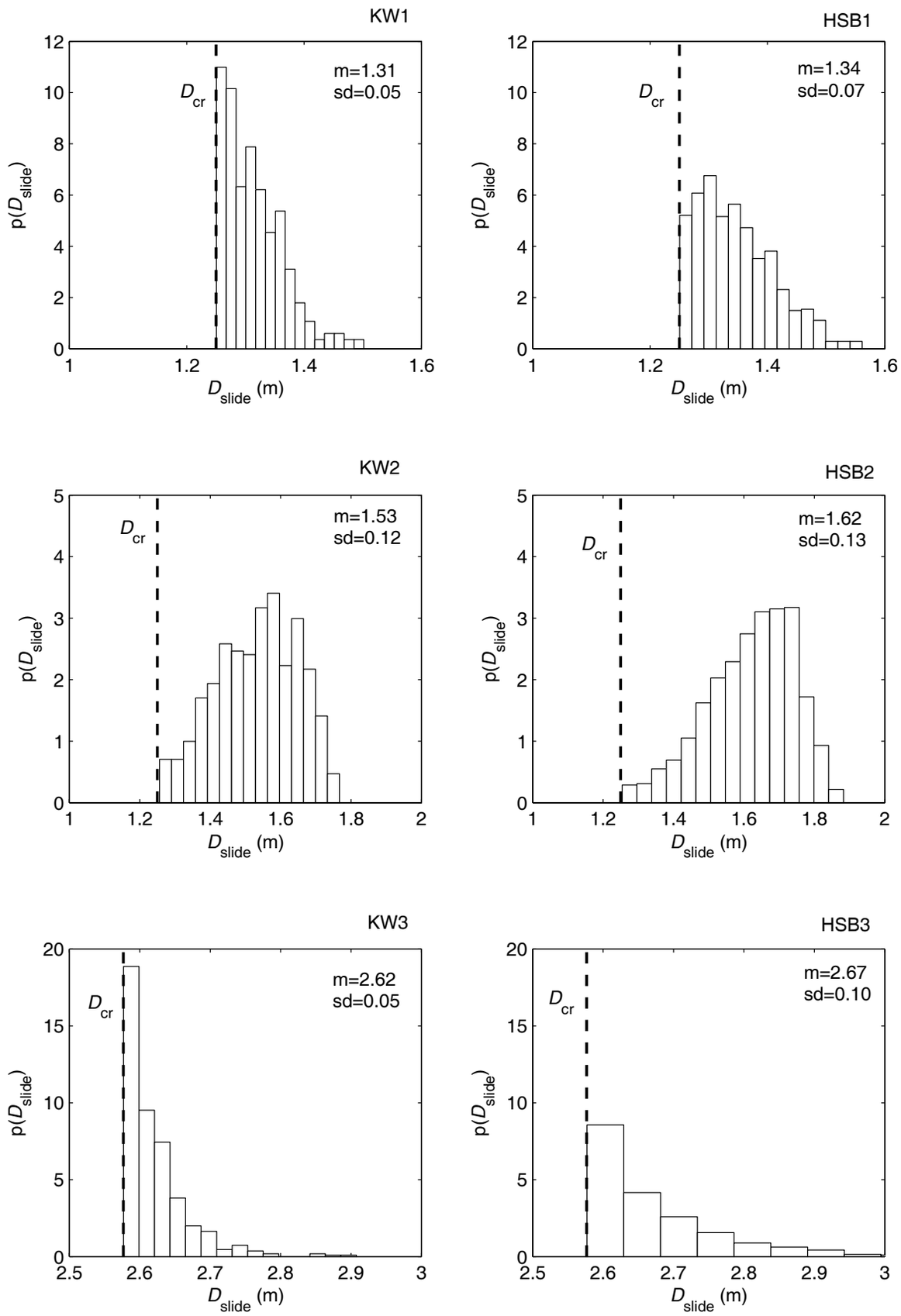

Figure 5.2: Probability distribution of scar depth (colluvium thickness when a landslide occurs) for hollows 1, 2 and 3, respectively. Left column: KW; right column: HSB model.

Figures 5.3 and 5.4 indicate how the probability distributions of the interarrival of the landslide-producing rain events (T_{slide}) and the corresponding rainfall intensities (R_{slide}) vary for the different hollows. As in the previous figure, the left and right columns show the results of the KW model and the HSB model, respectively. These results show that in hollow 1 (which has less convergence and a larger area), T_{slide} is close to T_{im} (supply limited regime), while in hollow 2 (which has more convergence and a smaller area), T_{slide} moves in the direction of T_r (event limited regime). Comparison of the left and right columns in Figure 5.4 also indicates that the values of R_{slide} (the rainfall intensity generating a landslide) are significantly different for the KW and HSB models. This is because the computation of the concentration time of the HSB model (Equation 5.23) includes the effect of diffusion.

Figure 5.5 shows the probability distribution of colluvium thickness for the different hollows corresponding to the KW (left column) and the HSB model (right column). As can be seen, as soon as the soil depth reaches the immunity depth, landslides begin to occur. Hollow 2 (second row in Figure 5.5) shows a significant difference between the KW and HSB models. This is because in hollow 2 (which lies in the event-limited regime), the value of T_r / T_{im} for the KW model is less than for the HSB model, indicating that landslides occur a longer time after D_{cr} for the HSB model. Hence, including a diffusion term in the steady-state hydrological model has a noticeable influence on the landslide probability.

In order to quantify the effect of variations of hollow geometrical parameters (e.g. D', L', A, a and β) and hollow hydrological parameters (e.g. S', h' and p) and to generalize the results obtain, different landslide regimes have been investigated for a wide range of hollow geometrical and hydrological parameters for gentle and steep slopes (see Figure 5.6). As can be seen, by changing the length (L'), slope (β) and shape (a) of several hollows, a wide range of Péclet number (Equation 5.2, dimensionless parameter for hollow geometry and hydrology), corresponding to the immunity period (T_{im}) and return period of triggering rainfall (T_r) has been obtained. In particular, we have investigated the relationship between the Péclet number of a large number of hollows and the ratio of T_r / T_{im}. Based on our model, different regimes can occur, which depend on the ratio between T_r and T_{im} (see Table 5.4). Figure 5.6 summarizes the results of this paper and shows how presented model allows to identify different landslide regimes as a function of hollow geometry, hydrology and climatology. Therefore, Péclet number (pe) as the index of geometry and hydrology, T_{im} as the index of temporal variability of colluvium thickness and T_r as the index of climatology can be used to investigate the probability distribution of shallow landslides in the different hollows.

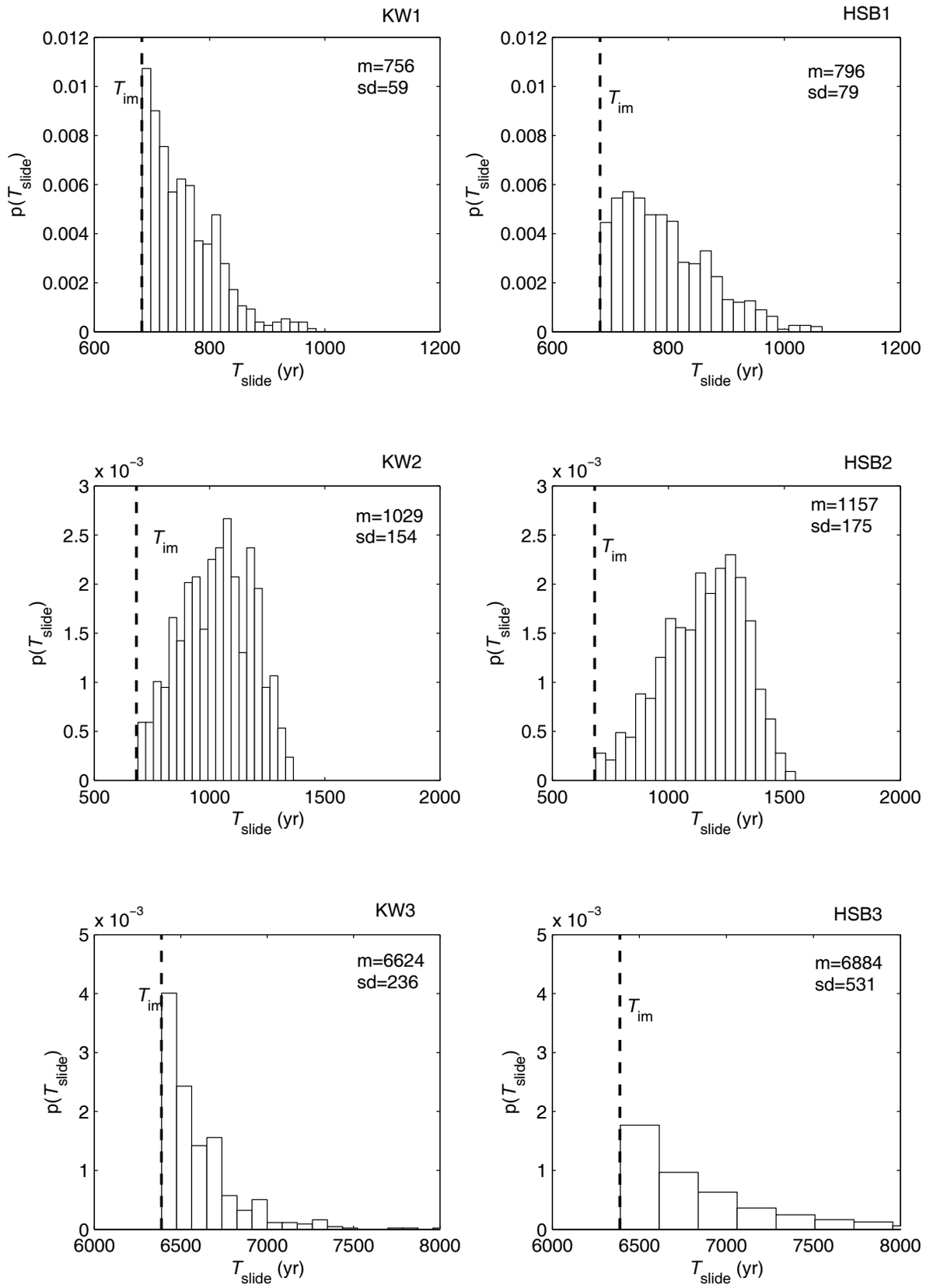

Figure 5.3: Probability distribution of landslide return period for hollows 1, 2 and 3, respectively. Left column: KW; right column: HSB model.

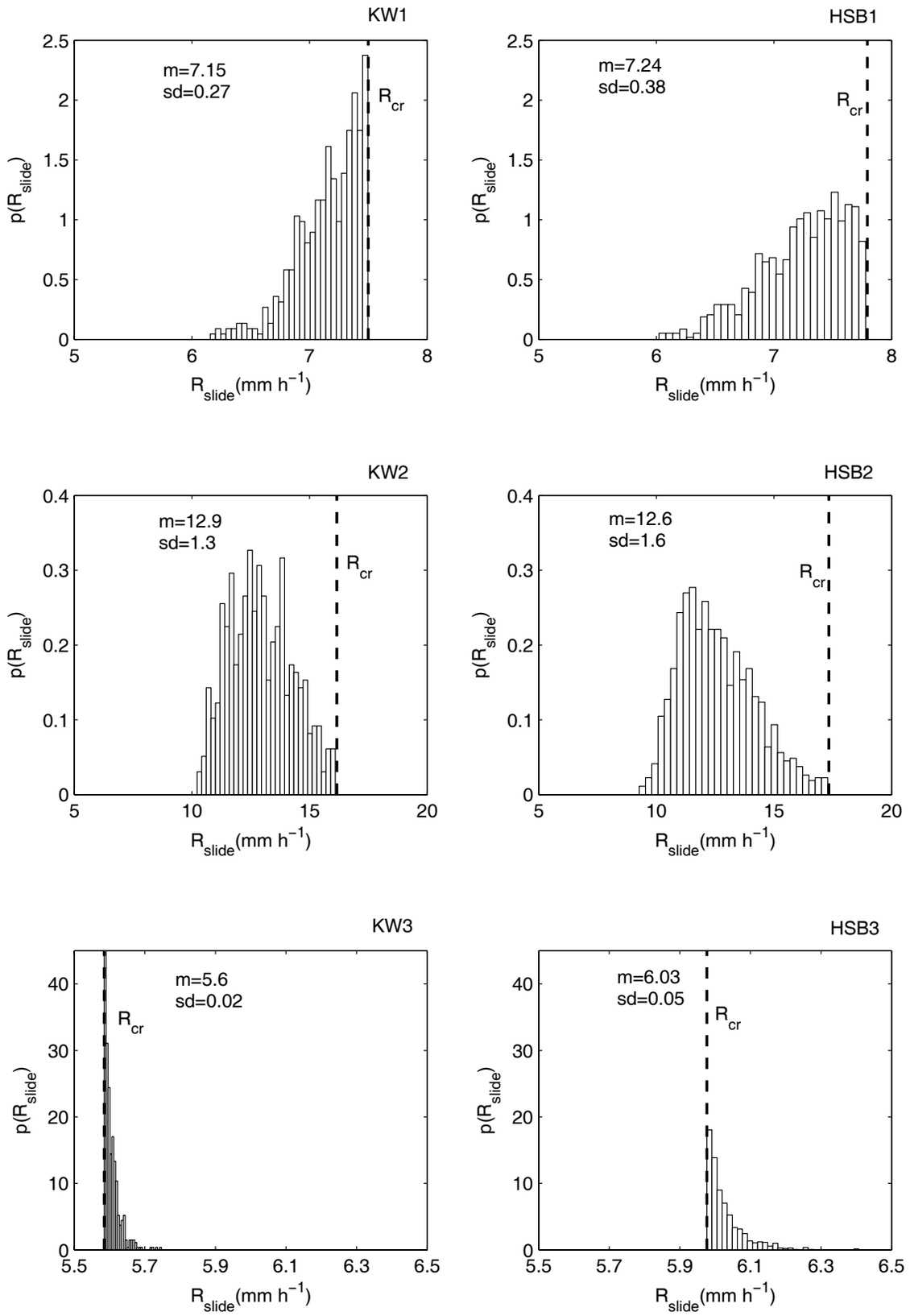

Figure 5.4: Probability distribution of the landslide triggering rainfall intensity for hollows 1, 2 and 3, respectively. Left column: KW; right column: HSB model.

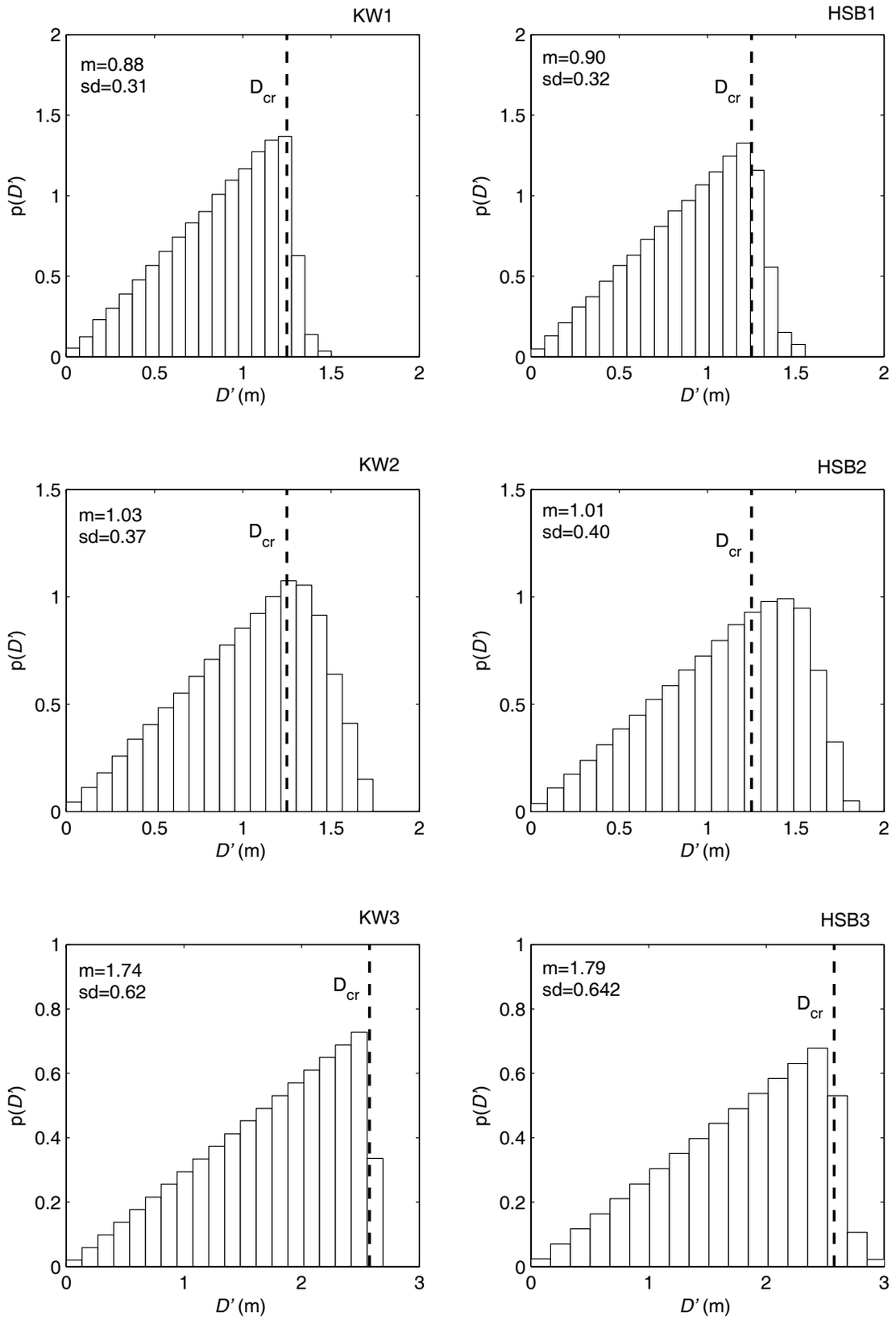

Figure 5.5: Probability distribution of colluvium thickness for hollows 1, 2 and 3, respectively. Left column: KW; right column: HSB model.

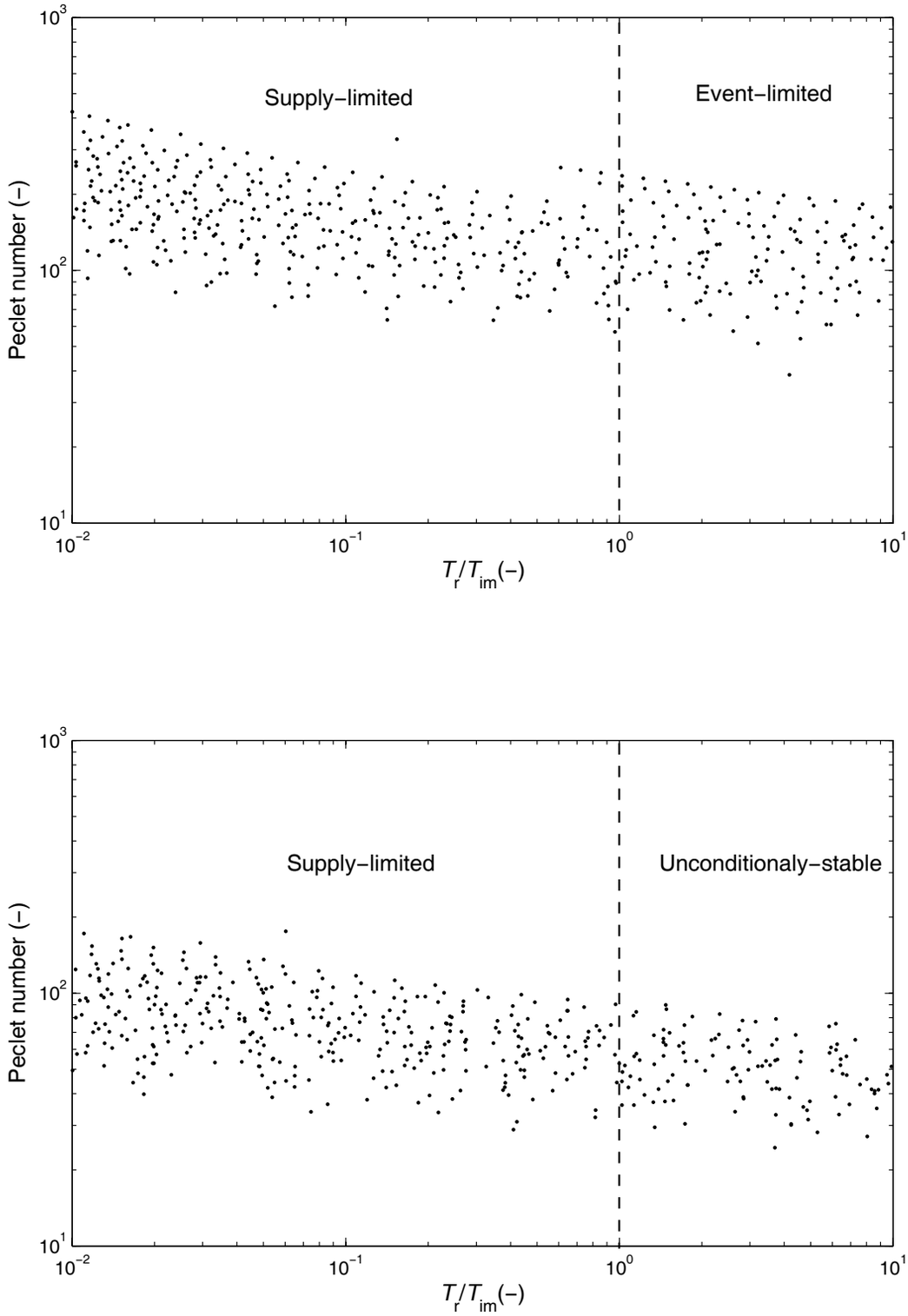

Figure 5.6: The relation between hollow geometry (*Pe*) and hollow stability and landslide regime in steep (top) and gentle hollows (bottom).

5.4. Conclusions

The aim of this paper was to investigate the effect of hollow geometry and hydrology on probability distribution of landslides in complex hollows (hollows with different length, slope and convergence degree). For that purpose and to relax the KW assumptions, we substituted a more realistic description of hollow hydrology (the linearized steady-state HSB model) in the work of *D'Odorico and Fagherazzi* (2003). The obtained model constitutes a probabilistic model of rainfall-induced shallow landsliding in complex hollows and allows to investigate the relation between the return period of rainfall, deposit thickness and landslide occurrence. The main assumptions of the presented model are:

- infinite planar slope stability analysis;
- steady-state hydrology;
- statistical model relating depth-duration-frequency of extreme precipitation based on Gumbel extreme value distribution;
- growth of colluvial deposits in hollow only due to transport of soil from uphill, not from physical weathering of underlying bedrock;
- and landslides scour hollow to bedrock.

Note that similar assumptions regarding hillslope hydrology and stability have been employed by other researchers (e.g. *Montgomery et al.*, 1998; *Iida*, 1999; *D'Odorico and Fagherazzi*, 2003; *Rosso et al.*, 2006).

The following conclusions can be drawn from our rainfall-induced landslide stability analysis in response to deposit thickness evolution in complex hollows:

(i) Although shallow landslides in hollows are mainly triggered by high rainfall intensities, deposit thickness also plays an important role in stability.

(ii) With other site variables constant, shallow landslides usually occur when the soil depth (deposits thickness) is between D_{cr} and $D_{\max}$ (as has been confirmed by other researchers, e.g. *Iida*, 1999; *D'Odorico and Fagherazzi*, 2003).

(iii) Given a deposit thickness, for each hollow there exists a critical rainfall intensity leading to the highest water table and subsequent landslide occurrence.

(iv) In general, when convergence degree of hollows increases, the time period between land slides (T_{slide}) decreases. This means that hollows with more convergence degree are generally more susceptible to landsliding.

(v) In addition to the effect of slope angle, plan shape also controls the subsurface flow and this process affects the probability distribution of landslide occurrence in complex hollows and should be considered in hollow stability analysis.

(vi) Finally, it can be concluded that incorporating a more realistic description of hollow hydrology (instead of the KW model) in landslide probability models is necessary, especially for hollows with high convergence degree (which are more susceptible to land sliding).

Chapter 6

Summary and conclusions

6. Summary and conclusions

6.1. Introduction

The hydrologic response of a hillslope to rainfall involves a complex, transient saturated-unsaturated interaction that usually leads to a water table rise. Rising pore water pressures can reduce the effective weight of the soil mass by producing an uplift force. An increase of saturated groundwater flow is the triggering mechanism for slope failure. Since the dynamic response of hillslopes is strongly dependent on plan shape, slope curvature and slope angle (*Troch et al.*, 2002; *Hilberts et al.*, 2004), a three dimensional model of dynamic hillslope hydrology is needed for stability analysis of complex hillslopes. The mathematical description of these flow processes results in the formulation of the 3D Richards equation, which is difficult to solve numerically. To overcome difficulties associated with three-dimensional models, low-dimensional hillslope models have been developed by Troch and co-workers. These models are able to treat geometric complexity in a simple way based on a concept presented by *Fan and Bras* (1998), resulting in a significant reduction in model complexity. These models can cope with varying hillslope width functions and bedrock slopes (*Hilberts et al.*, 2004). This final chapter will reflect on the most important conclusions from coupling these low-dimensional models with slope stability models in complex hillslopes and hollows and discuss the main objectives and research aims postulated in Chapter 1. Finally some ideas for future research are put forward.

6.2. A steady-state analytical slope stability model for complex hillslopes

The approach described in Chapter 2 provides an analytical hillslope stability model for assessing the relationship between slope geometry and slope stability in complex hillslopes. The model consists of a topography model, a steady-state hydrological model and the infinite slope stability assumption. The presented hydrological model takes account of the effects of topography on hillslope saturated storage through the plan shape and profile curvature. By varying these two parameters, nine basic hillslope shapes were used to compute their factor of safety (*FS*) for given hydraulic and hydrologic conditions. We have demonstrated that these nine basic hillslopes show quite different behavior from a slope stability viewpoint. It is shown that in addition to average bedrock slope angle, topographic characteristics (especially profile curvature and plan shape) of the hillslope control the subsurface flow and this process strongly affects slope stability by changing the soil strength. In particular, when the width function (plan shape) changes from divergent to convergent, hillslope stability generally decreases. This effect is more pronounced for concave length profiles. As a result, for a given plan shape (convergent, parallel or divergent) convex hillslopes are generally more stable than either concave or straight hillslopes, particularly when the average bedrock slope angle approaches the effective angle of internal friction.

Several assumptions have been made to derive the relationships in Chapter 2. Although the assumptions incorporated in the model limit its use, the model can determine relative

stability in different hillslopes with different profile curvatures and plan shapes. The first assumption is the use of the kinematic wave approximation for subsurface flow. The advantages of the kinematic wave approximation are, first, that analytical solutions exist, and second, that the model accounts explicitly for the profile curvature and plan shape (*Troch et al.*, 2002). The main disadvantage of the kinematic wave approximation is that it does not account for diffuse drainage; hence the model is not applicable for gently to moderately sloping terrains. Since the key element for initiation of shallow landslides is the average bedrock slope angle, this assumption is not expected to have a large influence on the slope stability analysis (except for convergent hillslopes).

Another assumption is that soil density above and below the water table is the same in the steady-state condition. The next step in our analysis has been to relax this assumption by combining the saturated storage hydrological model with a steady-state unsaturated storage hydrological model (Chapter 3). This has allowed us to derive soil moisture profiles defined by the constant rainfall rate and the lower boundary condition (i.e. the groundwater level) from which the unsaturated soil density can be computed. The performance of the infinite slope hypothesis compared to alternative approaches to estimate slope stability (such as the Bishop and Janbu methods) has also been investigated (Chapter 3).

6.3. Soil moisture storage and hillslope stability

The aim of this part of the research is to analyze the role of the geometric characteristics of hillslopes as well as the effect of the unsaturated zone storage on the hillslope stability in the steady-state hydrology. This was studied on the basis of computing and analyzing the factor of safety in two different manners. First, by means of the analytical model presented in Chapter 2 (*Talebi et al.*, 2007a). Second, by means of a more complex approach (i.e. non-constant soil depth associated with deep landslides) that accounts for the unsaturated zone storage and that relaxes the simplifying assumptions of the infinite slope stability model (Janbu's non-circular method and Bishop's simplified method). All methods were studied in two cases: with and without considering the soil moisture profile in the unsaturated zone. The effect of soil suction on soil cohesion was also incorporated.

We again applied the different hillslope stability models to nine characteristic hillslope types with three different profile curvatures (concave, straight, convex) and three different plan shapes (convergent, parallel, divergent). In order to generalize the results, we also applied the slope stability models to a wide range of plan shapes and profile curvatures. In the case of the infinite slope method for shallow landslides (with and without the unsaturated zone storage), the convergent hillslopes with concave profile curvature have the least stability in both cases. The divergent convex hillslopes have the most stability as they have less storage than other hillslopes.

To evaluate the critical slip surface for hillslopes with non-constant soil depth, Bishop's method was incorporated in the analytical model. In this case, not only the factor of safety is different in the hillslopes but also the location of the critical slip surface changes. The critical slip surface is located at the upstream end of the slope in the concave hillslopes and near the

outlet in the convex hillslopes. This is because the local slope angle (profile curvature) plays a key role in the slope stability. Therefore, it can be concluded that the location of the critical slip surface is more dependent on profile curvature than on plan shape. Overall, for a given plan shape (convergent, parallel or divergent) convex convergent hillslopes have slip surfaces with the minimum safety factor in the outlet region. To compare the stability of entire hillslopes, Janbu's non-circular method was incorporated in the analytical model with a slip surface at the bedrock. This method also shows that convergent hillslopes with concave profile curvature have the least stability.

A comparison of the results of the different slope stability models with and without considering the unsaturated zone storage shows that there is no noticeable difference between the two cases. This means that the bulk specific weight of the unsaturated zone can be considered equal to that of the saturated zone in the steady-state hydrology. Hence, the hillslope stability is completely determined by the water table dynamics. Therefore the effect of the unsaturated zone storage can safely be neglected in the steady-state hydrology. Finally, we conclude that the more complex approach (simplified Bishop method and Janbu's non-circular method) and a steady-state hydrology model can predict the critical slip surface and slope stability for hillslopes with different geometrical characteristics. Due to its limitation (steady-state hydrology) more research is needed to account for dynamical slope stability effects. In Chapter 4 we have presented a dynamic slope stability model for complex hillslopes.

6.4. A low-dimensional physically-based model of hydrologic control on shallow landsliding in complex hillslopes

In Chapter 4, a physically-based hillslope stability model is presented to investigate the dynamic controls of shallow landsliding for complex hillslopes. The presented model is composed of three parts: a topography model conceptualizing three-dimensional soil mantled landscapes, a dynamic hydrology model for shallow subsurface flow and water table depth (HSB model) (*Troch et al.*, 2003; *Hilberts et al.*, 2004) and an infinite slope stability method based on the Mohr-Coulomb failure law. The HSB model is based on the continuity and Darcy equations in terms of storage along the hillslope. The resulting Hillslope-Storage Boussinesq Stability Model (HSB-SM) is able to simulate rain-induced shallow landsliding in hillslopes with non-constant bedrock slope and non-parallel plan shape. Based on the HSB-SM model, the dynamic response of complex hillslopes during drainage and recharge events depends very much on the slope angle, plan shape and slope curvature.

In the HSB-SM model, the rate of daily precipitation is substituted by the recharge rate directly. This means that the variations of the unsaturated zone storage have been ignored (note that soil moisture in the unsaturated zone has been calculated by Darcy's law with a unit gradient assumption). To relax this assumption, the slope stability analysis has also been investigated based on coupling the saturated and unsaturated storages (*Hilberts et al.*, 2007). To investigate the effect of the unsaturated zone storage on hillslope stability under time-varying conditions, this model has been combined with the infinite slope stability method.

Both methods yield comparable results, illustrating the hillslope stability is mainly determined by the water table dynamics (saturated soil moisture storage). These results are confirmed by others (e.g. *Iverson*, 2000; *Iida*, 2004; *Rosso et al.*, 2006; *Talebi et al.*, 2007b). Therefore, we can safely use the original HSB model (*Troch et al.*, 2003; *Hilberts et al.*, 2004) for stability analysis in hillslopes with different plan shapes and profile curvatures.

The results of the stability analysis for different recharge rates (using the HSB-SM model) indicate clear differences in the stability of different hillslope types for the same soil condition. In all cases (different recharge rates), convergent hillslopes with concave and straight profiles become unstable faster than others. This is because the convergent hillslopes drain much more slowly than the divergent hillslopes (*Troch et al.*, 2003) and this process increases the saturated zone storage, which consequently decreases the factor of safety quickly. In contrast, in the divergent hillslopes which drain fast, even with 50 mm recharge per day, the slopes remain stable.

With respect to the important role of subsurface flow on slope stability (e.g. *Borga et al.*, 2002; *Matsushi et al.*, 2006), the relation between variations of subsurface flow and the factor of safety has also been studied. Based on the results obtained by the HSB-SM model, the minimum safety factor coincides with the maximum rate of subsurface flow. In fact, an increase of subsurface flow leads to a decrease of stability in all hillslopes and vice versa. As the current model is limited to event-based analyses, further research is needed to present a probabilistic model of rainfall-triggered shallow landslides for complex hillslopes with changing rainfall input. This probabilistic model has been presented in Chapter 5.

6.5. Application of a probabilistic model of rainfall-induced shallow landslides to complex hollows

The aim of this chapter was to generalize a probabilistic model of rainfall-induced shallow landslides in complex hollows to investigate the relation between return period of rainfall, deposit thickness and landslide occurrence. The basis of this model is the same as the work presented by *D'Odorico and Fagherazzi* (2003), whose model describes the long-term evolution of colluvial deposits through a probabilistic soil mass balance at a point. Further building blocks of their model are: an infinite-slope stability analysis; a steady-state kinematic wave model of hollow groundwater hydrology; and a statistical model relating intensity, duration, and frequency of extreme precipitation. With respect to the limitation of the kinematic wave hydrology for gentle slopes and especially for hillslopes with convergent plan shape or a concave profile (*Hilberts et al.*, 2004), we incorporated a more realistic description of hollow hydrology (HSB model) (*Troch et al.*, 2003; *Berne et al.*, 2005) in the stochastic landslide model. We applied the presented model in four realistic hollows. The results obtained by the KW and HSB models show significant differences, as in the KW model the diffusion term is ignored.

We generalize our results by examining the stability of several hollow types with different plan shapes (different convergence degrees). For each hollow type, the minimum value of the landslide-triggering saturated depth corresponding to the triggering precipitation

(critical recharge rate) is computed for steep and gentle hollows. Long term analysis of shallow landslides by the presented model illustrates that all hollows show a quite different behavior from the stability view point. In hollows with more convergence, landslide occurrence is limited by the supply of deposits (supply limited regime) or the occurrence of rainfall events (event limited regime) while hollows with low convergence degree are unconditionally stable regardless of the soil thickness or rainfall intensity. Overall, our results show that in addition to the effect of slope angle, plan shape (convergence degree) also controls the subsurface flow and this process affects the probability distribution of landslide occurrence in different hollows. Finally, we conclude that incorporating a more realistic description of hollow hydrology (instead of the KW model) in landslide probability models is necessary, especially for hollows with a high convergence degree, which are more susceptible to landsliding.

The main assumptions of the presented model are: infinite planar slope stability analysis; steady-state hydrology (no antecedent moisture); statistical model relating intensity-duration-frequency of extreme precipitation based on the Gumbel extreme value distribution; growth of colluvial deposits in the hollow only due to transport of soil from uphill, not from physical weathering of the underlying bedrock; landslides scour the hollow to the bedrock. Note that similar assumptions regarding hillslope hydrology and stability have been employed by other researchers (e.g. *Montgomery et al.*, 1998; *Iida*, 1999; *D'Odorico and Fagherazzi*, 2003; *Rosso et al.*, 2006).

6.6. Ideas for future research

As vegetation plays an important role in improving slope stability and preventing mass movements (e.g. *Waldron*, 1977; *Ziemer*, 1981; *Sidle et al.*, 1985; *Greenway*, 1987; *Abe and Ziemer*, 1991; *Wu*, 1995; *Gray and Sotir*, 1996; *Montgomery et al.*, 2000; *Norris et al.*, 2006), this component should be incorporated in the models presented in this thesis. Two ways are considered in which vegetation can affect slope stability: changes in the soil moisture regime and contribution to soil strength by the roots (*O'Loughlin*, 1974; *Wu et al.*, 1979; *Sidle*, 1991; *Schmidt et al.*, 2001). The first way is not particularly important for shallow landslides that occur during an extended rainy season, except possibly in the tropics and subtropics, where evapotranspiration is high throughout the year (*Sidle*, 2006). By incorporating models (e.g. *Waldron*, 1977; *Wu et al.*, 1979; *Gray and Sotir*, 1996) to estimate the root resistance per unit area in the dynamic slope stability model (HSB-SM model, *Talebi et al.*, 2007c), an integrated hillslope stability model can be presented. To consider the effect of evapotranpiration and interception, a water balance model for the unsaturated zone can also be incorporated in the presented model. Therefore, incorporating the vegetation component in the dynamic slope stability model is suggested as a next step for this research.

Mapping areas susceptible to landslides is essential for land-use management and should become a standard tool to support land management decision-making. Recent advances in incorporating advanced GIS and DEM technology into distributed, physically based modeling (e.g. *Montgomery and Dietrich*, 1994; *Wu and Sidle*, 1995; *Dhakal and Sidle*,

2003; *Iida*, 2004; *Hong et al.*, 2007) has facilitated the prediction of landslides at the catchment scale. Therefore, a next idea following this line of research could be landslide hazard mapping by incorporating the integrated hillslope stability model (the developed HSB-SM model) with GIS tools. For doing this, an effort should be made to scale up from hillslope to catchment. The result would be an improved slope stability screening tool. This objective is met by uniformly describing and completely mapping all potentially unstable slope areas in the watershed. Finally, landform hazard classification is linked to the identified sensitivity to land management practices.

References

Abe, K., and R. R. Ziemer (1991), Effect of tree roots on shallow seated landslides, USDA Forest Service, *Gen. Tech. Rep*., *PSW-GTR-130*, 11–20.

Anderson, M. G., and M. J. Kemp (1991), Towards an improved specification of slope hydrology in the analysis of slope instability problems in the tropics, *Progr. Phys. Geogr.*, *15* (l), 29-52.

Andersen, S. A., and N. Sitar (1995), Analysis of rainfall-induced debris flows, *Journal of Geotechnical Engineering*, 544-552.

Au, S. W. C. (1998), Rain-induced slope instability in Hong Kong, *Eng. Geol., 51*, 1–36.

Berne, A., R. Uijlenhoet and P. A. Troch (2005), Similarity analysis of subsurface flow response of hillslopes with complex geometry, *Water Resour. Res., 41*, W09410, doi:10.1029/2004WR003629.

Beven, K. J., and M. J. Kirkby (1979), A physically-based variable contributing area model of basin hydrology, *Hydrol. Sci. Bull., 24*, 43-69.

Bishop, A. W. (1955), The use of the slip circle in the stability analysis of slopes, *Geotechnique*, *5,* 7-17.

Bogaard, T. A., J. T. Buma and C. J. M. Klawer (2004), Testing the potential of geochemical techniques for identifying hydrological systems within landslides in partly weathered marls, *Geomorphology, 58*, 1-4, 323-338.

Borga, M., G. Dalla Fontana, C. Gregoretti and L. Marchi (2002), Assessment of shallow landsliding by using a physically based model of hillslope stability, *Hydrol. Process., 16*: 2833-2851.

Borga, M., G. Dalla Fontana, D. D. Ros and L. Marchi (1998), Shallow landslide hazard assessment using a physically based model and digital elevation model, *Environ. Geol.*, *35* (2-3), 81-88.

Boussinesq, J. (1877), Essai sur la theorie des eaux courantes, *Mem. Acad. Sci. Inst. France, 23*, 1-680.

Brutsaert, W., (2005), *Hydrology: An Introduction*, Cambridge University Press.

Cai, F., K. Ugai, A. Wakai and Q. Li (1998), Effects of horizontal drains on slope stability under rainfall by three-dimensional finite element analysis, *Computers and Geotechnics, 23*, 255-275.

Campbell, G. (1974), A simple method for determining unsaturated conductivity from moisture retention data, *Soil Sci., 117*(6), 311-314.

Chow, W.T., D. R. Maidment and L. W. Mays (1988), *Applied Hydrology*, McGraw-Hill, New York.

Claessens, L. (2005), *Modeling Landslide Dynamics in Forested Landscapes*. PhD Thesis, Wageningen University, 143 p.

Claessens, L., J. M. Schoorl and A. Veldkamp (2007), Modeling the location of shallow landslides and their effects on landscape dynamics in large watersheds: An application for Northern New Zealand, *Geomorphology, 87*, 16–27.

Clap, R. B. and G. M. Hornberger (1978), Emprical equations for some soil hydraulic properties, *Water Resour. Res., 14*(4), 601-604.

Cruden, D. M. (1991), A simple definition of a landslide, *Bulletin of International Association of Engineering Geology, 43*, 27-29.

Dai, F. C. and C. F. Lee (2001), Frequency-volume relation and prediction of rainfall-induced landslides, *Eng. Geol., 59*, 253–266.

Dhakal, A. S. and R. C. Sidle (2003), Long-term modeling of landslides for different forest management practices, *Earth Surf. Process. Landforms, 28*, 853-868.

Dhakal, A. S. and R. C. Sidle (2004), Pore water pressure assessment in a forest watershed: Simulations and distributed field measurements related to forest practices, *Water Resour. Res., 40*, W02405, doi:10.1029/2003WR002017.

Dietrich, W. E., and T. Dunne (1978), Sediment budget for a small catchment in mountainous terrain. Zeitschrift fur Geomorphologie, *Supplementband, 29*, 191–206.

Dietrich, W. E., C. J. Wilson and S. L. Reneau (1986), Hollows, colluviums, and landslides in soil-mantled landscapes*, In: Hillslope Processes*, edited by A. D. Abrahams, pp. 361 – 388, Allen and Unwin, Concord, Mass.

D'Odorico, P., and S. Fagherazzi (2003), A probabilistic model of rainfall-triggered shallow landslides in hollows: A long-term analysis, *Water Resour. Res., 39*: 1262. doi: 10.1029/2002WR001595.

D'Odorico, P., S. Fagherazzi and R. Rigon (2005), Potential for landsliding: Dependence on hyetograph characteristics, *J. Geophys. Res., 110*, F01007, doi: 10.1029/2004JF000127.

Evans, I. S. (1980), An integrated system of terrain analysis and slope mapping, Zeitschrift fur Geomorphologie, *Supplementband, 36,* 274-295.

Fan, Y., and R. L. Bras (1998), Analytical solutions to hillslope subsurface storm flow and saturation overland flow, *Water Resour. Res., 34*(4): 921-927.

Fell, R., O. Hungr, S. Leroueil and W. Riemer (2000), Geotechnical engineering of the stability of natural slopes, and cuts and fills in soil, Key Note Lecture at International Conference on Geotechnical and Geological Engineering, Melbourne, Australia, 21 – 121.

Fernands, N. F., A. L. C. Netto and W. A. Lacerda (1994), Subsurface hydrology of layered colluvium mantles in unchanneled valleys-south-eastern Brazil, *Earth Surf. Process. Landforms, 19*, 609-626.

Finlay, P. J., R. Fell, P. K. Maguire (1997), The relationship between the probability of landslide occurrence and rainfall, *Can. Geotech. J., 34*, 811–824.

Floris, M., and F. Bozzano (2007), Evaluation of landslide reactivation: a modified rainfall threshold model based on historical records of rainfall and landslides, *Geomorphology*, doi: 10.1016/j.geomorph.2007.04.009.

Frattini, P., G. B. Crosta, N. Fusi and P. D. Negro (2004), Shallow landslides in pyroclastic soil : a distributed modeling approach for hazard assessment, *Eng. Geol., 73*, 277–295.

Fredlund, D. G., N. R. Morgenstern and R. A. Widger (1978), The shear strength of unsaturated soil, *Can. Geotech. J., 15*, 313-321.

Gan, J. K., D. G. Fredlund and H. Rahardjio (1988), Determination of shear strength parameters of an unsaturated soil using the direct shear test, *Can. Geotech. J., 25*, 500-510.

Gardner, W. R. (1958), Some steady-state solutions of the unsaturated moisture flow equation with application to evaporation from a water table, *Soil Sci.,* 228-332.

Giannecchini, R. (2006), Relationship between rainfall and shallow landslides in the southern Apuan Alps (Italy), *Nat. Hazards Earth Syst. Sci., 6*, 357–364.

Gray, D. H., and R. B. Sotir (1996), *Biotechnical and Soil Bioengineering Slope Stabilization. A Practical Guide for Erosion Control*, John Wiley and Sons, New York.

Greenway, D. R. (1987), Vegetation and slope stability, In: *Slope stability, Geothechnical Engineering and Geomorphology*, edited by M. G. Anderson and K. S. Richards, pp. 187-230, John Wiley & Sons, Chichester, UK.

Hack, J. T. (1965), Geomorphology of the Shenandoah Valley, Virginia and West Virginia, and origin of the residual ore deposits. *US Geol Surv Prof Pap* 484.

Han, J., and D. Leshchinsky (2004), Limit equilibrium and continuum mechanics-based numerical methods for analyzing stability of MSE walls, *17th ASCE Engineering Mechanics Conference*, June 13-16, University of Delaware, Newark, DE, USA.

Haneberg, W. C., and A. Onder Gocke (1994), Rapid water level fluctuations in a thin colluvium landslide west of Cincinnati, *Ohio. US Geol. Surv. Bull.* 2059 C, 1–16.

Harp, E. L., W. G. Wells II, and J. G. Sarmiento (1990), Pore pressure response during failure in soils, Geol. Soc. Am. Bull., 102(4), 428-438.

Heimsath, A. M., W. E. Dietrich, K. Nishiizumi and R. C. Finkel (1997), The soil production function and landscape equilibrium: *Nature, 388*, 358–361.

Heimsath, A. M., W. E. Dietrich, K. Nishiizumi, R. C. Finkel (2001), Stochastic processes of soil production and transport: erosion rates, topographic variation and cosmogenic nuclides in the Oregon Coast Range. *Earth Surf. Process Landforms, 26*, 531–552.

Hennrich, K., M. J. Crozier (2004), A hillslope hydrology approach for catchment-scale slope stability analysis, *Earth Surf. Process. Landforms, 29,* 599-610.

Hilberts, A., E. Van Loon, P. A. Troch and C. Paniconi (2004), The hillslope-storage Boussinesq model for non-constant bedrock slope, *J. Hydrol., 291*, 160-173.

Hilberts, A., P. A. Troch, C. Paniconi and J. Boll (2007), Low-dimensional modeling of hillslope subsurface flow: the relationship between rainfall, recharge, and unsaturated storage, *Water Resour. Res., 43*, W03445, doi: 10.1029/2006WR006496.

Hong, Y., R. Adler and G. Huffman (2007), Use of Satellite Remote Sensing Data in mapping of global shallow landslides Susceptibility, *Nat Hazards*, doi: 10.1007/s11069-006-9104-z.

Ibsen, M. L., and N. Casagli (2004), Rainfall patterns and related landslide incidence in the Porretta-Vergato region, Italy, *Landslides, 1*, 143–150.

Iida, T. (1999), A stochastic hydro-geomorphological model for shallow landsliding due to rainstorm. *CATENA, 34,* 293-313.

Iida, T. (2004), Theoretical research on the relationship between return period of rainfall and shallow landslides, *Hydrol. Processes, 18*, 739–756.

Iverson, R. M. (2000), Landslide triggering by rain infiltration, *Water Resour. Res., 36,* 1897-1910.

Janbu, N. (1954), Application of composite slip surface for stability analysis, Proceedings of the European Conference on the Stability of Earth Slopes, 3, 43-49.

Jiao, J. J., X. S. Wang and S. Nandy (2005), Confined groundwater zone and slope instability in weathered igneous rocks in Hong Kong, *J. Eng. Geol., 80*, 71-92.

Keefer, D. K., and M. C. Larsen (2007), Assessing Landslides hazards, *Science, 316,* 1136-1138, doi: 10.1126/science.1143308 (in Perspectives).

Kirkby, M. J. (1985), A model for the evolution of regolit-mantled slopes, In: *Models in Geomorphology*, Woldenburg MJ (ed.). Allen and Unwin, Winchester, MA, 213-237.

Lan, H. X., C. F. Lee, C. H. Zhou and C. D. Martin (2005), Dynamic characteristic analysis of shallow landslides in response to rainfall event using GIS, *Environ Geol, 47*, 254–267.

Magirl, C. S., R. H. Webb, M. Schaffner, S. W. Lyon, P. G. Griffiths, C. Shoemaker, C. Unkrich, S. Yatheendradas, P. A. Troch, E. Pytlak, D. C. Goodrich, S. L. E. Desilets, A. Youberg and P. A. Pearthree (2007), Impact of Recent Extreme Arizona Storms, *Eos, Trans. Amer. Geophys. Union, Vol. 88*, No. 17.

Malet, J. P., Th. W. J. Van Asch, R. Van Beek and O. Maquaire (2005), Forecasting the behavior of complex landslides with a spatially distributed hydrological model, *Nat. Hazards Earth Syst. Sci., 5*, 71–85.

Matsushi, Y., T. Hattanji and Y. Matsukura (2006), Mechanisms of shallow landslides on soil-mantled hillslopes with permeable and impermeable bedrocks in the Boso Peninsula, Japan, *Geomorphology, 76*, 92– 108.

Montgomery, D. R., and W. E. Dietrich (1994), A physically based model for the topographic control on shallow landsliding, *Water Resour. Res., 30*, 1153-1171.

Montgomery, D. R., W. E. Dietrich, R. Torres, S. P. Anderson, J. T. Heffner and K. Loague (1997), Hydrologic response of a steep, unchanneled valley to natural and applied rainfall, *Water Resour. Res., 33*, 91– 109.

Montgomery, D. R., K. Sullivan and H. M. Greenberg (1998), Regional test of a model for shallow landsliding, *Hydrol. Process.,12*, 943-955.

Montgomery, D. R., K. N. Schmidt, H. M. Greenberg and W. E. Dietrich (2000), Forest clearing and regional landsliding, *Geology, 28*, 311–314.

Ng, C. W. W., and Q. Shi (1998), A numerical investigation of the stability of unsaturated soil slopes subjected to transient seepage, *Computers and Geotechnics, 22*, 1, 1–28.

Norris, J. E., L. H. Cammeraat, A. Stokes and I. Spanos (2006), The use of vegetation to improve slope stability, *Geotech. Geol. Eng., 24*, 427–428.

Oeberg, A. L., and G. Saellfors (1997), Determination of shear strength parameters of unsaturated silts and sand based on the water retention curve, *Geotech. Test. J., 20* (1), 40-48.

O'Loughlin, C. L. (1974), A study of tree root strength deterioration following clearfelling, *Can. J. For. Res., 4*(1), 107-113.

Onda, Y., M. Tsujimura and H. Tabuchi (2004), The role of subsurface water flow paths on hillslope hydrological processes, landslides and landform development in steep mountains of Japan, *Hydrol. Proces., 18*, 637– 650.

Paniconi, C., P. Troch, E. Van Loon and A. Hilberts (2003), Hillslope-storage Boussinesq model for subsurface flow and variable source areas along complex hillslopes: 2-Intercomparison with a three-dimensional Richards equation model, *Water Resour. Res., 39*(11), doi: 10.1029/2002WR001730.

Pellenq, J., J. Kalma, G. Boulet, G. M. Saulnier, S. Wooldridge and Y. Kerr (2003), A disaggregation scheme for soil moisture based on topography and soil depth, *J. Hydrol., 276,* 112–127.

Pennock, D. J., B. J. Zebarth, E. de Jong (1987), Landform classification and soil distribution in Hummocky Terrain, Saskatchewan, *Canada. Geoderma, 40*, 297-315.

Qiu, Y., B. Fu, J. Wang and L. Chen (2001), Soil moisture variation in relation to topography and land use in a hillslope catchment of the Loess Plateau, China, *J. Hydrol., 240*, 243–263.

Reichenbach, P., M. Cardinali, P. De Vita and F. Guzzetti (1998), Regional hydrological thresholds for landslides and floods in the Tiber River basin (Central Italy), *Environ Geol 35* (2–3), 146–159.

Reneau S.L. and Dietrich W.E. (1987), The importance of hollows in debris flow studies: example from Marin County, California. In: Costa JE, Wieczorek GF (eds) Debris flows/avalanches: process, recognition, and mitigation, *Geol Soc Am Rev Eng Geol, 7*: 165-180.

Rezzoug, A., A. Schumann, P. Chifflard, H. Zepp (2005), Field measurement of soil moisture dynamics and numerical simulation using the kinematic wave approximation, *Adv. Water Resour., 28*, 917-926.

Ridolfi, L., P. D'Odorico, A. Porporato and I. Rodriguez-Iturbe (2003), Stochastic soil moisture dynamics along a hillslope, *J. Hydrol.., 272*, 264-275.

Ritter, J. B. (2004), *Landslides and Slope Stability Analysis*, Department of Geology, Wittenberg University (available at: www.capital.edu/Internet/Estrada.config?resource=7095).

Rockhold, M. L., C. S. Simmons and M. J. Fayer (1997), An analytical solution technique for one-dimensional, steady vertical water flow in layered soils, *Water Resour. Res., 33*, 897-902.

Rosso, R., M., C. Rulli and G. Vannucchi (2006), A physically based model for the hydrologic control on shallow landsliding, *Water Resour. Res., 42*, W06410, doi:10.1029/2005WR004369.

Schmidt, K. M., J. J. Roering, J. D. Stock, W. E. Dietrich, D. R. Montgomery, and T. Schaub (2001), The variability of root cohesion as an influence on shallow landslide susceptibility in the Oregon Coast Range, *Can. Geotech. J., 38*, 995-1024.

Sidle, R. C. (1984), Shallow groundwater fluctuations in unstable hillslopes of coastal Alaska, Z. *fur Gletscherkunde und Glazialgeol., 20*, 79-95.

Sidle, R. C. (1991), A conceptual model of changes in root cohesion in response to vegetation management, *J. Environ. Quality, 20*(1), 43-52.

Sidle, R. C. (1992), A theoretical model of the effects of timber harvesting on slope stability, *Water Resour. Res., 28*(7), 1897-1910.

Sidle, R. C. (2006), Field observations and process understanding in hydrology: essential components in scaling, *Hydrol. Processes, 20*, 1439-1445.

Sidle, R. C., and H. Ochiai (2006), *Landslides: Processes, Prediction, and Land Use*, Water Resour. Monogr. Ser., vol. 18, AGU, Washington, D. C.

Sidle, R. C., A. J. Pearce, and C. L. O'Loughlin (1985), *Hillslope Stability and Land Use*, Water Resour. Monogr. Ser., vol. 11, AGU, Washington, D. C.

Sidle, R. C. and D. N. Swanston (1982), Analysis of a small debris slide incoastal Alaska, *Can. Geotech. J., 19*, 167-174.

Stock, J., and W. E. Dietrich (2003), Valley incision by debris flows: Evidence of a topographic signature, *Water Resour. Res., 39* (4), 1089, doi:10.1029/2001WR001057.

Talebi, A., P. A. Troch and R. Uijlenhoet (2007a), A steady-state analytical hillslope stability model, *Hydrol. Proces., 21,* doi:10.1002/hyp.6881.

Talebi, A., R. Uijlenhoet and P. A. Troch (2007b), Soil moisture storage and hillslope stability, *Nat. Hazards Earth Syst. Sci., 7*, 523-534.

Talebi, A., R. Uijlenhoet and P. A. Troch (2007c), A low-dimensional physically-based model of hydrologic control on shallow landsliding in complex hillslopes, accepted in *Earth Surf. Process. Landforms* (in press).

Terlien, M.T.J. (1997), Hydrological landslide triggering in ash-covered slopes of Manizales (Colombia), *Geomorphology, 20*, 165-175.

Terlien, M.T.J. (1998), The determination of statistical and deterministic hydrological landslidetriggering thresholds, *Environ Geol, 35*, 124–130.

Teuling, A. J., and P. Troch (2005), Improved understanding of soil moisture variability dynamics, *Geophys. Res. Lett., 32*, doi: 10.1029/2004GL021935.

Torres, R., W. E. Dietrich, D. R. Montgomery, S. P. Anderson, K. Loague (1998), Unsaturated zone processes and the hydrologic response of a steep, unchanneled catchment, *Water Resour. Res., 34*(8), 1865-1874, 10.1029/98WR01140.

Troch, P. A., C. Paniconi and E. Van Loon (2003), Hillslope-storage Boussinesq model for subsurface flow and variable source areas along complex hillslopes: 1-Formulation

and characteristic response, *Water Resour. Res., 39*(11):1316, doi: 10.1029/2002WR001728.

Troch, P. A., E. Van Loon and A. Hilberts (2002), Analytical solutions to a hillslope-storage kinematic wave equation for subsurface flow, *Adv. Water Resour., 25*, 637-649.

Tsai, T. L., and J. C. Yang (2006), Modeling of rainfall-triggered shallow Landslide, *Environ Geol*, *50*, 525–534, doi: 10.1007/s00254-006-0229-x.

Tsao, T. M., M. K. Wang, M. C. Chen, Y. Takeuchi, S. Matsuura and H. Ochiai (2005), A case study of the pore water pressure fluctuation on the slip surface using horizontal borehole works on drainage well, *Engineering Geology, 78*, 105– 118.

Tsaparas, I., H. Rahardjo, D. G. Toll and E. C. Leong (2002), Controlling parameters for rainfall induced landslides, *Computers and Geotechnics, 29*, 1–27.

Tsuboyama, Y., R. C. Sidle, S. Noguchi, S. Murakami and T. Shimizu (2000), A zero-order basin-its contribution to catchment hydrology and internal hydrological processes, *Hydrol. Proces., 14*, 387-401.

Tsukamoto, Y. and T. Ohta (1988) Runoff processes on a steep forested slope, *J. Hydrol., 102*, 165-178.

Vanapalli, S. K., D. G. Fredlund, D. E. Pufahl and A. W. Clifton (1996), Model for the prediction of shear strength with respect to soil suction, *Can. Geotech. J., 33* (3), 379–392.

Van Asch, Th. W. J., M. R. Hendriks, R. Hessel and F. Rappange (1996), Hydrological triggering conditions of landslides in varved clays in the French Alps, *Eng. Geol., 42*, 239–251.

Van Beek, H. (2002), Assessment of the Influence of Changes in Land Use and Climate on Landslide Activity in a Mediterranean Environment. PhD Thesis, Utrecht University, 363 p.

Van Genuchten, M. T. (1980), A closed-form equation for predicting the hydraulic conductivity of unsaturated soils, *Soil Sci. Soc. Am. J., 44*, 892-898.

Waldron, L. J. (1977), The shear resistance of root-permeated homogeneous and stratified, *Soil Sci. Soc. Am. J., 41*, 843–848.

Wilkinson, P. L., M. G. Anderson, D. M. Lloyd and J. P. Renaud (2002), An integrated hydrological model for rain-induced landslide prediction, *Earth Surf. Process. Landforms, 27*, 1285-1297.

Wilkinson, P. L., S. M. Brooks and M. G. Anderson (2000), Design and application of an automated non-circular slip surface search within a combined hydrology and stability model (CHASM), *Hydrol. Proces., 14*, 2003-2017.

Wu, T. H. (1995), Slope stabilization. *In Slope Stabilization and Erosion Control*. Eds. R. P. C. Morgan & R. J. Rickson, pp. 221–264, Spon, London.

Wu, T. H., W. P. Mckinnel and D. N. Swanston (1979), Strenght of tree roots and landslides on Prince of Wales Island, Alaska, *Can. Geotech. J., 16*, 19-33.

Wu, W., and R. C. Sidle (1995), A distributed slope stability model for steep forested basins, *Water Resour. Res., 31*(8), 2097-2110.

Zaitchik, B. F., H. M. Van Es and P. J. Sullivan (2003), Modeling slope stability in Honduras: parameter sensitivity and scale of aggregation, *Soil Sci. Soc. Am. J., 67*, 268-278.

Ziemer, R. R. (1981), The role of vegetation in the stability of forested slopes, Proc. *Int. Union of Forestry Research Organizations*, XVII World Congress, Kyoto, Japan vol. 1, 297–308.

Samenvatting

De hydrologische reactie van een helling op regen gaat gepaard met een complexe, niet-stationaire interactie tussen de onverzadigde en verzadigde zones van de bodem, die in de meeste gevallen tot een stijging van de grondwaterspiegel leidt. Een toename in verzadigde grondwaterstroming kan het bezwijken van hellingen tot gevolg hebben. Om betrouwbare simulaties te kunnen uitvoeren van de stabiliteit van hellingen op landschapsschaal zijn eenvoudige (laag-dimensionale), maar fysisch realistische modellen nodig die kunnen omgaan met de drie-dimensionale vorm van hellingen waarin stroming en berging van grondwater plaatsvindt, zodat hydrologische processen op hellingsschaal op een correcte manier worden gerepresenteerd. In dit proefschrift wordt het verband tussen de vorm, de hydrologie en de stabiliteit van complexe hellingen en nissen onderzocht.

In dit proefschrift worden verschillende modellen gepresenteerd die worden gebruikt om de stabiliteit van negen karakteristieke hellingtypen (landschapselementen) te onderzoeken, met drie verschillende krommingen in de lengterichting (concaaf, recht en convex) en drie in de dwarsrichting (convergent, parallel en divergent). Naast het testen van deze modellen voor negen verschillende hellingtypen wordt er een algemeen verband tussen de krommingen van de landschapselementen (hellingen) in lengte- en dwarsrichting en een veiligheidsfactor afgeleid voor een gegeven hellinglengte. Onze resultaten laten zien dat de stabiliteit van hellingen toeneemt als de kromming van het lengteprofiel van concaaf naar convex verandert. In termen van krommingen van het dwarsprofiel neemt de stabiliteit toe als de vorm verandert van convergent naar divergent, ongeacht de vorm van het lengteprofiel. Analyses van de veiligheidsfactor laten zien dat deze minimaal is als de grondwaterstroming maximaal is. Met andere woorden, de stabiliteit neemt altijd af met een toenemende grondwaterstroming, ongeacht de vorm van de helling. Na een regenbui worden convergente hellingen met concave en rechte profielen sneller instabiel dan andere hellingen, terwijl divergente convexe hellingen stabiel blijven (zelfs na intense regen). Er is ook gebleken dat hellingen met een variabele bodemdikte (mogelijk diepe aardverschuivingen) en met een convex lengteprofiel en een convergent dwarsprofiel een minimale veiligheidsfactor hebben op het uitstroompunt. Samenvattend kan gezegd worden dat, naast de hellingshoek van het onderliggende gesteente, de krommingen van een helling in lengte- en dwarsrichting een grote invloed hebben op de stabiliteit ervan.

Met betrekking tot het verband tussen het voorkomen van regen en de instabiliteit van hellingen is een probabilistisch model van door regen geïnitieerde ondiepe aardverschuivingen in complexe nissen gebruikt om het verband tussen de herhalingstijd van regen, de depositiedikte en het voorkomen van aardverschuivingen te onderzoeken. Een lange-termijn analyse van ondiepe aardverschuivingen gesimuleerd met dit model laat zien dat alle nissen zich anders gedragen uit het oogpunt van stabiliteit. Tenslotte kan er worden geconcludeerd dat het nodig is om een realistischere beschrijving van de hydrologie van nissen te gebruiken (het hillslope-storage Boussinesq model in plaats van een kinematische golf model) voor het modelleren van de kans op aardverschuivingen, in het bijzonder voor zeer convexe nissen, die het meest gevoelig zijn voor aardverschuivingen. Dit model kan

worden gebruikt als hulp bij het onderzoeken van het verband tussen de herhalingstijd van regen en het voorkomen van aardverschuivingen in relatie tot bodemproductie (depositiedikte) in complexe nissen.

Kort gezegd was het doel van dit proefschrift om theoretisch te begrijpen hoe hydrologische processen (grondwaterstroming en de dynamica van de grondwaterspiegel) de stabiliteit van de bodem van complexe hellingen en nissen beïnvloeden. De gepresenteerde modellen kunnen op een breed vlak worden toegepast bij het analyseren van de stabiliteit van hellingen vanwege de relatieve eenvoud van deze (laag-dimensionale) modellen.

Netherlands Research School for the
Socio-Economic and Natural Sciences of the Environment

CERTIFICATE

The Netherlands Research School for the
Socio-Economic and Natural Sciences of the Environment
(SENSE), declares that

Ali Talebi

Born on: 21 September 1969 at: Isfahan, Iran

has successfully fulfilled all requirements of the
Educational Programme of SENSE.

Place: Wageningen Date: 17 January 2008

the Chairman of the SENSE board	the SENSE Director of Education
Prof. dr. R. Leemans	Dr. C. Kroeze

The SENSE Research School declares that Mr. Ali Talebi has successfully fulfilled all requirements of the Educational PhD Programme of SENSE with a work load of 54 ECTS, including the following activities:

SENSE PhD courses:

- Environmental Research in Context
- Research Context Activity: "Writing of research proposal on 'Water erosion at the hillslope scale' and public communication of dissertation results".
- The Art of Modelling
- Land use and Landscape Dynamics: Concept, Tools and Uncertainties
- Uncertainty Modelling and Analysis

Other Phd and MSc courses:

- Introduction Geo-information Science
- Hydraulic and Hydrometry
- Processes and Models related to water erosion
- English language courses: Writing English, Academic Writing I, Academic Writing II, Scientific Writing and English - Fluency Speaking

Poster Presentation:

- European Geosciences Union, general Assembly, 2 – 7 April 2006, Vienna, Austria

Deputy director SENSE
Dr. A. van Dommelen

Curriculum Vitae

Ali Talebi, 21 sepember 1969, Esfandaran, Esfahan, Iran.

1983 – 1987:

High school (Diploma in biological sciences), Adl School, Esfahan

1988 – 1992:

B.Sc. period in Natural Resources Engineering (Range and watershed management), Faculty of Natural Resources, Tehran University, Tehran (Karaj), Iran.

1993 – 1997:

M.S. period in Watershed Management Engineering, Faculty of Natural Resources, Tarbiat Modarres University, Noor, Iran.

Research project entitled:

"Investigation of the effective factors on mass movement (landslides)"

1996 – 2002:

Member of the scientific board, Faculty of Natural Resources, Yazd University, Yazd, Iran.

2003 – 2008:

PhD period in Hydrology and Quantitative Water Management Group, Centre for Water and Climate, Department of Environmental Sciences, Wageningen University, Wageningen, The Netherlands.

Research project entitled:

"The relation between geometry, hydrology and stability of complex hillslopes examined using low-dimensional hydrological models"

2008:

Netherlands Research School diploma for the Socio-economic and Natural Sciences of the Environment (SENSE).

E-mail: talebisf@yazduni.ac.ir ,

talebisf@yahoo.com

List of publications in scientific journals:

Talebi, A., P. A. Troch and R. Uijlenhoet (2007), A steady-state analytical hillslope stability model, *Hydrological Processes*, 21, doi:10.1002/hyp.6881.

Talebi, A., R. Uijlenhoet and P. A. Troch (2007), Soil moisture storage and hillslope stability, *Natural Hazards and Earth System Sciences*, 7, 523-534.

Talebi, A., R. Uijlenhoet and P. A. Troch (2007), A low-dimensional physically-based model of hydrologic control on shallow landsliding in complex hillslopes, *Earth Surface Processes and Landforms* (in press).

Talebi, A., R. Uijlenhoet and P. A. Troch (2007), Application of a probabilistic model of rainfall-induced shallow landslides to complex hollows, *Natural Hazards and Earth System Sciences* (submitted).

جهت تجزیه و تحلیل پایداری دامنه های با اشکال مختلف توپوگرافی مورد استفاده قرار گیرد. بر اساس نتایج بدست آمده و با تغییر بارندگی روزانه در همه انواع دامنه ها، دامنه های همگرآ با پروفیل طولی مقعر و صاف سریع تر از دامنه های دیگر به حالت ناپایداری می رسند. این فرایند به این علت است که دامنه های همگرآ آهسته تر از دامنه های دیگر زهکش شده و در نتیجه ذخیره اشباع خاک افزایش یافته و نهایتا پایداری کاهش می یابد. در مقابل دامنه های واگرآ که سریع تر زهکش می شوند، حتی در بارندگی 50 میلی متر در روز هم پایدار می مانند. با توجه به نقش مهم جریانهای زیر سطحی در پایداری دامنه ها رابطه بین تغییرات جریانهای زیر سطحی و ضریب پایداری هم مورد بررسی قرار گرفته است. بر اساس یافته های حاصل از مدل (HSB-SM model, Talebi et al., 2007) حداقل ضریب پایداری با حداکثر دبی جریانهای زیر سطحی منطبق می باشد. در حقیقت اینگونه می توان بیان کرد که افزایش جریانهای زیر سطحی منجربه کاهش پایداری در همه اشکال دامنه ها می شود.

فصل پنجم:کاربرد یک مدل احتمالاتی زمین لغزشهای سطحی (ایجاد شده توسط بارندگی) در دامنه های مرکب

مقاله ارائه شده به مجله (*Natural Hazards and Earth system sciences*, 2007)

هدف از این فصل ارائه یک مدل احتمالاتی جهت بررسی رابطه بین دوره بازگشت بارندگی ضخامت رسوبات و وقوع لغزش می باشد. الگوی مدل بر اساس مدل ارائه شده توسط دودوریکو و فقرازی (D'Odorico and Fagherazzi (2003,) می باشد که تکامل طولانی مدت رسوبات را از طریق یک مدل احتمالاتی بیلان خاک بررسی می کند. بخش های دیگر مدل ارائه شده از این قرار است: معادله پایداری شیب (روش شیب نامحدود)، یک مدل هیدرولوژی آبهای زیر زمینی بر اساس موج جنبشی (KW) و یک مدل آماری مربوط به شدت مدت و فراوانی بارندگیهای حداکثر. با توجه به محدودیت مدلهای هیدرولوژی موج جنبشی در شیب های ملایم و مخصوصا همگرآ (Troch et al., 2003; Berne) در این فصل ما یک مدل واقعی تر از هیدرولوژی دامنه (Hilberts et al., 2004) et al., 2005) را وارد مدل احتمالاتی لغزش می کنیم. مدل ارائه شده ما در چهار دامنه حقیقی در طبیعت مورد ارزیابی قرار می کیرد. نتایج بدست آمده از روش KW وHSB اختلافات معنی داری نشان می دهد چراکه در روشKW بخش پخشیدگی (Diffusion) نادیده گرفته می شود. نهایتا مدل ارائه شده در انواع دره های با درجه همگرایی مختلف بکار برده می شود. برای هرنوع دره، حداقل عمق اشباع و میزان بارندگی لازم (که می تواند باعث لغزش شود) در شیب های تند و ملایم محاسبه می شود. تجزیه و تحلیل طولانی مدت لغزشهای سطحی توسط مدل ارائه شده به وضوح مشخص می کند که همه دره ها یک رفتار کاملا متفاوت از نظر پایداری نشان می دهند. در دره های با درجه همگرایی بیشتر، احتمال لغزش به وجود رسوبات و وقوع بارندگی ارتباط دارد، درحالیکه دره های با همگرایی کمتربدون توجه به وجود رسوبات و وقوع بارندگی پایدار هستند. سرانجام ما نتیجه می گیریم که جایگزین نمودن یک مدل واقعی هیدرولوژی دامنه (HSB) به جای مدل موج جنبشی (KW) در مدلهای پایداری شیب ضروری می باشد (مخصوصا در دره های با همگرایی زیاد که مستعد لغزش می باشند). بدین ترتیب، این تحقیق نشان می دهد که علاوه بر زاویه شیب، شکل پلان دامنه و دره نیز جریانهای زیرسطحی را کنترل نموده و این فرایند در توزیع احتمالی زمین لغزش در دره ها و دامنه های مختلف اثر می گذارد.

همکاران Talebi et al., 2007) و روش شیب های نامحدود (Infinit slope stability method) صورت گرفته است. در مورد دوم نیز پایداری دامنه های مختلف با استفاده از روشهای بیشاپ (Bishop, 1954) و یانبو (Janbu 1955) و در دو حالت مختلف (با و بدون در نظر گرفتن رطوبت منطقه غیر اشباع) مورد تجزیه و تحلیل قرار گرفته است. ضمنا تاثیررطوبت منطقه غیر اشباع در چسبندگی خاک نیز در همه مدل های پایداری وارد گردیده است. علاوه بر بررسی نه دامنه اصلی (با توجه به شکل پلان و انحنای کف) مدل های ارائه شده برای طیف وسیعی از دامنه های موجود در طبیعت مورد تجزیه و تحلیل قرار گرفته است. بر اساس یافته های ما، در دامنه های با خاک کم عمق (مستعد به زمین لغزشهای سطحی) دامنه های همگرا با پروفیل طولی مقعر کمترین پایداری را در هر دو حالت (با و بدون در نظر گرفتن رطوبت منطقه غیر اشباع) نشان می دهند. در مقابل، دامنه های محدب واگرآ (که کمترین ذخیره رطوبتی را دارند) بیشترین پایداری را نشان می دهند.

جهت بررسی سطح لغزش بحرانی در دامنه های با عمق خاک متغیر (مستعد به لغزشهای عمیق) روش بیشاپ در مدل تحلیلی پایداری (طالبی و همکاران Talebi et al., 2007) وارد گردید. نتایج حاصله نشان می دهد نه تنها ضریب پایداری در دامنه های مختلف متفاوت است، بلکه محل سطح لغزش نیزبا توجه به شکل پلان و انحنای کف تغییر می کند. بطوریکه در دامنه های مقعر سطح لغزش در بالادست دامنه و در دامنه های محدب نزدیک به خروجی دامنه واقع می شود. بنابر این می توان گفت محل سطح لغزش بحرانی بیشتر به پروفیل طولی دامنه مرتبط است تا به شکل پلان آن. نتیجتا برای یک شکل پلان مشخص دامنه (همگرا، واگرا و موازی)، دامنه های محدب همگرا کمترین ضریب پایداری را در قسمت خروجی دامنه دارند. علاوه بر مدل بیشاپ مدل غیر دایره ای یانبو (Janbu, 1955) نیز درمدل تحلیلی پایداری (طالبی و همکاران Talebi et al., 2007) وارد گردید. نتایج حاصل از این مدل ارائه شده نیز یافته های قبلی را تایید نموده، بطوریکه دامنه های همگرآ با پروفیل مقعر کمترین پایداری را نشان می دهند. با توجه به نتایج یکسان در دو حالت رطوبتی بررسی شده (با و بدون در نظر گرفتن رطوبت منطقه غیر اشباع) می توان نتیجه گرفت که در حالت ماندگار هیدرولوژی جهت بررسی پایداری دامنه می توان وزن مخصوص خاک اشباع و غیر اشباع را یکسان فرض نمود و پایداری دامنه ها کاملا تحت تاثیر تغییرات سطح آب زیرزمینی تعیین می گردد. با توجه به محدودیت های مدل ارائه شده در این بخش (حالت ماندگار هیدرولوژی) در فصل چهارم مدل پایداری با در نظر گرفتن حالت دینامیک هیدرولوژی ارائه می گردد.

فصل چهارم: یک مدل فیزیکی یک بعدی برای کنترل هیدرولوژیکی زمین لغزشهای سطحی در دامنه های مرکب

مقاله در حال چاپ در مجله (*Earth Surface Processes and Landforms*, 2007)

در این فصل یک مدل فیزیکی جهت بررسی کنترل دینامیکی زمین لغزشهای سطحی در دامنه های مرکب ارائه می گردد. مدل ارائه شده شامل سه قسمت می باشد: یک مدل توپوگرافی با در نظر گرفتن مرفولوژی سه بعدی دامنه، یک مدل هیدرولوژی دینامیک جهت جریانهای زیر سطحی و سطح آب زیر زمینی دامنه (Troch et al., 2003; Hilberts, 2004) ویک مدل پایداری (شیب بی نهایت) بر اساس قانون موهر-کلمب. مدل ارائه شده در این بخش (Hillslope Storage Boussinesq Stability Model, HSB-SM) قادر است لغزشهای ایجاد شده توسط بارندگی را در دامنه های با بستر متغیر و اشکال مختلف مورد بررسی قرار دهد. بر اساس این مدل، عکس العمل دینامیکی دامنه های مرکب در طی بارندگی بستگی زیادی به شیب کف شکل پلان و انحنای کف بستر دارد. در این مدل میزان بارندگی روزانه با مقدار تغذیه ورودی (Recharge) جایگزین می گردد. این بدین معنی است که از تغییرات رطوبت خاک در منطقه غیر اشباع صرفنظر گردیده است (شایان ذکر است رطوبت منطقه غیراشباع بر مبنای قانون دارسی و با فرض تغییرات یکنواخت محاسبه شده است). جهت فائق آمدن بر این فرض پایداری دامنه های مختلف بر اساس جفت نمودن رطوبت منطقه اشباع و غیر اشباع (Hilberts et al., 2007) مورد بررسی قرار گرفته است. بررسی پایداری در هر دو حالت نتایج قابل مقایسه ای می دهد، بطوریکه پایداری دامنه عمدتا بر اساس تغییرات سطح آب (ذخیره اشباع خاک) تعیین می گردد. بنابر این مدل ارائه شده توسط تورخ و همکاران (Troch et al., 2003) بطورایمنی می تواند

خلاصه تحقیق:

فصل اول: مقدمه

عکس العمل هیدرولوژیکی یک دامنه نسبت به بارندگی باعث ارتباط متقابل منطقه اشباع-غیراشباع شده که معمولا منجر به بالا آمدن سطح آب در دامنه می شود. افزایش سطح آب و فشار آن با ایجاد یک نیروی بالایی می تواند باعث کاهش نیروی موثر توده خاک گردد. افزایش جریان زیرزمینی اشباع باعث ایجاد یک مکانیسم ما شه ای جهت ناپایدار کردن دامنه می شود. از آنجا که عکس العمل دینامیکی یک دامنه قویا بستگی به شکل پلان، انحنای شیب کف و زاویه شیب دارد، یک مدل سه بعدی دینامیکی هیدرولوژی دامنه جهت آنالیز پایداری دامنه های مرکب (غیر یکنواخت) مورد نیاز می با شد. معمولا جهت بررسی سه بعدی جریان آب زیر زمینی از مدل سه بعدی ریچارد استفاده می شود که حل این معادله بصورت سه بعدی بسیار مشکل می باشد. جهت جبران این مشکل اخیرا تورخ و همکارانش (Troch et al. 2002, 2003) مدلهای کم بعد تری توسعه داده و ارائه کرده اند. این مدلها کلیه اشکال دامنه ها را بر اساس ایده فن و براس (Fan and Bras, 1980) در نظر گرفته و پیچیدگی مدلهای سه بعدی را به شکل معنی داری کاهش می دهد. ضمنا این مدلها تغییرات عرض دامنه و انحنای کف بستر (مورفولوژی سه بعدی دامنه) را در نظر می گیرد، لذا در این تحقیق سعی بر آن است تا با توسعه مدل سه بعدی مورفولوژی دامنه و جریانهای زیر زمینی، پایداری دامنه های مرکب مورد تجزیه و تحلیل قرار گیرد.

فصل دوم: یک مدل پایداری شیب در شرایط ماندگار هیدرولوژی برای دامنه های مرکب
مقاله چاپ شده در مجله (*Hydrological Processes*, 2007)

ایده ارائه شده در این بخش یک مدل پایداری جهت بررسی رابطه بین شکل دامنه شامل عرض دامنه (همگرا، واگرا و موازی) و انحنای کف (محدب، مقعرو صاف) با هیدرولوژی و پایداری دامنه های های مرکب می باشد. این مدل از سه قسمت تشکیل شده است: یک مدل توپوگرافی، یک مدل هیدرولوژی در حالت ماندگار و یک مدل پایداری در شیب های نامحدود. مدل هیدرولوژیکی ارائه شده، اثر توپوگرافی دامنه را (از طریق شکل پلان و انحنای پروفیل) در برمی گیرد. با تغییر این دو عامل توپوگرافی ، نه شکل اصلی جهت بررسی پایداری دامنه های مختلف مورد استفاده قرار گرفت. بر اساس نتایج بدست آمده علاوه بر شیب کف، خصوصیات توپوگرافی دامنه (مخصوصا شکل پلان و انحنای کف) جریانهای زیر سطحی دامنه را کنترل نموده و این فرایند باعث تغییر مقاومت خاک شده و نتیجتا در پایداری دامنه اثر می گذارد. در واقع وقتی که عرض دامنه از حالت واگرآ به حالت همگرآ تغییر شکل می دهد، معمولا پایداری دامنه کاهش می یابد. این تاثیر در دامنه های با پروفیل مقعر کاملا واضح است. بنابراین برای یک شکل پلان مشخص (همگرا، واگرا و موازی)، دامنه های محدب معمولا پایداری بیشتری نسبت به دامنه های دیگر (مقعر و موازی) دارند. با توجه به یکسان دانستن وزن مخصوص خاک اشباع و غیر اشباع در حالت ماندگار هیدرولوژی در مدل ارائه شده، در فصل بعد اثر رطوبت منطقه غیر شباع در پایداری دامنه مورد بررسی قرار می گیرد.

فصل سوم: ذخیره رطوبت خاک و پایداری دامنه
مقاله چاپ شده در مجله (*Natural Hazards and Earth system sciences*, 2007)

همانطور که قبلا ذکر شد در این بخش نقش رطوبت منطقه غیر اشباع در پایداری دامنه های مرکب (دامنه های مختلف از نظر توپوگرافی) مورد تجزیه و تحلیل قرار می گیرد. این موضوع بر پایه محاسبه و تجزیه و تحلیل ضریب پایداری دامنه در دو حالت مختلف (با و بدون در نظر گرفتن رطوبت منطقه غیر اشباع) در دامنه های مرکب و با استفاده از دومدل مختلف پایداری مورد مطالعه قرار گرفته است. مورد اول با استفاده از مدل تحلیلی پایداری (طالبی و

به نام خداوند بخشنده و مهربان

دانشگاه واگنینگن هلند
دپارتمان علوم محیطی (مرکز مطالعات آب و اقلیم)
گروه هیدرولوژی و مدیریت کمی آب

رساله دکترای تخصصی (PhD)

عنوان:

رابطه بین شکل هندسی، هیدرولوژی و پایداری دامنه های مرکب (غیر یکنواخت) با استفاده از مدلهای هیدرولوژیکی یک بعدی

علی طالبی
دی ماه 1386

* This research was made possible with the financial support from **Ministry of Science, Researches and Technology (MSRT), of the Islamic Republic of Iran.**

Cover pages:
Front: shows a shallow landslide in the west of Iran (Mahdavifar, 2005).
Back: shows the distribution of shallow and deep landslides in Iran (Reference: National Geoscience Database of IRAN, http://www.ngdir.ir/landslide/PLandSlideMap.asp?#Nod).